

BIOTECHNOLOGICAL INVENTION OF CALOXINS

- A NOVEL CLASS OF ALLOSTERIC INHIBITORS

SPECIFIC FOR

PLASMA MEMBRANE CALCIUM PUMP ISOFORMS

BIOTECHNOLOGICAL INVENTION OF CALOXINS  
- A NOVEL CLASS OF ALLOSTERIC INHIBITORS  
SPECIFIC FOR  
PLASMA MEMBRANE CALCIUM PUMP ISOFORMS

By

MAGDALENA MARIA SZEWCZYK

A Thesis

Submitted to the School of Graduate Studies  
in Partial Fulfillment of the Requirements  
for the Degree  
Doctor of Philosophy

McMaster University

© Copyright by Magdalena Maria Szewczyk, June 2011

Doctor of Philosophy (2011)

McMaster University

(Biology)

Hamilton, Ontario

TITLE: Biotechnological invention of caloxins - a novel class of allosteric inhibitors  
specific for plasma membrane calcium pump isoforms

AUTHOR: Magdalena Maria Szewczyk (McMaster University)

SUPERVISOR: Professor A.K. Grover

NUMBER OF PAGES: xiv, 156

## ABSTRACT

This work used biotechnology to invent new caloxins - allosteric peptide inhibitors of plasma membrane  $\text{Ca}^{2+}$  pumps (PMCA) needed to understand the  $\text{Ca}^{2+}$  signalling in coronary artery.

PMCA are encoded by genes PMCA1-4. Defects in PMCA expression have been associated with several pathologies. The major objectives of my thesis were to determine the expression of PMCA isoforms in the smooth muscle and the endothelium of coronary artery and to invent high affinity and specificity caloxins for the isoforms present in these tissues.

In Aim 1 it was determined that the total PMCA protein and activity was much greater in smooth muscle than in endothelium. Both tissues expressed only PMCA1 and PMCA4, with  $\text{PMCA4} > \text{PMCA1}$  in smooth muscle and  $\text{PMCA1} > \text{PMCA4}$  in endothelium. Therefore, the search for PMCA1 and 4 selective caloxins using phage display technique was conducted.

Aim 2 was to invent PMCA1 selective inhibitors. Caloxin 1b3 was invented as the first known PMCA1 selective inhibitor. It inhibited PMCA1  $\text{Ca}^{2+}$ - $\text{Mg}^{2+}$ -ATPase with higher affinity than PMCA2, 3 or 4. Aims 1 and 2 were consistent with the greater potency of caloxin 1b3 than a known PMCA4 selective caloxin 1b1 in increasing cytosolic  $\text{Ca}^{2+}$  concentration in endothelial cells.

Aim 3 was to obtain ultrahigh selectivity and affinity PMCA4 bidentate inhibitor using the previously invented PMCA4 selective caloxins 1c2 and 1b2. In the first step the affinity of caloxin 1b2 was improved by limited mutagenesis to obtain caloxin 1c4. Caloxin 1c4 had 5-6 times higher affinity than caloxin 1b2 for inhibiting PMCA4 activity. Optimization of the bidentate caloxins from caloxin 1c2 and 1c4 was also attempted.

The novel caloxins may aid in elucidating the role of PMCA1 and PMCA4 in the physiology and pathophysiology of coronary artery and other tissues.

## PUBLICATIONS

*List of Publications as a result of the present study:*

Szewczyk MM, Pande J, Akolkar G, Grover AK (2010). Caloxin 1b3: A novel plasma membrane  $\text{Ca}^{2+}$ -pump isoform 1 selective inhibitor that increases cytosolic  $\text{Ca}^{2+}$  in endothelial cells. *Cell Calcium* 48:352-357

Szewczyk MM, Davis KA, Samson SE, Simpson F, Rangachari PK, Grover AK (2007)  $\text{Ca}^{2+}$ -pumps and  $\text{Na}^{+}$ - $\text{Ca}^{2+}$ -exchanger in vascular endothelium versus smooth muscle: activity, abundance and isoforms. *J Cell Mol Med* 11:129-38

Pande J, Mallhi KK, Sawh A, Szewczyk M.M, Simpson F, Grover AK (2006) Aortic smooth muscle and endothelial plasma membrane  $\text{Ca}^{2+}$  pump isoforms are inhibited differently by the extracellular inhibitor caloxin 1b1. *Am J Physiol Cell Physiol* 290: C1341-C1349

*List of Publications related to present study:*

Pande J, Szewczyk MM, Grover AK (2011) Allosteric inhibitors of plasma membrane Ca pumps: Invention and applications of caloxins. *World J Biol Chem.* 26: 39-47

Pande J, Szewczyk MM, Grover AK (2010). Phage display: concept, innovations, applications and future. *Biotechnol Adv* 28:849-58

Szewczyk MM, Pande J, Grover AK (2008). Caloxins: a novel class of selective plasma membrane  $\text{Ca}^{2+}$  pump inhibitors obtained using biotechnology. *Pflugers Arch* 456:255-66

Pande J, Szewczyk MM, Kuszczak I, Grover S, Escher E, Grover AK. (2008) Functional effects of caloxin 1c2, a novel engineered selective inhibitor of plasma membrane  $\text{Ca}^{2+}$ -pump isoform 4, on coronary artery *J Cell Mol Med* 12:1049-60

## **ACKNOWLEDGEMENTS**

I would like to express my sincere gratitude, first and foremost, to my supervisor Dr. Ashok Grover, for the excellent mentorship and patience he has provided me with and that he has believed in me since the beginning.

I would like to thank Sue Samson for friendship as well as technical assistance as well as all lab members I had pleasure to work with especially Jyoti Pande, Ivy Kuszczak, Kim Davis, Gauri Akolkar and Warda Khan.

I would like to acknowledge Gauri Akolkar and Warda Khan for helping me with experiments.

I would like to also acknowledge the CIHR and HSFO for providing me scholarship.

To all my closest family members - my husband, daughter, parents-in-law and my sister, thank you for all your help, support and patience.

## TABLE OF CONTENTS

ABSTRACT.....	III
PUBLICATIONS.....	V
ACKNOWLEDGEMENTS.....	VII
LIST OF ILLUSTRATIONS.....	XI
LIST OF ABBREVIATIONS.....	XIII
1.0 INTRODUCTION.....	1
1.1 Major players of calcium dynamics.....	1
1.2 Coronary artery structure and function.....	2
1.2.1 The effect of $[Ca^{2+}]_i$ increase in EC and SMC on vascular contractility....	5
1.2.1.1 Vascular smooth muscle.....	5
1.2.1.2 Vascular endothelium.....	7
1.3 Pathways which decrease $[Ca^{2+}]_i$ .....	10
1.4 Plasma Membrane $Ca^{2+}$ ATPases.....	11
1.4.1 General properties.....	11
1.4.2 PMCA structure.....	13
1.4.3 PMCA isoforms.....	16
1.4.4 PMCA regulation.....	18
1.4.1.1 Regulation by calmodulin.....	18
1.4.1.2 Regulation by phosphorylation.....	20
1.4.1.1 Regulation by acidic phospholipids.....	22
1.4.1.2 Regulation by proteases.....	23
1.4.5 PMCA distribution.....	24
1.4.6 Molecular partners for PMCA.....	26
1.4.7 PMCA and disease processes.....	28
1.5 Approaches used today to study the role of PMCA.....	32
1.5.1 Genetic techniques.....	32
1.5.2 Inhibitors.....	34
1.6 Allosterism, as applied to P-type ATPase inhibitors.....	35
1.7 Phage display - a tool for the development of allosteric inhibitors.....	36
1.8 Caloxins –concepts and classification.....	38
1.8.1 Series A caloxins.....	40
1.8.2 Series B caloxins.....	41
1.8.3 PMCA isoform selective caloxins.....	41

1.8.3.1	The invention of first PMCA isoform selective allosteric inhibitor-caloxin 1c2	43
1.8.4	Applications of caloxins	44
1.9	Problem definition and objectives	46
2.0	MATERIALS AND METHODS	49
2.1	Materials	49
2.2	Membrane isolation	51
2.2.1	Rabbit duodenal mucosa (RDM)	51
2.2.2	Leaky erythrocyte ghosts	52
2.2.3	Pig coronary artery smooth muscle membranes	53
2.2.4	Cultured pig coronary artery endothelium and HEK293 cells	54
2.3	Pig coronary artery endothelium and HEK293 cell culture	54
2.4	Protein estimation	55
2.5	Western blotting	55
2.6	Isolation of fresh EC	57
2.7	RNA isolation	58
2.8	RT-PCR	59
2.9	Screening Ph.D-12 library for binding to a synthetic exdom (biopanning)	60
2.10	Assay to determine phage selectivity for the PMCA1 exdom1X target	62
2.11	Phage amplification and precipitation	63
2.12	Determining phage titers	64
2.13	Picking phage clones and plasmid isolation	64
2.14	Screening the phage using PMCA affinity chromatography	65
2.14.1	Affinity chromatography with RDM PMCA	65
2.14.2	Affinity chromatography with erythrocyte ghosts PMCA	67
2.15	Construction of Ph.D caloxin 1b3-like peptide library	68
2.15.1	Synthesis of a duplex from single stranded oligonucleotides	69
2.15.2	Digestion of the oligonucleotide duplex	69
2.15.3	Preparation of the M13KE vector	70
2.15.4	Ligation of digested oligonucleotide duplex into digested M13KE vector.	70
2.15.5	Transformation of XL2-Blue MRF' ultracompetent cells	71
2.16	Construction of the Ph.D caloxin 1b2-like peptide library	71
2.17	Construction of the phage expressing bidentate peptides	72
2.18	Coupled enzyme ATPase assay	75
2.18	[Ca <sup>2+</sup> ] <sub>i</sub> determination in endothelial cells	77
2.18	Data Analysis	78

3.0	RESULTS .....	79
3.1	Aim1: PMCA isoform expression in pig arterial SMC and EC.....	79
3.1.1	PMCA mRNA expression.....	79
3.1.2	PMCA protein expression.....	82
3.1.2	PMCA Ca <sup>2+</sup> -Mg <sup>2+</sup> -ATPase activity .....	84
3.2	Aim2: Invention of PMCA1 selective caloxins .....	86
3.2.1	Tissue selection for PMCA1 .....	86
3.2.2	Phase I: Biopanning .....	91
3.2.3	Phase II: Screening by affinity chromatography with RDM PMCA .....	92
3.2.3.1	Optimization of affinity chromatography .....	92
3.2.3.2	Screening results .....	93
3.2.4	Phase III: Competition experiment .....	96
3.2.5	Inhibition of PMCA Ca <sup>2+</sup> -Mg <sup>2+</sup> -ATPase activity in coupled enzyme assay by caloxin 1b3 and 1b4.....	98
3.2.6	Effects of caloxin 1b3 on [Ca <sup>2+</sup> ] <sub>i</sub> in endothelium .....	102
3.2.7	Mutagenesis of caloxin 1b3 .....	104
3.3	Aim 3: The invention of ultra high affinity PMCA4 selective bidentate caloxins .....	109
3.3.1	Mutagenesis of caloxin 1b2 .....	109
3.3.1.1	Phase III: Competition of phage clones selected in phase II .....	111
3.3.1.2	Inhibition of PMCA by mutants of caloxin 1b2. ....	113
3.3.2	The invention of bidentate caloxins.....	115
3.3.2.1	Preliminary results with bidentate caloxin 1c2-1b2.....	116
3.3.2.2	Bidentate caloxin 1c2-1c4 creation using M13 phage display library..... .....	118
4.0	DISCUSSION .....	120
4.1	Differences in the PMCA isoforms in smooth muscle and endothelium.....	120
4.2	The invention of a PMCA1 selective caloxin .....	124
4.2.1	Physiological and pathophysiological implications.....	125
4.2.2	Role of exdom1 in PMCA reaction cycle .....	127
4.3	Advances in biotechnology.....	129
4.3.1	Phage propagation related contamination .....	129
4.3.2	Differentiating between closely related targets.....	130
4.3.3	Bidentate inhibitors.....	131
4.4	Conclusions and Future experiments .....	132
5.0	REFERENCES .....	134
6.0	APPENDIX 1: To determine caloxin 1c2-binding to PMCA protein .....	153

## LIST OF ILLUSTRATIONS

### *Figure number*

Fig. 1.	Key players in $\text{Ca}^{2+}$ -dynamics	3
Fig. 2.	The effect of $[\text{Ca}^{2+}]_i$ increase in endothelium and smooth muscle on vascular contractility	9
Fig. 3.	PMCA structure and comparison of extracellular domains (Exdoms) sequences between human PMCA isoforms 1-4	15
Fig. 4.	Bidentate peptides expressed on M13 phage	74
Fig. 5.	PMCA isoform expression in pig vascular tissues examined using RT-PCR	81
Fig. 6.	PMCA isoform expression analyzed by Western blots	83
Fig. 7.	Comparison of PMCA isoform expression in pig coronary artery EC and SMC analyzed by Western blots	84
Fig. 8.	Relative values of PMCA activity and total PMCA protein abundance in Western blots in pig coronary artery EC and SMC.	85
Fig. 9.	Overview of the screening procedure to obtain isoform selective caloxins	87
Fig. 10.	PMCA isoform expression in HEK293 cells and RDM examined using RT-PCR.	89
Fig. 11.	PMCA1 protein expression in HEK293 and RDM plasma membrane enriched fraction	89
Fig. 12.	PMCA1 and PMCA4 isoform expression in mucosa from different parts of rabbit intestine	90
Fig. 13.	Selectivity of phage population obtained upon biopanning	92
Fig. 14.	Western blot analysis of RDM PMCA1 eluted from calmodulin-agarose column	94
Fig. 15.	Caloxin 1b3 and 1b4 inhibition of PMCA activity in rabbit duodenal mucosa measured by coupled enzyme assay	99
Fig. 16.	The effect of caloxin 1b3 on PMCA activity in rabbit duodenal mucosa (PMCA1) and human erythrocyte ghosts (PMCA4) measured by coupled enzyme assay	100
Fig. 17.	Caloxin 1b3 inhibition of $\text{Ca}^{2+}$ - $\text{Mg}^{2+}$ ATPase activity of PMCA1-4 measured in the coupled enzyme assay	101
Fig. 18.	The effect of caloxin 1b3 on $\text{Mg}^{2+}$ ATPase activity in RDM membranes and human erythrocyte ghosts measured by coupled enzyme assay	102
Fig. 19.	The effect of caloxins 1b3 and 1b1 on $[\text{Ca}^{2+}]_i$ in cultured pig coronary artery endothelial cells	103
Fig. 20.	PMCA4 inhibition by 25 $\mu\text{M}$ the caloxin1b2 mutant peptides	113
Fig. 21.	Caloxin 1c4 concentration dependence of inhibition of PMCA4	114
Fig. 22.	Inhibition of PMCA activity in leaky human erythrocyte ghosts by the bidentate caloxin 1c2-1b2	116

***Table number***

Table 1.	Caloxins	40
Table 2.	Antibodies/proteins and dilutions used for Western blot analysis	56
Table 3.	PMCA isoform specific Primers for PCR analysis	61
Table 4.	Adsorbents and eluants used in selectivity test	63
Table 5.	Binding efficiency in each round of phase I	95
Table 6.	Phage clones obtained after competition experiment in affinity chromatography with RDM PMCA	97
Table 7.	Testing small-scale caloxin 1b3-like peptide library	105
Table 8.	Characterization of the Ph.D caloxin 1b3-like peptide library	106
Table 9.	Phage clones selected after 1 round of screening of the caloxin 1b3-like peptide library	107
Table 10.	Characterization of the phage clones selected after competition	118
Table 11.	Testing Ph.D caloxin 1b2-like peptide library diversity	110
Table 12.	Characterization of Ph.D caloxin 1b2-like peptide library	100
Table 13.	Phage binding efficiency in each experiment of phase II	111
Table 14.	Phage clones obtained in Phase II screening of caloxin 1b2-like peptide library	111
Table 15.	Frequencies of clones (mutants of caloxin 1b2) selected in competition experiment for binding to PMCA4	112
Table 16.	Sequences of bidentate peptides	118
Table 17.	Binding efficiency in each of competition experiments of phage displaying bidentate peptides	119

### LIST OF ABBREVIATIONS

Bpa	Benzoylphenylalanine
BSA	bovine serum albumin
Ca <sup>2+</sup>	ionized calcium
[Ca <sup>2+</sup> ] <sub>i</sub>	cytosolic Ca <sup>2+</sup> concentration
cAMP	adenosine 3',5'-cyclic monophosphate
CBD	calmodulin binding domain
cGMP	guanosine 3',5'-cyclic monophosphate
EC	endothelial cell(s)
EDTA	(ethylenedinitrilo)-tetraacetic acid
EGTA	ethylene glycol-bis(β-aminoethyl ether)-N,N,N',N'-tetraacetic acid
eNOS	endothelial nitric oxide synthase
exdom	extracellular domain
HEK293	human embryonic kidney cell line
HEPES	N-2-hydroxyethylpiperazine-N'-2-ethanesulfonic acid
HRP	horseradish peroxidase
IP <sub>3</sub>	inositol 1,4,5-trisphosphate
IP <sub>3</sub> R	IP <sub>3</sub> receptor
K <sub>Ca</sub>	calcium activated potassium channels
K <sub>d</sub>	dissociation constant
KLH	keyhole limpet hemocyanin
K <sub>i</sub>	inhibition constant
LB	Luria broth
MLCK	myosine light chain kinase
MLCP	myosine light chain phosphatase
mNCX	mitochondrial Na <sup>+</sup> /Ca <sup>2+</sup> exchanger
NADH	nicotinamide adenine dinucleotide (reduced form)
NCX	Na <sup>+</sup> /Ca <sup>2+</sup> exchanger
NCKX	Na <sup>+</sup> /Ca <sup>2+</sup> /K <sup>+</sup> exchanger
nNOS	neuronal nitric oxide synthase
NO	nitric oxide
Orai-1	calcium release-activated calcium channel protein 1
PBS	phosphate buffered saline
PEG	polyethylene glycol
pfu	plaque forming unit
Ph.D	phage display peptide library
PKA	cAMP dependent protein kinase
PKC	calcium dependent protein kinase
PKG	cGMP dependent protein kinase
PMCA	plasma membrane Ca <sup>2+</sup> ATPase(s)
P2X	cation-permeable ligand gated ion channels
RDM	rabbit duodenal mucosa
ROCC	receptor operated Ca <sup>2+</sup> channel
RyR	ryanodine receptor

SEM	standard error of the mean
SER	sarco/endoplasmic reticulum
SERCA	sarco/endoplasmic reticulum Ca <sup>2+</sup> ATPase(s)
sGS	soluble guanylate cyclase
SMC	smooth muscle cell(s)
SOCC	store operated Ca <sup>2+</sup> channel
STIM1	Stromal interaction molecule 1
TM	transmembrane
TRIS	tris(hydroxymethyl)aminomethane
TRP	transient receptor potential
TUPs	target unrelated proteins
VOCC	voltage operated Ca <sup>2+</sup> channels

## **1.0. Introduction**

The regulation of intracellular calcium concentration ( $[Ca^{2+}]_i$ ) is essential for cell homeostasis and cellular signal transduction. Plasma Membrane  $Ca^{2+}$  ATPases (PMCA), encoded by 4 genes, are the only high affinity calcium extrusion systems (Brini et al. 2011; Carafoli 1991; Di Leva et al. 2008; Szewczyk et al. 2007). Different cells express different PMCA isoforms (Burette et al. 2003; Carafoli 1991; Strehler et al. 2001). There are a number of pathologies associated with failed PMCA function (Brini et al. 2009; Carafoli 2004; Ficarella et al. 2007; Heyliger et al. 1987; Kozel et al. 1998; Kurnellas et al. 2010; Kwan et al. 1979; Lehotsky et al. 2002; Missiaen et al. 2000; Monteith et al. 2007; Oceandy et al. 2006; Schuh et al. 2004). However, the exact role of each isoform in physiology and pathology has been hindered due to lack of isoform selective inhibitors. The overall objective of this research was to determine the PMCA gene expression in pig coronary artery endothelium and smooth muscle and to invent high affinity allosteric inhibitors of PMCA, that are specific for the isoforms expressed in the coronary artery. Before proceeding onto the details of the research proposal, an overview of the following is provided:  $Ca^{2+}$  homeostasis, differences in  $Ca^{2+}$  handling in coronary artery endothelial cells (EC) and smooth muscle cells (SMC), structure, regulation and role of PMCA, limitations of the methods currently used to study PMCA and PMCA inhibitors.

### **1.1. Major players of calcium dynamics**

Homeostasis of  $[Ca^{2+}]_i$  is a prerequisite for healthy cell life. Since  $Ca^{2+}$  is a universal signal transduction molecule, its concentration must be kept at low levels in resting cells and increased only during brief periods of cell excitation (Carafoli 1987;

Carafoli 2002). After signal transmission  $[Ca^{2+}]_i$  is lowered by extrusion by PMCA,  $Na^+/Ca^{2+}/(K^+)$  exchangers (NC(K)X), sequestration into the sarco/endoplasmic reticulum (SER) by SER  $Ca^{2+}$  pump (SERCA) and a number of cytosolic  $Ca^{2+}$  buffering and binding proteins (Carafoli 1991; Carafoli et al. 2001; Carafoli 2002; Missiaen et al. 1991; Philipson et al. 2002; Schnetkamp 2004; Wuytack et al. 2002). The SER can store  $Ca^{2+}$  at concentrations up to 10-15 mM that can be released upon stimulation of inositol 1,4,5,-trisphosphate ( $IP_3$ ) receptors ( $IP_3R$ ) and ryanodine receptors (RyR) (Dawson 1997; Fill et al. 2002; Meldolesi et al. 1998). Cell stimulation can also lead to  $Ca^{2+}$  entry into cells via voltage operated calcium channels (VOCC), receptor operated calcium channels (ROCC), storage operated calcium channels (SOCC) and the reverse mode of NC(K)X (Lacinova 2005; Philipson et al. 2002; Shuttleworth 2004; Wang et al. 2008). Mitochondria may also sequester or release  $Ca^{2+}$  via a mitochondrial uniporter or mitochondrial  $Na^+/Ca^{2+}$  exchanger, respectively (Carafoli 2003; Kirichok et al. 2004). Fig. 1 shows the major players involved in  $[Ca^{2+}]_i$  dynamics.

## **1.2. Coronary artery structure and function**

Coronary arteries supply oxygenated blood to the heart. Vascular tone is an important factor in regulating coronary blood flow. Any obstruction in coronary blood flow e.g. by atherosclerotic plaque formation, may cause serious pathologies, such as heart failure, arrhythmia or heart attack (Duncker et al. 2004; Kralios et al. 1998). The major vessels for coronary circulation are the left main coronary artery, which divides into left anterior descending and circumflex branches, and the right main coronary artery (Danas 2002).

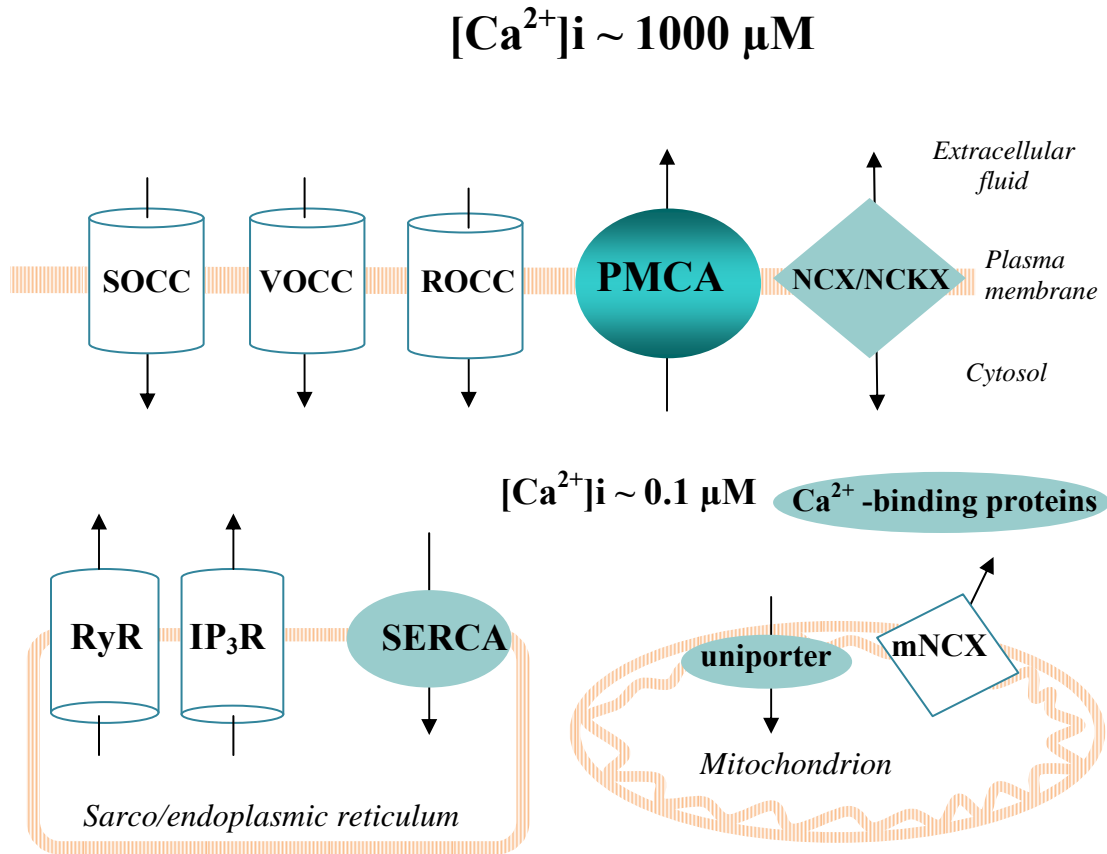


**Fig.1. Key players in Ca<sup>2+</sup>-dynamics.** Receptor activation may produce membrane depolarization, opening of voltage operated Ca<sup>2+</sup> channels (VOCC), receptor operated Ca<sup>2+</sup> channels (ROCC) and/or phospholipase C activation to produce IP<sub>3</sub>, which in turn releases Ca<sup>2+</sup> from sarco/endoplasmic reticulum (SER) via IP<sub>3</sub> receptors (IP<sub>3</sub>R). Ca<sup>2+</sup> can also induce Ca<sup>2+</sup> release from SER via ryanodine receptors (RyR). Calcium depletion from SER activates storage activated Ca<sup>2+</sup> channels (SOCC). Mitochondria may sequester or release Ca<sup>2+</sup> via mitochondrial uniporter and mitochondrial Na<sup>+</sup>/Ca<sup>2+</sup> exchanger (mNCX), respectively. Various Ca<sup>2+</sup> binding proteins can buffer Ca<sup>2+</sup> in the cytosol and in the SER lumen. Increase in intracellular Ca<sup>2+</sup> concentration ( $[Ca^{2+}]_i$ ) leads to tissue specific responses and is then decreased to its resting levels. Ca<sup>2+</sup> can be removed from the cell by plasma membrane Ca<sup>2+</sup> pump (PMCA), Na<sup>+</sup>-Ca<sup>2+</sup>-exchanger (NCX), Na<sup>+</sup>-Ca<sup>2+</sup>-K<sup>+</sup> exchanger (NCKX) or sequestered into SER by SER Ca<sup>2+</sup> pump (SERCA). The exchangers may also bring calcium inside the cell.

These arteries originate from the aorta just above the aortic valve and branch into smaller arteries over the surface of the heart. These superficial arteries branch further into epicardial arteries but also into arteries penetrating the ventricular wall and then connect to the capillary network of the heart. This capillary network is responsible for the exchange of oxygen and other substrates to the heart cells. The small arteries and arterioles in the microcirculation are the primary sites of vascular resistance, and therefore the primary site for regulation of blood flow (Coats 2003; Danias 2002).

A coronary artery is composed of three tissue layers: intima, media and adventitia. The innermost layer, the intima, consists of endothelium. EC functions as a selective barrier between blood and the underlying tissues, which regulate the passage of gases, fluid and various molecules across their cell membranes (Busse et al. 2006; Danias 2002; Moncada et al. 2006). The EC reacts with physical and chemical stimuli within the circulation and participates in vascular homeostasis, vasomotor tone, immune and inflammatory responses and angiogenesis (Basu et al. 2008; Busse et al. 2006; Danias 2002; Rodriguez et al. 2009). EC injury, activation or dysfunction leads to pathological processes such as atherosclerosis, loss of semi-permeable membrane function, vessel remodeling and thrombosis (Chesterman 1988; Danias 2002; Sima et al. 2009). The next layer, the media, consists of elastic fibers and SMC, which compose the majority of the arterial wall. SMC control arterial diameter and thus blood pressure by their ability to contract and relax in response to various stimuli (Johns et al. 1987). Excessive constriction or relaxation of smooth muscle leads to hypertension and hypotension, respectively (Bohr et al. 1988). The outermost layer, the adventitia is composed mainly of collagen bundles

which function as mechanical support (Gutterman 1999). It also contains fibroblasts and nerve fibers. Larger arteries are surrounded by perivascular fat, which may secrete various molecules, such as adiponectin, and play a role in local control of blood flow (Yiannikouris et al. 2010).

### **1.2.1. The effect of $[Ca^{2+}]_i$ increase in EC and SMC on vascular contractility**

SMC and EC differ in their response to increases in  $[Ca^{2+}]_i$ : contracting and paracrine, respectively (Fig. 2). In this section the major routes of  $[Ca^{2+}]_i$  increase in SMC and EC will be described.

#### **1.2.1.1. Vascular smooth muscle**

In SMC, an increase in  $[Ca^{2+}]_i$  activates  $Ca^{2+}$ -calmodulin dependent myosin light chain kinase, leading to increased phosphorylation of the 20-kDa myosin light chains, cross-bridge formation between the myosin heads and the actin filaments and eventually, SMC contraction (Consigny 1991). Phosphorylation of 20-kDa myosin light chains and the contractile state is balanced by the actions of myosin light chain phosphatase. SMC can also be contracted via  $Ca^{2+}$ -independent pathways triggered by production of diacylglycerol and protein kinase C (PKC) activation as well as by activation of Rho-kinase, integrin-linked kinase or zipper-interacting protein kinase (Sward et al. 2003; Wilson et al. 2005; Zhang et al. 1994).

$[Ca^{2+}]_i$  can be increased by  $Ca^{2+}$  release from SER or  $Ca^{2+}$  entry from outside. Activation of various G-protein coupled receptors by neurotransmitters or hormones, e.g. noradrenaline (norepinephrine), adrenaline (epinephrine), angiotensin II, endothelin-1,

histamine, adenosine or vasopressin leads to conformational changes which promote binding of heterotrimeric G protein with  $G\alpha/q$  subunit (Bhalla et al. 1987; Bouallegue et al. 2007; Ishida et al. 1997; Miller et al. 2000; Waugh 1962; Yaar et al. 2002). The binding activates  $G\alpha/q$  so that it releases guanosine diphosphate and binds guanosine triphosphate leading to the dissociation of  $G\alpha/q$  and complex of  $\beta\gamma$  subunits. Dissociated  $G\alpha/q$  activates its downstream target, phospholipase C, to hydrolyze the membrane lipid phosphatidylinositol 4,5-bisphosphate into  $IP_3$  and diacylglycerol.  $IP_3$  is water-soluble and diffuses through the cytoplasm to the SER, where it binds to the  $IP_3R$  receptor causing  $Ca^{2+}$  release (Dawson 1997).

$Ca^{2+}$  can enter the cell through various calcium channels and also the reverse mode of NCX (Bolton et al. 1992; Hirota et al. 2007; Lamont et al. 2002; Navedo et al. 2007; Saleh et al. 2008). Membrane depolarization leads to opening of L-type VOCC (Navedo et al. 2007). ATP released from perivascular nerves activates purinergic ligand gated calcium channels (P2X) (Lamont et al. 2002). Other possibilities are the various isoforms of the transient receptor potential cation channel family (TRPC). TRPC are non-selectively permeable to cations, with variable selectivity of calcium over sodium among the different members (Owsianik et al. 2006). TRPC3, 6 and 7 are of interest because they are activated by diacylglycerol that is formed together with  $IP_3$  upon G-protein coupled receptor activation (Albert et al. 2005; Peppiatt-Wildman et al. 2007; Saleh et al. 2006). Extracellular calcium entry may sensitize SER channels ( $IP_3R$  and RyR) prior to their full activation and is important for calcium induced calcium release from SER (Wray et al. 2010). The initiation of calcium induced calcium release may depend either

on activation of IP<sub>3</sub>R by IP<sub>3</sub> or RyR by Ca<sup>2+</sup> and is then amplified by regenerative Ca<sup>2+</sup> release by either the RyRs or IP<sub>3</sub>R, depending on the cell type (Dai et al. 2006; Wray et al. 2010). The process often appears as a wave traveling down the length of the cell (Iino et al. 1994; Iino et al. 1994). An increase in [Ca<sup>2+</sup>]<sub>i</sub> may, in turn, stimulate the Ca<sup>2+</sup> activated chloride channel, which leads to membrane depolarization and opening of VOCC (Pacaud et al. 1989). The depolarization can spread to neighboring cells through gap junctions (Jacobsen et al. 2007). On the other hand, Ca<sup>2+</sup> also stimulates large conductance Ca<sup>2+</sup>-activated potassium channels, which hyperpolarize the cell and negatively regulate VOCC, playing a role in vasodilation (Dick et al. 2010).

#### **1.2.1.2. Vascular endothelium**

In EC, an increase in [Ca<sup>2+</sup>]<sub>i</sub> leads to activation of nitric oxide synthase (eNOS) and production of nitric oxide (NO) from L-arginine (Moncada et al. 2006). NO diffuses to SMC and activates soluble guanyl cyclase to produce guanosine 3',5'-cyclic monophosphate (cGMP). Increased cGMP levels inhibit VOCC and activate myosin light chain phosphatase through cGMP dependent protein kinase leading to dephosphorylation of myosin light chains and SMC relaxation (Consigny 1991). Recently the role of calcium activated potassium channels in endothelium-dependent vasodilation was proposed (Dick et al. 2010). Activation of these channels by Ca<sup>2+</sup> leads to EC membrane hyperpolarization. The hyperpolarization may spread into SMC through gap junctions connecting EC to SMC, which can potentially enable direct electrical coupling (Dora 2010).

Similar to SMC, in EC  $[Ca^{2+}]_i$  can increase upon activation of the  $IP_3$  signaling pathway and release of calcium from SER. This can be accomplished by activation of G protein coupled receptors by thrombin, histamine, bradykinin and receptor protein kinases by growth factors (Dzau et al. 1991; Glusa et al. 1988; Hecker et al. 1992; Wennmalm et al. 1991). In contrast to SMC, EC are conventionally considered ‘electrically non-excitable’ and devoid of voltage-operated  $Ca^{2+}$  channels. However, in pulmonary, adrenal and brain microvascular endothelium, the L-type and/or T-type VOCC current has been observed, but the role of influx via VOCC in EC still remains to be specified (Vinet et al. 1999; Yakubu et al. 2002; Zhou et al. 2006). Agonist induced store depletion leads to activation of store operated calcium entry which is an important  $Ca^{2+}$  entry route in EC (Cioffi et al. 2010). It contains three major components; stromal interaction molecule 1 (STIM1, calcium sensor in ER/SR), calcium release-activated calcium channel protein 1 (Orai1) and TRPC. STIM1 senses the depletion of  $Ca^{2+}$  from the ER, and then oligomerizes, translocates to junctions adjacent to plasma membrane and helps to organize Orai1 or TRPC channels in the membrane. It has been reported that vascular endothelial cells express all seven members of TRPC (Yip et al. 2004). TRPC (isoforms 3, 6, 7) can also act independently, as receptor operated calcium channels since they are activated by the diacylglycerol produced in  $IP_3$  pathway. EC also express various types of P2X which expression may differ depending on vascular bed (Ray et al. 2002). It was suggested that in vascular EC, the rise in intracellular calcium resulting from shear stress is due to calcium entry through P2X type 4 (Yamamoto et al. 2006).

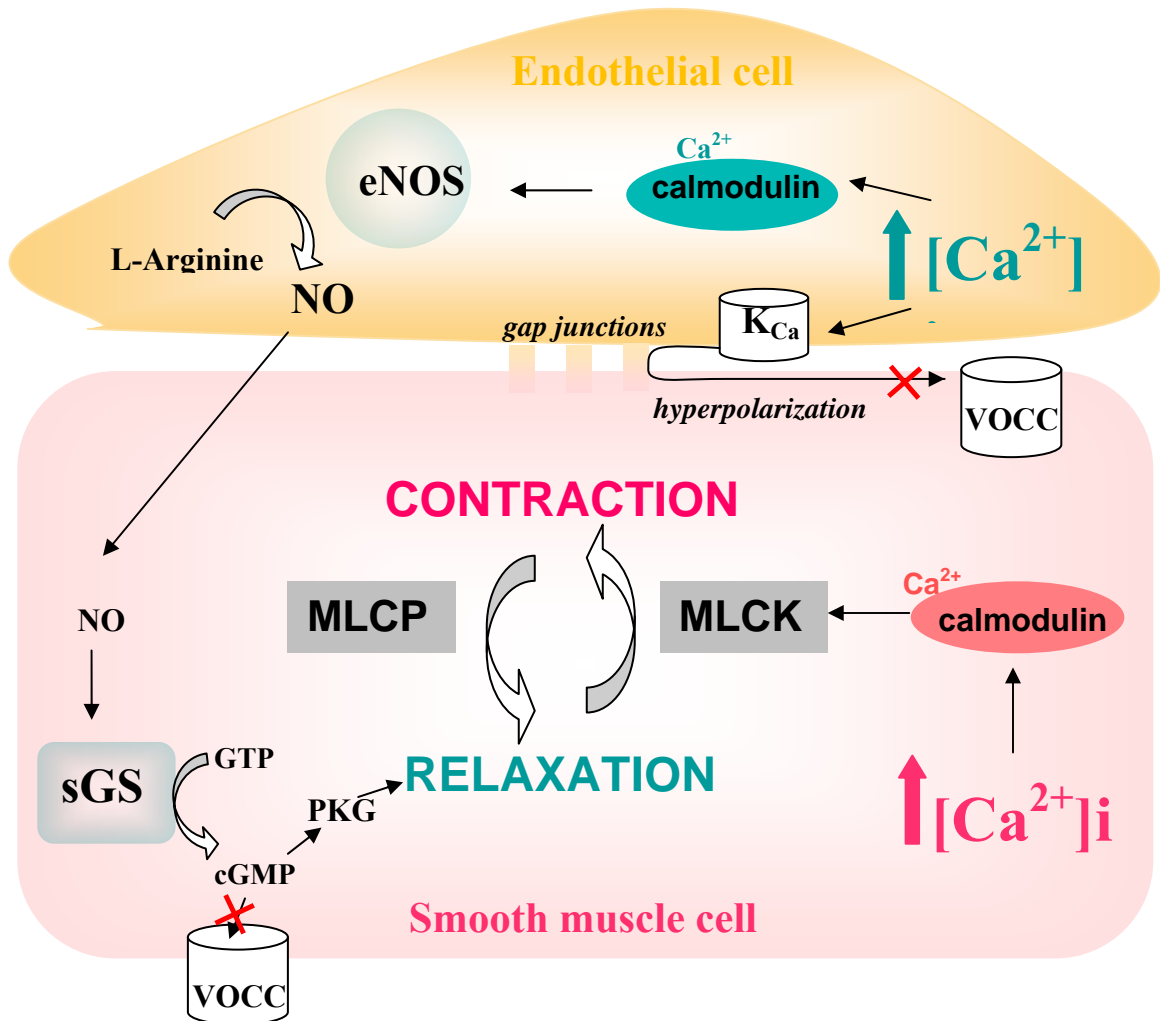


**Fig. 2. The effect of  $[Ca^{2+}]_i$  increase in endothelium and smooth muscle on vascular contractility.** The increase of  $[Ca^{2+}]_i$  in endothelium leads to activation of endothelial NO synthase (eNOS) by calcium-calmodulin and NO production. NO diffuses to SMC, where it activates soluble guanyl cyclase (sGS) and cGMP production. cGMP activates myosin light chain phosphatase through cGMP dependent protein kinase (PKG) and inhibits voltage operated calcium channels (VOCC) leading to smooth muscle relaxation. When  $[Ca^{2+}]_i$  rises in endothelium, the cells hyperpolarize due to opening of calcium-activated potassium channels ( $K_{Ca}$ ). This hyperpolarization spreads to adjacent smooth muscle cells through gap junctions and inhibits VOCC function. In contrast an increase in  $[Ca^{2+}]_i$  in smooth muscle leads to activation of myosine light chain kinase (MLCK) and smooth muscle contraction.

### 1.3. Pathways which decrease $[Ca^{2+}]_i$

After short periods of increase of  $[Ca^{2+}]_i$  following cell stimulation,  $[Ca^{2+}]_i$  has to return to its resting levels. There are three major systems which can decrease  $[Ca^{2+}]_i$ : calcium pumps, ion exchangers and the mitochondrial electrophoretic uniporter (Carafoli 1991; Kirichok et al. 2004; Philipson et al. 2002; Wuytack et al. 2002).  $Ca^{2+}$  can also be buffered by reversible complexation with  $Ca^{2+}$  binding proteins within the cell (Haeseleer et al. 2002). Three classes of  $Ca^{2+}$  pumps have been described in mammals: PMCA which transports  $Ca^{2+}$  out of the cell, SERCA that sequester  $Ca^{2+}$  inside the SER, nuclear envelope and to some degree into Golgi apparatus and  $Ca^{2+}$  pump of the Golgi membranes. Interestingly, this pump can also transport  $Mn^{2+}$ , which is a cofactor of many enzymes found in the Golgi compartment (Van Baelen et al. 2004). All  $Ca^{2+}$  pumps have a high affinity for  $Ca^{2+}$  (nanomolar range) which differs among isoforms and splice variants. The plasma membrane may also contain low affinity (micromolar range) calcium transporting ion exchangers: NCX and NCKX, which, depending on ions concentrations, may transport calcium out or bring calcium into the cell (Philipson et al. 2002). NCX exchanges 3  $Na^+$  for 1  $Ca^{2+}$  and NCKX co-transport  $Ca^{2+}$  and  $K^+$  in exchange for 4  $Na^+$  and thus both are electrogenic. Mitochondria also play a role in transporting cytosolic  $Ca^{2+}$ . They possess a low affinity, high-speed electrophoretic uniporter that is located in the inner membrane (Kirichok et al. 2004). The uniporter is coupled to oxidative phosphorylation, and uses the electropotential gradient across the inner mitochondrial membrane to drive  $Ca^{2+}$  into the mitochondrion. Since the focus of

this thesis is on developing selective inhibitors of PMCA, this pump is described here in detail.

#### **1.4. Plasma Membrane $\text{Ca}^{2+}$ ATPases**

PMCA are the only high affinity calcium extrusion system in mammalian cells (Brini et al. 2009; Carafoli 1991; Di Leva et al. 2008). They convert the energy of ATP hydrolysis into transmembrane  $\text{Ca}^{2+}$  transport against its electrochemical gradient. PMCA play an important role in calcium homeostasis by keeping low calcium concentration inside the cell, as well as in calcium signaling by affecting other protein functions through local  $[\text{Ca}^{2+}]_i$  regulation. They were first discovered in 1961 as an ATPase activity in red blood cell membranes (Dunham et al. 1972). Five years later, in 1966, it was discovered that these ATPases pump  $\text{Ca}^{2+}$  out of the cytosol (Vincenzi et al. 1967). Since then, tremendous progress has been made in elucidating PMCA expression, properties and their role in health and disease, which will be discussed in detail in following sections.

##### **1.4.1. General properties**

PMCA belong to the P2 subfamily of P-type ion transport ATPases, which are characterized by the formation of a high energy acylphosphate during their reaction cycle (Apell 2004; Moller et al. 1996). Phosphorylation occurs between the  $\gamma$  phosphate of the hydrolyzed ATP and the conserved aspartate (D) residue of the P-type ATPase consensus sequence (SDKTGT). According to the E1E2 model of the P-type ATPase reaction cycle it is suggested that PMCA cycles between two main conformational states denoted as E1

and E2 (Carafoli et al. 2000). The E1 conformation has high affinity binding sites for  $\text{Ca}^{2+}$  facing the cell interior and the E2 form has low affinity  $\text{Ca}^{2+}$  binding sites facing the extracellular surface. Following  $\text{Ca}^{2+}$  binding, the E1 form is phosphorylated by ATP to form a high energy intermediate -  $(\text{Ca}^{2+})\text{E1P}$ . Next, the pump undergoes a conformational change into the E2 state while translocating  $\text{Ca}^{2+}$  to the extracellular surface where  $\text{Ca}^{2+}$  is released. The counter transport  $\text{H}^+$  ion binds to the E2P form, leading to its dephosphorylation. Finally, the E2 returns to the E1 state with the release of the counter transport ion. The pump is suggested to have 1:1 stoichiometry with one  $\text{Ca}^{2+}$  being translocated with the hydrolysis of each molecule of ATP. This is in contrast to the SERCA pump, which has a stoichiometry of 2  $\text{Ca}^{2+}$  per one ATP hydrolyzed. Consistently, PMCA has a Hill coefficient of 1 for  $\text{Ca}^{2+}$ , while SERCA has a Hill coefficient of 2 (Grover et al. 1986).

PMCA operates as a  $\text{Ca}^{2+}/\text{H}^+$  exchanger, however its stoichiometry still remains controversial. Work done on neuronal cells and on purified PMCA protein reconstituted in liposomes suggests that PMCA is electroneutral and exchanges 2  $\text{H}^+$  for each  $\text{Ca}^{2+}$  extruded (Niggli et al. 1987; Thomas 2009). However, experiments done by Hao et. al. suggest partial PMCA electrogenic with 1:1  $\text{Ca}^{2+}:\text{H}^+$  transport process (Hao et al. 1994).

PMCA has high affinity for  $\text{Ca}^{2+}$  ( $K_d = 0.2\text{-}0.5 \mu\text{M}$  measured under optimal conditions) and it is active even during the resting  $\text{Ca}^{2+}$  concentration, indicating its important role in the fine tuning of  $[\text{Ca}^{2+}]_i$  (Di Leva et al. 2008; Missiaen et al. 1991).

### 1.4.2. PMCA structure

Although first cloned in 1988, the 3D structure of PMCA has not been yet determined. Based on the structural template of SERCA pump, hydropathy plots, and proteolytic digestion, PMCA, like other P-type ATPases, is predicted to have 10 transmembrane spanning helices (TM 1-10) (Fig.3.) (Carafoli et al. 1982; Carafoli 1997; Moller et al. 1996). Eighty percent of the pump mass together with its amino and carboxy termini is located on the cytosolic side of the membrane. The cytosolic domains of PMCA contain three major functional domains: actuator, catalytic and regulatory.

The actuator domain consists of a short intracellular loop between TM2 and TM3. The domain contains a conserved TGES sequence where glutamate seems to play an important role in the dephosphorylation of the E2P conformation in the reaction cycle of both SERCA and the Na<sup>+</sup> pump (Clausen et al. 2004; Toustrup-Jensen et al. 2003). The loop has been predicted to consist of antiparallel  $\beta$  strands in which several conserved glycines would form the hairpin turns. Mutations of these glycines result in loss of ATPase activity (Andersen et al. 1989; Ghislain et al. 1987). It also contains the stretch of basic amino acids involved in binding acidic phospholipids (see section 1.4.4.3), splice site A (see section 1.4.3) and the site for binding C-terminal tail involved in PMCA autoinhibition process (see section 1.4.4.1).

The largest loop, connecting TM4 and TM5, contains the catalytic domain and the two sequences conserved among all P-type ATPases. The **KGA** sequence found within the nucleotide binding domain which contains a lysine residue involved in ATP binding and the **SDKTGLT** sequence found within the phosphorylation domain containing a

conserved phosphorylated aspartate residue. The phosphorylation domain also contains a hinge region which brings the catalytic aspartic acid and the ATP-binding site located within the catalytic domain in close spatial contact during the reaction cycle allowing for aspartate phosphorylation and formation of the high energy intermediate during PMCA reaction cycle. The catalytic loop, in addition to actuator domain, is involved in PMCA autoinhibition since it also binds the C-terminal tail.

The C-terminal tail protruding into the cytosol from TM10, called the regulatory domain, is much longer than in the other  $\text{Ca}^{2+}$  ATPases. It contains a calmodulin binding domain (CBD) which in the absence of  $\text{Ca}^{2+}$ -calmodulin serves as an inhibitory domain by binding to two sites (one on actuator and one on catalytic domain) and preventing PMCA catalytic turnover. Recent data suggested that D<sup>1080</sup>, located 5 residues upstream from the CBD is an essential residue that may assist in orienting the regulatory carboxyl terminus to the catalytic sites of PMCA to form a stable inhibited conformation. The mutation of this residue into asparagine, alanine or lysine substantially increased basal PMCA activity in the absence of calmodulin (Paszty et al. 2002). The C-terminal tail also contains phosphorylation sites for protein kinases A (PKA) and C (PKC) and binding sites for many regulatory proteins and acidic phospholipids all of which affect PMCA functionality (see section 1.4.4). Since the second splice site (splice site C) is located within the regulatory domain, PMCA splice variants differ in their regulation.

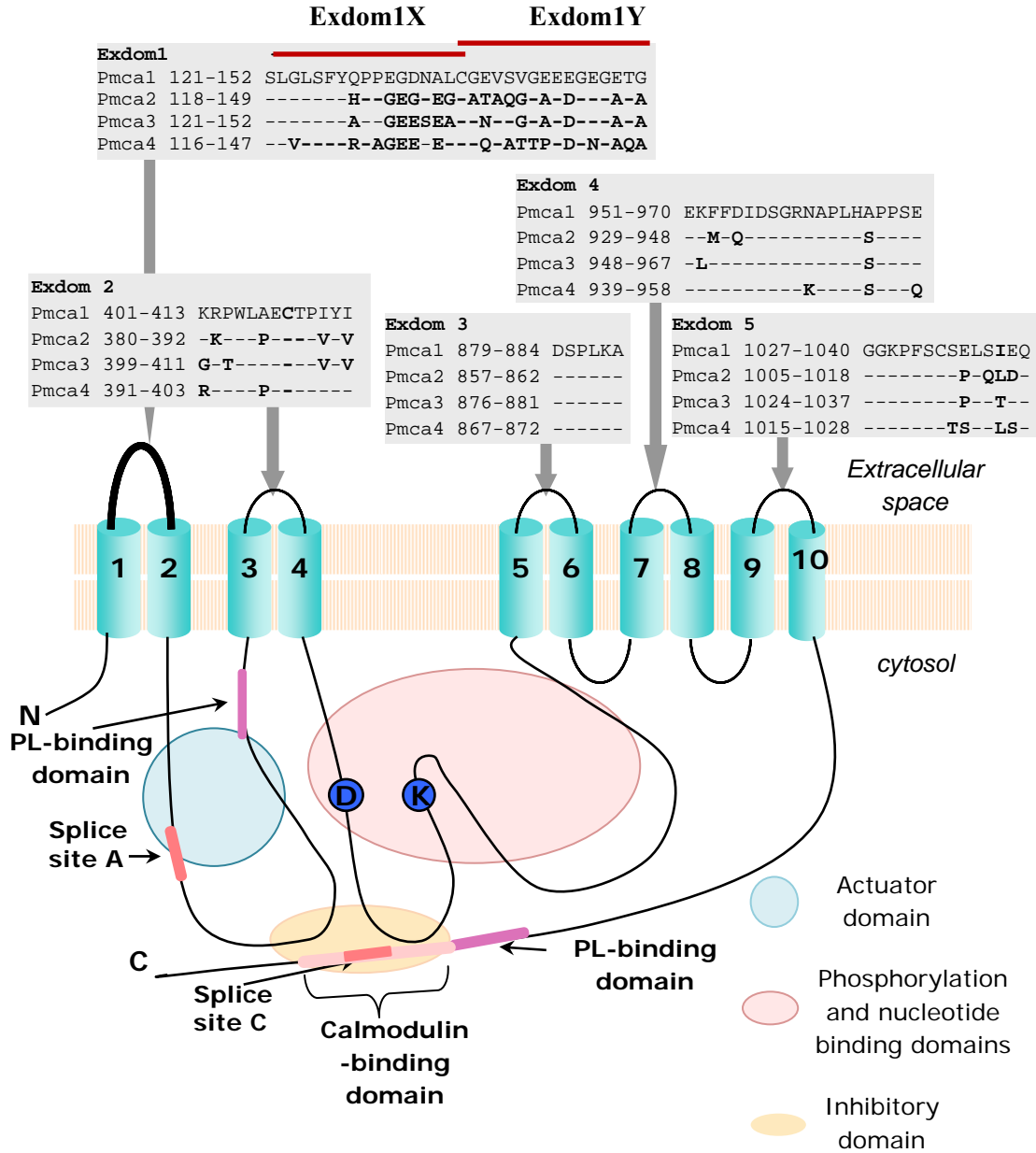


**Fig. 3. PMCA structure and comparison of extracellular domains (Exdoms) sequences between human PMCA isoforms 1-4. Identical exdom amino acids are marked as “-”. Transmembrane regions are numbered 1-10. N – amino terminal end, P – phosphorylation site, aspartate residue, C-carboxy terminal end, D- conserved aspartate residue phosphorylated during reaction cycle, K- conserved lysine residue involved in ATP binding, PL-phospholipids.**

The TMs are connected on the outside with 5 short loops called putative extracellular domains (exdoms) (Fig.3). The sequences of these exdoms do not have any significant homology with other proteins. Exdom1, connecting TM 1 and 2, is the largest and the most divergent among all PMCA isoforms. Together with exdom5, exdom1 contains cysteine in the middle indicating their possible role in tertiary structure. Exdoms 2, 4 and 5 are shorter with only minor differences among PMCA isoforms. Exdom 3 is a very short loop and is conserved among all PMCA isoforms and among different species, with this sequence also being present in *Drosophila* (Szewczyk et al. 2008). It is not known what functions, if any, exdoms play in the reaction cycle of PMCA. However, based on information obtained for SERCA it can be suggested that they may undergo tremendous conformational changes during PMCA reaction cycle (Toyoshima et al. 2002).

#### **1.4.3. PMCA isoforms**

In mammalian cells PMCA are encoded by four separate genes (*ATP2B1-4*) located in humans on different chromosomal loci 12q21-q23, 3p25-p26, Xq28 and 1q25-q32. However, alternative splicing gives many theoretically possible variants, out of which about 30 have been detected at cDNA levels (Brini & Carafoli 2009). PMCA contain two splice sites - one at the actuator domain (splice site A) and one on the C-terminal tail (splice site C) (see Fig.3). In all PMCA isoforms the splicing at site A involves the insertion (variant x) or exclusion (variant z) of a small 36-42 nt long exon. All PMCA1 isoforms are x variants and for PMCA3 and 4 both variants x and z were detected. PMCA2 alternative splicing is more complex, because it involves the

combination of insertion or deletion either of three exons (36, 42 or 60 nt): variant z (all excluded), variant w (all included), variant x (exon 42 nt included) and variant y detected only in rat (exon 39 nt or 60 nt included). The differential splicing at site A seems not to affect PMCA function, however, recent studies indicate its role in PMCA membrane targeting. In polarized cells such as auditory system stereocilia and mammary gland epithelium, PMCAw variant is exclusively targeted to apical membranes, regardless of the splicing pattern at site C (Chicka et al. 2003; Hill et al. 2006; Reinhardt et al. 2004).

The splicing at site C is more complex due to the occurrence of splice sites internal to exons. The exclusion of exons results in PMCAb splice variants. The insertion of the alternatively spliced large exon (splice variants a) changes the reading frame leading to the occurrence of stop codons resulting in protein truncation, so that PMCAa variants are shorter than PMCAb variants. The multiple internal donor sites within the spliced exons and the insertions of other small exons (PMCA2 and 3) lead to the creation of five different PMCA1 variants (a-e), three PMCA2 variants (a- c), six PMCA3 variants (a-f) and four PMCA4 variants (a-d). Interestingly, the PMCA3e variant is generated when a “read through” of the 154-nt exon occurs, adding 88 nt of the following intron and a poly(A) tail. The splicing at site C affects the C-terminal half of the CBD and the region downstream to it. Therefore, splicing would affect PMCA regulation by calmodulin, protein kinases and the PDZ domain containing proteins (see section 1.4.4. and 1.4.6).

#### **1.4.4. PMCA regulation**

The distinct feature of PMCA among other P-type ATPases is long C-terminal tail which contains various sites for PMCA regulation. In its unstimulated state PMCA has a low  $\text{Ca}^{2+}$  affinity ( $K_d \sim 10 \mu\text{M}$ ). However, there are various mechanisms, which increase PMCA affinity for  $\text{Ca}^{2+}$  to 0.2-0.5  $\mu\text{M}$  (Enyedi et al. 1987). In the following section PMCA regulation by calmodulin, protein kinases, acidic phospholipids and proteases will be described.

##### **1.4.4.1. Regulation by calmodulin**

Calmodulin regulates PMCA in a calcium specific manner by direct interaction with the CBD located on C-terminal tail of PMCA (see Fig. 3). In the absence of calmodulin, CBD acts as an autoinhibitory sequence by binding to two sites, one within the actuator domain and another within the catalytic domain, compromising access to the active site (Falchetto et al. 1991; Falchetto et al. 1992). Calcium activated calmodulin binding to CBD releases the autoinhibition and increases the  $\text{Ca}^{2+}$  affinity of the pump and the rate of ion transport (Carafoli et al. 1994; Monteith et al. 1995). Experiments with fluorescently labelled calmodulin revealed that at low calcium concentrations a population of PMCA-calmodulin complexes exists in which the autoinhibitory domain is not dissociated (Osborn et al. 2004). It is suggested that the existence of this complex provides a mechanism for the rapid response of the pump to the subsequent  $\text{Ca}^{2+}$  signaling events in the cell. Interestingly, calmodulin binds to PMCA through its C-terminal lobe, which differs from binding to other calmodulin dependent enzymes (Elshorst et al. 1999). The CBD sequence analysis showed that the first 18 N-terminal

amino acids are identical and the next 10 differ significantly between PMCA isoforms suggesting that these C-terminal amino acids control the rates of interaction with calmodulin. They also differ between splice variants due to the occurrence of splice site C within the CBD. The effect of alternative splicing on calmodulin binding has been extensively studied on PMCA4a and PMCA4b isoforms (Enyedi et al. 1994; Verma et al. 1996). The CBD of PMCA4a (49 amino acids) is much longer than that of PMCA4b (28 amino acids) and contains a region which is not involved in calmodulin binding. Moreover, the autoinhibitory region of PMCA4b is divided between the CBD and a downstream region, whereas in PMCA4a only the CBD contributes to autoinhibition. The C-terminal structure of isoforms may be the reason for observed higher affinity of PMCA4b for calmodulin and apparent higher affinity for  $\text{Ca}^{2+}$  and more effective PMCA autoinhibition. As compared to PMCA4b, the 4a isoform has higher basal activity at any given concentration of  $\text{Ca}^{2+}$  in the absence of calmodulin. The similar pattern of difference between splice variants a and b has been observed in PMCA2 isoforms (Elwess et al. 1997). Such a difference may have the consequence of more restricted tissue distribution of splice variants a, which appear to be prevalent in excitable cells. A higher basal activity and in consequence lower dependence on calmodulin may be important in that environment, where elevated  $[\text{Ca}^{2+}]_i$  levels and frequent  $\text{Ca}^{2+}$  fluctuations occur. The alternative splicing may also influence pH dependence of calmodulin binding (Enyedi et al. 1994). In the PMCA1 isoform, variants other than b contain a histidine rich region, which favours calmodulin binding at lower pH. This

feature may be the reason that PMCA1c and d are the most abundant in skeletal muscle, where acidic conditions may temporarily exist.

#### **1.4.4.2. Regulation by phosphorylation**

The downstream portion of the C-terminal tail of all PMCA following splice site C is very rich in serine and threonine residues (17-31%), but their distribution and absolute position vary greatly between isoforms and splice variants. The effect of phosphorylation by PKA, protein PKC, src kinase and focal adhesion kinase has been observed in various PMCA isoforms (Monteith et al. 1995; Penniston et al. 1998). Generally, phosphorylation may influence PMCA activity leading directly to the removal of inhibition or indirectly by interference with calmodulin binding.

Among all isoforms only PMCA1b-d contain the PKA consensus sequence KRNSS downstream to the CBD. In vitro studies showed that phosphorylation of PMCA1b at Ser 1178 leads to an increase in  $\text{Ca}^{2+}$  affinity and maximal velocity and that phosphorylation is inhibited by calmodulin (James et al. 1989). The stimulation of the  $\text{Ca}^{2+}$  pump by calmodulin and PKA is non-additive suggesting that phosphorylation increases activity by relieving autoinhibition. It should be noted that although most cells express PMCA1b, PKA stimulation is not observed in all of them indicating that other mechanisms are involved in this process. One of the reasons may include targeted PKA translocation. In parotid acinar cells, activated PKA translocated specifically into apical regions of the cell (Baggaley et al. 2007). As a result, only the apical portion of PMCA1 has been phosphorylated by PKA followed by increased  $\text{Ca}^{2+}$  clearance in the apical region.

PKC regulates PMCA activity in an isoform specific manner. In general, PKC stimulation increases  $\text{Ca}^{2+}$  extrusion by PMCA (Enyedi et al. 1996; Kuo et al. 1991; Werth et al. 1996). PKC has been shown to phosphorylate the conserved threonine within the CBD, however, the residues downstream from the CBD seem to be more readily phosphorylated. In PMCA4b, threonine phosphorylation within the CBD led to pump activation and attenuation of calmodulin stimulation, possibly due to relieving autoinhibition (Wang et al. 1991). In contrast, the phosphorylation of the serine residue within the inhibitory domain downstream to the CBD in PMCA4b led to only partial stimulation of the pump, while the stimulatory effect of calmodulin was retained (Enyedi et al. 1996). Although PMCA2a and 3a are also readily phosphorylated by PKC, the phosphorylation does not change basal pump activity (Enyedi et al. 1997). However, it interferes with calmodulin binding which may lead to reduced calcium efflux in cells expressing those isoforms. PMCA2b and 3b are poor substrates for PKC and PMCA4a phosphorylation does not affect basal activity and calmodulin stimulation (Enyedi et al. 1997).

Phosphorylation may also lead to PMCA deactivation. In thrombin-activated platelets, Tyr-1176 phosphorylation of PMCA4b, probably mediated by focal adhesion kinase, resulted in reduction of PMCA activity by approximately 40% (Dean et al. 1997; Wan et al. 2003). Moreover, PMCA activity in purified platelet plasma membranes was inhibited by 75% following tyrosine phosphorylation by src kinase (pp60src) (Dean et al. 1997).

#### **1.4.4.3. Regulation by acidic phospholipids**

Acidic phospholipids, in particular phosphatidylserine, phosphatidylinositol, phosphatic acid and cardiolipin, are very potent PMCA activators (Carafoli et al. 1982; Carafoli 1991; Niggli et al. 1981). Of these, phosphatidylinositol bisphosphate is one of the most potent (Carafoli et al. 1982; Choquette et al. 1984). Stimulation of phospholipase C, by receptors linked to G-proteins, leads to the breakdown of phosphatidylinositol bisphosphate into IP<sub>3</sub> and diacylglycerol, which have no effect on the activity of the pump (Carafoli 1991). The decreased levels of phosphatidylinositol bisphosphate may reduce PMCA activity and therefore enhance the rise in cytosolic calcium levels. Phospholipid activation makes PMCA insensitive to calmodulin activation, but PMCA activation by calmodulin may be enhanced upon phospholipid binding. Phospholipids stimulate the pump by increasing the Ca<sup>2+</sup> affinity and the rate of transport (Enyedi et al. 1987; Niggli et al. 1981). They are more effective activators as compared to calmodulin as they do not require Ca<sup>2+</sup> for their effect (Niggli et al. 1981). Reconstitution of PMCA in liposomes containing different proportions of acidic phospholipids revealed that the minimal content of acidic phospholipids in the environment of the PMCA necessary for full stimulation is about 40% (Niggli et al. 1981). There are two separate phospholipid binding regions in the pump: one corresponding to the carboxyl-terminal calmodulin binding domain and the second situated in the immediately preceding third membrane-spanning domain (Fig. 3). The deletion of the second one results in a fully active PMCA with high affinity for Ca<sup>2+</sup>, a characteristic of the pump activated by acidic phospholipids (Pinto et al. 2002).

#### 1.4.4.4 Regulation by proteases

PMCA is a substrate of intracellular proteases such as calpain and caspases (1 and 3) (Paszty et al. 2002; Salamino et al. 1994). Calpain is  $\text{Ca}^{2+}$ -dependent protease. In its first step it removes the CBD from PMCA which results in the formation of a 124 kDa constitutively active fragment, while further calpain-dependent cleavage causes the formation of 100 kDa and smaller fragments (James et al. 1989; Salamino et al. 1994). Different PMCA isoforms differ in their sensitivity to calpain cleavage. *In vitro* studies on purified PMCA1, 2 and 4 isoforms revealed that calpain slowly degrades PMCA2 and 4 to a large, constitutively active fragment, while PMCA1 is rapidly and completely degraded (Guerini et al. 2003). Calpain has been shown to play a role in human erythrocyte function and platelet activation *in vivo* (Salamino et al. 1994). However, in both cases calpain degraded PMCA completely, leading to increased  $[\text{Ca}^{2+}]_i$  levels, which was prevented by calpain inhibitors.

PMCA is also a substrate for caspase-3 cleavage indicating the role of PMCA in apoptosis. Caspase-3 cleaved PMCA4b at Asp<sup>1080</sup> to a 120 kDa constitutively active fragment during an early phase of apoptosis induced by either receptor mediated or mitochondrial pathways (Paszty et al. 2002; Paszty et al. 2007). It suggests that the cleavage may have a role in protecting apoptotic cells from excessive  $\text{Ca}^{2+}$  overload and in consequence secondary necrosis. In contrast, other studies suggested that cleavage by caspase-3 inhibited PMCA4 activity and promoted internalization of PMCA4 stably expressed in Chinese hamster ovary cells. It seems that other cell-specific processes may be involved in PMCA regulation by caspase-3 (Schwab et al. 2002).

#### **1.4.5. PMCA distribution**

All tissues and cell types express at least one PMCA isoform. Individual isoforms show developmental, cell and subcellular patterns of expression; suggesting that they participate in cell-specific and spatially segregated intracellular  $\text{Ca}^{2+}$  regulation. In situ hybridization experiments on mouse embryos revealed that PMCA1 is the first isoform expressed from the earliest time point analyzed (9.5 days post coitum) (Zacharias et al. 1999). All other PMCA isoforms were detected around 12.5 day onwards. PMCA2 was confined to the developing nervous system and PMCA4 was widely expressed, but at the lowest levels compared to other isoforms. This is in contrast to expression levels in adults, where it is found in many tissues at high levels. Interestingly, PMCA3 which in adults has a restricted expression pattern, was expressed widely during early development and starting around 16.5 days it showed more restricted expression being high in nervous system, limb skeletal muscle and lung.

Various tissues express different PMCA isoforms. In general, PMCA1 and PMCA4 are the most ubiquitously expressed isoforms, while PMCA2 and 3 are expressed in a much more restricted manner (Stauffer et al. 1995; Strehler et al. 2001). The brain expresses the greatest abundance and diversity of PMCA isoforms and splice variants (Burette et al. 2003; Filoteo et al. 1997). The hippocampus expresses PMCA genes 1, 3, and 4, and the cerebellum has higher levels of PMCA2 and 3. Within the brain PMCA2 is mostly expressed in specialized cell types such as cerebellar Purkinje cells and cochlear hair cells, but significant levels of this isoform can also be found in uterus, liver, kidney and in lactating mammary glands (Faddy et al. 2008; Silverstein et al. 2006;

Stauffer et al. 1995). PMCA3 expression is even more restricted with high levels in choroid plexus (Eakin et al. 1995). Various organs show a very restricted pattern of PMCA isoform expression. In retinal neurons PMCA2 is localized to rod bipolar cells, horizontal cells, amacrine cells, and ganglion cells, and PMCA3 is predominantly expressed in horizontal cells and spiking neurons, including both amacrine and ganglion cells (Krizaj et al. 2002). PMCA4 is selectively expressed in both synaptic layers. Certain unique splice variants of PMCA are expressed in specific cell types like PMCA2w/a, which is found only in the hair cells of the inner ear (Hill et al. 2006). Cell-type specific expression of PMCA isoforms has also been observed in stratified corneal epithelium, where there are differences in the PMCA isoforms expressed in different cells layers (Marian et al. 2005; Talarico, Jr. et al. 2005).

Within the cell PMCA may not be distributed uniformly in plasma membrane. The spatially distinct demands of  $\text{Ca}^{2+}$  influx and efflux observed especially in polarized cells, like epithelial and neuronal cells may determine the differential distribution of PMCA isoforms in the plasma membrane. This type of organization is important for the role which the cell plays in the organism and its role as a signaling molecule. Duodenal mucosa cells express PMCA1b localized in basolateral membrane (Howard et al. 1993). The localization allows the calcium absorbed from intestine by mucosa to be pumped out of the cell by PMCA1b into the interstitial space where it enters the blood (Hoenderop et al. 2005). In many cell types, PMCA has been shown to localize in domains rich in cholesterol and sphingolipids named lipid rafts or in specialized flask-shaped invaginated lipid rafts containing caveolin called caveolae (Cho et al. 2005; Darby et al. 2000;

Fujimoto 1993; Hammes et al. 1998; Sepulveda et al. 2006). These specialized domains are rich in receptors, channels, signal transducers, effectors and structural proteins which allow for signal integration and local  $\text{Ca}^{2+}$  signaling (Razani et al. 2002; Shaul et al. 1998). Neuronal NO synthase (nNOS) was also found to localize in caveolae (Daniel et al. 2006; Venema et al. 1997). In cerebellum, synaptic plasma membranes express all PMCA isoforms, but only PMCA4 was exclusively localized in lipid rafts (Sepulveda et al. 2006). PMCA4b has also been shown to localize in caveolae where it can interact with nNOS and regulate its activity (Oceandy et al. 2007). Thus, the PMCA isoforms exhibit tissue, cell and subcellular-specific expression that may reflect differences in their  $[\text{Ca}^{2+}]_i$  handling requirements, indicating that  $\text{Ca}^{2+}$  extrusion is highly regulated and functionally integrated with  $\text{Ca}^{2+}$ .

#### **1.4.6. Molecular partners for PMCA**

PMCA may interact with numerous proteins. The interaction may result in the recruitment and maintenance of particular PMCA splice variants in specific membrane domains. It may also be involved in the modulation of signal transduction pathways.

Most partners of PMCA have been found to interact with the PDZ binding domain, which is present in the C-terminal end of PMCA isoforms 2b and 4b. Both isoforms interact with the PDZ containing membrane-associated guanylate kinase family of kinases (SAP), which are associated with the cortical actin cytoskeleton and are thought to act as scaffolding or clustering proteins for various membrane receptors and transporters (DeMarco et al. 2001). Confocal immunofluorescence microscopy revealed the exclusive presence and colocalization of PMCA4b and SAP97 in the basolateral

membrane of polarized Madin-Darby canine kidney epithelial cells. In hippocampal neurons, PMCA2b was abundant throughout the somatodendritic compartment where it colocalized with SAP90. PMCA2b was shown to interact with the PDZ protein Na<sup>+</sup>/H<sup>+</sup> exchanger regulatory factor 2 (DeMarco et al. 2002). In polarized Madin-Darby canine kidney cells the interaction enhanced the apical concentration of PMCA2w/b by anchoring the pump to the apical membrane cytoskeleton. The PDZ-mediated PMCA4b-nNOS interaction in an *in vitro* expressing system using human embryonic kidney cells (HEK293), as well as in a neuronal cell line, cardiomyocytes and SMC, was shown to down-regulate NO production (Gros et al. 2003; Mohamed et al. 2009; Oceandy et al. 2007). The observed decrease of nNOS activity, which is Ca<sup>2+</sup>-calmodulin dependent, was caused by Ca<sup>2+</sup> depletion in the immediate proximity of the enzyme. The Ca<sup>2+</sup> depletion is also the cause of the downregulation of calcium/calmodulin-dependent serine protein kinase by PDZ mediated interaction with PMCA4b. This kinase is a co-activator of the transcription of T-element containing promoters and overexpression of PMCA4b was shown to down-regulate the T-element-dependent reporter activity (Schuh et al. 2003). It is also proposed that during platelet activation PMCA4b interacts with F-actin via PDZ-containing protein CLP36 and translocates to filopodia (Bozulic et al. 2007).

Other than the PDZ- binding domain, the main intracellular loop of PMCA (between TM4 and 5) and N-terminus may also interact with partner proteins. Tumour suppressor Ras-Associated Factor 1 (Ras-1), alpha-1 syntrophin and calcineurin were shown to bind to the main intracellular loop. Co-expression of tumour suppressor Ras-1 and PMCA4b inhibited the epidermal growth factor-dependent activation of Ras,

suggesting a role for PMCA4b in the modulation of Ras-mediated signaling (Armesilla et al. 2004). The overexpression of alpha-1 syntrophin increased the inhibitory effect of the PMCA on NOS-1 activity. This complex has been found in cardiac myocytes (Williams et al. 2006). Both PMCA4 and 2 interact with the catalytic subunit of calcineurin A, which displaces a nuclear factor of activated T-cell binding to calcineurin, and subsequently inhibits signal transmission (Buch et al. 2005). The N-terminal part of PMCA1, 3 and 4 interacts with 14-3-3 $\epsilon$  protein, which modulates cell signaling, intracellular trafficking, transcription and apoptosis (Di Leva et al. 2008; Rimessi et al. 2005).

#### **1.4.7. PMCA and disease processes**

Changes in the levels of expression or activity of various PMCA isoforms have been associated with several pathologies including heart disease, hypertension, carcinogenesis, cataract formation, diabetes and neurodegenerative diseases (Brini et al. 2009; Tempel et al. 2007).

Gene knock-out studies have shown an essential housekeeping role for PMCA1, since PMCA1 null mice are embryolethal (Prasad et al. 2004). The presence of a null mutation in heterozygous PMCA1 mice did not cause major defects, however, increased apoptosis of vascular smooth muscle was observed (Okunade et al. 2004). Some cancer types are associated with altered expression of the PMCA1 gene. Studies on oral squamous cell carcinoma have suggested an epigenetic inactivation of PMCA1 gene as a frequent and early event during oral carcinogenesis (Saito et al. 2006). In contrast, increased PMCA1 expression has also been observed in breast cancer (Lee et al. 2002).

In vascular smooth muscle cells, the regulation of PMCA1 expression by the transcription factor c-Myb may control cell proliferation. In neuronal cells PMCA1 is suggested to be involved in neurite extension. The blocking of PMCA1 production in the neuronal cell line (PC6) with antisense RNA impaired the cell's ability to extend normal neurites in response to neuronal growth factor without interference with its signaling (Brandt et al. 1996). An increase in the level of PMCA1 expression is associated with the loss of  $Ca^{2+}$  homeostasis observed in human cataract lenses (Marian et al. 2008). Studies using a cultured human lens epithelial cell line have shown that oxidative stress, a major contributor to cataract development, also induces changes to the level of expression of PMCA1 (Marian et al. 2008).

Changes in the levels of PMCA2 have been reported in several diseases including hearing defects, decreased milk production, multiple sclerosis, spinal cord injury, cancer, cataract and Huntington disease. Both natural and generated mutants of PMCA2 are known (Prasad et al. 2004). PMCA2 null mice exhibit deafness and ataxia, whereas the heterozygous mice are predisposed to age or noise related hearing loss. Two human families have been described in which mutations in the PMCA2 gene are linked to the insurgence of deafness. In one, a homozygous mutation in the cadherin gene caused hearing loss in all five siblings, however three siblings with a mutation in the PMCA2 gene (heterozygous) showed more profound hearing loss (Schultz et al. 2005). In the other family, profound deafness was present only when a mutation in the cadherin 23 gene was present together with a mutation in the PMCA2 gene (Ficarella et al. 2007). Besides being a regulator of  $Ca^{2+}$  homeostasis, PMCA2 has been shown to be essential

for  $\text{Ca}^{2+}$  secretion in milk by mammary epithelial cells (VanHouten et al. 2007). An increase in levels of PMCA2 is seen during lactation, which decreases again upon weaning. In PMCA2 knock-out mice the level of  $\text{Ca}^{2+}$  in the milk was found to be strongly reduced (Reinhardt et al. 2004). Although, an up-regulation of SERCA2b and the Golgi apparatus  $\text{Ca}^{2+}$  pump occurs under these conditions it was inadequate to compensate for the loss of PMCA2 (Reinhardt et al. 2000). After lactation PMCA2 levels are down-regulated. The loss of PMCA2 expression leads to  $[\text{Ca}^{2+}]_i$  elevation and sensitizes epithelial cells to apoptosis (VanHouten et al. 2007). An increase in levels of PMCA2 was observed in breast cancer cell lines where it can protect cells from apoptosis (Lee et al. 2005; VanHouten et al. 2010). It is suggested that high PMCA2 expression in breast cancers is associated with poor outcome. PMCA2 expression is also altered in cataract lenses as compared to age-matched clear lenses (Marian et al. 2008). A transcriptional down-regulation of PMCA2 has recently been found in several mouse models of Huntington disease and in the brains of patients suffering from this disease, where it may contribute to the chronic cellular  $\text{Ca}^{2+}$  overload (Kuhn et al. 2007). In animal models of multiple sclerosis the decrease in PMCA2 transcript and protein levels and the correlation between expression and disease course was observed (Nicot et al. 2005). In spinal cord neurons, decreased levels of PMCA2 not only led to increased calcium overload in spinal cord neurons, but also to decreased collapsin response mediator protein 1 levels, which was followed by cell death (Kurnellas et al. 2010).

Lack of availability of PMCA3 knockout animals has limited studies on PMCA3 physiology and pathology. PMCA3 is expressed at high levels in the choroid plexus and

may thus play a role in regulating ionic composition of the cerebrospinal fluid which is essential in brain function and development (Eakin et al. 1995). PMCA3 mRNA levels in the placenta correlate with neonatal bone mineral content, bone area, placental weight and birth weight suggesting that it may be crucial in calcium absorption by fetal bones (Martin et al. 2007).

PMCA4 is ubiquitously expressed and could thus represent a housekeeping gene together with PMCA1. However in contrast to PMCA1, PMCA4 null mouse embryos survive and appear normal. The major phenotypic change observed in null mice is male infertility due to loss of sperm hypermotility (Withers et al. 2006). It is not surprising, since PMCA4 is the predominant isoform in testis (Wilhelm et al. 2008). In addition to defects in sperm motility, a loss of PMCA4 impaired phasic contractions and caused apoptosis in the portal vein smooth muscle studied *in vitro* in some mice strains (Okunade et al. 2004). Since PMCA4 also plays a role as a modulator of  $Ca^{2+}$  signaling pathways, the alterations in its expression levels may affect other protein functions. PMCA4b interacts with nNOS via the PDZ domain and downregulates its activity by decreasing  $[Ca^{2+}]_i$  and preventing  $Ca^{2+}$ -calmodulin dependent nNOS activation (Gros et al. 2003; Mohamed et al. 2009; Oeandy et al. 2007). Overexpression of PMCA4b in mice leads to an increase in arterial reactivity and increased blood pressure (Gros et al. 2003). In cardiomyocytes, the overexpression attenuated the  $\beta$ -adrenergic inotropic response (Mohamed et al. 2009). PMCA4b may also interact with calcineurin and inhibit calcineurin/nuclear factor of activated T cells pathway which is involved in hypertrophic growth induction in cardiac myocytes (Wu et al. 2009). In human failing hearts, PMCA4

protein expression decreased by 60% as compared to the normal hearts. In hypertrophic mouse hearts following transverse aortic constriction PMCA4 was also downregulated by 25%. Gene targeting of PMCA4 increased the susceptibility of hearts to hypertrophy, whereas its cardiac-specific inducible expression rendered it anti-hypertrophic in response to pressure overload. Downregulation of PMCA4 leads to impaired platelet aggregation (Jones et al. 2010). Type one and two diabetes mellitus is associated with an increase in the level of PMCA4 expression in platelets and megacaryocytes which leads to abnormalities in platelet maturation and is suggested to play a role in the onset and/or progression of macrovascular complications (Chaabane et al. 2007). PMCA4 expression levels may change during cancerogenesis. Differentiation of HT-29 colon cancer cells was associated with an upregulation of PMCA4, whereas breast cancer cell lines show decreased PMCA4 levels.

### **1.5. Approaches used today to study the role of PMCA**

The major approaches used to study the role of PMCA are genetic techniques such as gene knock-out or altered gene overexpression and inhibition of PMCA by pharmacological agents. However, all the methods have their drawbacks and in some cases the results obtained by different methods often give inconclusive results.

#### **1.5.1. Genetic techniques**

Animal models with ablated PMCA genes were used to delineate the physiological roles of PMCA1, 2 and 4 (Liu et al. 2007; Prasad et al. 2004; Prasad et al. 2007; Shull 2000). The PMCA3 null mice have not been yet developed. The major

drawback in the method is that mice seem to adapt to PMCA loss and sometimes the results are strain dependent. PMCA1 is essential for embryogenesis since PMCA1 knock-out is embryolethal. Therefore, the model cannot be used for studying the role of PMCA1 in adult mice physiology. Although PMCA4 is ubiquitously expressed, PMCA4 ablation affects mostly bladder function (bladders in the PMCA4 null mice are smaller than in the wild type, as is the response of the bladder smooth muscle to carbachol) and sperm motility. Certain phenotypes, such as impaired portal vein smooth muscle contractions, were observed in PMCA4-ablated mice in a strain dependent manner (Okunade et al. 2004). PMCA2 has unique properties (fast kinetics) and is found ubiquitously in the central nervous system and heart, however PMCA2 null mice show only balance and hearing defects and decreased milk production.

Intracellular calcium concentration has to be tightly regulated which is reflected in the plasticity and the adaptability of various  $\text{Ca}^{2+}$  transporters and sensors in the cell. Normally expressed at low levels in most cells, PMCA is often difficult to overexpress at high levels and also it may not be properly targeted to plasma membrane (Adamo et al. 1992; Guerini et al. 2003). The overexpression of PMCA4b altered the gene expression of endogenous mouse PMCA1, PMCA4, SERCA2 and  $\text{IP}_3\text{R1}$  indicating that adaptation processes take place, when manipulating PMCA levels (Guerini et al. 2003; Liu et al. 1996). Most of the cells express more than one PMCA isoform. This is one of the possible reasons that the effect of gene ablation is mostly observed in cells which express one PMCA isoform or when the proper cell function depends on high levels of PMCA, which cannot be compensated by other systems. Because PMCA2w/a is the only PMCA

isoform present in outer hair cells and vestibular hair cells in the ear, the biochemical properties of this pump must account fully for the physiological features of transmembrane  $\text{Ca}^{2+}$  pumping in the bundles and therefore the loss of this isoform leads to hearing defects (Kozel et al. 1998). The expression of PMCA2 increases 100-fold during lactation and PMCA4 is the predominant isoform in testis therefore the gene loss cannot be fully compensated by other PMCA genes and it leads to decreased milk production and loss of sperm motility, respectively (Faddy et al. 2008; Wilhelm et al. 2008).

### **1.5.2. Inhibitors**

Selective PMCA inhibitors seem to be the best tool for studying the role of PMCA in physiological and pathological conditions. There are known specific inhibitors for SERCA (thapsigargin and cyclopiazonic acid) and NCX (XIP, KB-R7943 and SEA0400). PMCA and NCX can expel  $\text{Ca}^{2+}$  from the cell and without inhibitors specific for PMCA it is difficult to delineate the role of these proteins in cell function. Eosin and vanadate have been used extensively in studies on PMCA (Boyer et al. 2001; Bredeston et al. 2004; Gunaratne et al. 2006; Kennedy et al. 1996; Krstic et al. 2009; Tiffert et al. 2001). Eosin modulates PMCA activity by interfering with its ATP binding, however, it also inhibits the  $\text{Na}^+$  pump and SERCA pump (Skou et al. 1981). Vanadate is a phosphate analog that inhibits various ATPases in its +5 oxidation state. It has been used as a PMCA inhibitor even though it has a higher affinity for the  $\text{Na}^+$  pump than for PMCA. Vanadate inhibits  $\text{Na}^+$ - $\text{K}^+$ -ATPase with an affinity 2500x higher than that for PMCA (Cantley, Jr. et al. 1977). It also inhibits the SERCA pump. The inhibition of  $\text{Na}^+$ - $\text{K}^+$ -

ATPase results in changes to  $\text{Na}^+$  and  $\text{K}^+$  gradients. Any change in those gradients may influence NCX activity. The reduction of vanadate to + 4 valency state may affect its inhibitory potential and/or alter its specificity, adding another dimension of complexity in interpreting the results. Therefore, neither eosin nor vanadate would delineate the role of PMCA from that of NCX.

### **1.6. Allostereism, as applied to P-type ATPase inhibitors**

Allosteric sites have been exploited as novel pharmacological targets. Allosteric modulation results from the binding of molecules at a different site from that of the active site. There are a number of advantages in using allosteric modulators as preferred therapeutic agents over classic orthosteric ligands. In contrast to allosteric sites, orthosteric sites could not have been changed greatly during evolution in order to accommodate the function to be performed. Therefore allosteric sites are more diverse and have greater specificity than the active sites of enzymes and receptors. P-type ATPases such as PMCA, SERCA and  $\text{Na}^+$ -pump shuttle between different conformational states during reaction cycle. Several allosteric inhibitors of SERCA and  $\text{Na}^+$ -pump have been discovered, which have proven useful as research and therapeutic tools. Thapsigargin has a high affinity (subnanomolar dissociation constant) for and is a very specific SERCA inhibitor. It binds tightly to the E2 form of the pump in the cavity surrounded by the TM3, TM5 and TM7 and prevents it from converting into its E1 form, which is required for catalytic function (Toyoshima et al. 2002). The use of thapsigargin, has led to an exploration of the roles of SERCA in signal transduction and calcium homeostasis, as well as in the analysis of its structure during reaction cycle. Ouabain, a

Na<sup>+</sup> pump selective inhibitor, binds to the first extracellular loop and TM4. It exerts its inhibitory activity by interacting with the M5-M6 loop that is involved in cation binding by restricting its flexibility (Qiu et al. 2005). Digoxin, another Na<sup>+</sup> pump selective inhibitor, was also shown to inhibit by binding to exodomains (Keenan et al. 2005). Other than for research purposes, digoxin is used therapeutically for atrial fibrillation and congestive heart failure (Falk et al. 1991; Reddy et al. 1997). Since PMCA specific inhibitors are required to understand the role of PMCA in Ca<sup>2+</sup> homeostasis and cell signaling and available active site inhibitors (vanadate, eosin) are highly nonspecific, the development of allosteric site based inhibitors is of great importance.

### **1.7. Phage display - a tool for the development of allosteric inhibitors**

Phage display is a technology, where exogenous (poly)peptides are expressed on the surface of a bacteriophage particle. The technology is extensively used in various applications such as screening for modulators of both the active and allosteric sites of the enzyme, receptor agonists and antagonists, analysis of protein–protein interactions, epitope mapping, vaccine design or generating target specific antibodies (Benhar 2001; Bottger et al. 2009; Bratkovic 2009; Carmen et al. 2002; Pande et al. 2010). The DNA fragment encoding a foreign (poly)peptide is inserted into the genome of the filamentous phage and the peptide is displayed as a fusion to one of the coat proteins on the surface of phage. The use of filamentous bacteriophage as a cloning vector or for the display of the foreign peptides has several advantages (Pande et al. 2010). The filamentous phage genome can tolerate insertions in the non essential regions without disrupting phage packaging and infectivity; however, the size of the insert is often restricted. It is stable

under a broad range of selection conditions such as pH and temperature. The infection with filamentous phages is not lethal so it can accumulate in high concentrations in the infected bacterial cells. A decrease in the rate of cell growth is seen in the infected cells causing turbid plaques in agarose-embedded bacteria allowing for easy isolation of distinct phage clones.

The most common bacteriophage used in phage display is the M13 filamentous phage (Kehoe et al. 2005; Smith et al. 1997). It is composed of single stranded circular DNA encapsulated in approximately 2700 copies of the major coat protein pXIII. One end of the phage particle is capped by the two minor proteins pIII and pVI, 5 copies each, while the other end displays 3-5 copies of pVII and pIX. The minor coat protein pIII is involved in infection process. It attaches to the receptor at the tip of the F pilus of the host *Escherichia coli*. In phage display, the foreign peptides can be displayed at the N-terminus of coat proteins pIII, pVII, pVIII, pIX and C-terminus of pVI.

Phage display libraries expressing random peptides have been used extensively for the invention of enzyme inhibitors (Casares et al. 2010; Jani et al. 2005; Kadam et al. 2010; Kristan et al. 2009; Szewczyk et al. 2008). It has its application for allosteric enzyme inhibitors, since any part of the enzyme can be used as a target. Usually the random oligonucleotides are inserted between the coat protein pIII and the coding sequence for the signal peptide. The random peptides varying in size from 6 to 42 amino acids have been successfully displayed as a fusion to N-terminus of the pIII (Burrill et al. 1995; McConnell et al. 1996). The peptides can be displayed in linear, as well as cyclised form, where the randomized sequence is flanked by a pair of cysteine residues. Under

non-reducing conditions the cysteines will spontaneously form a disulfide cross-link, resulting in phage display of cyclized peptides. Such structurally constrained phage display random peptide libraries have been screened successfully for targets that did not bind a ligand from the linear random peptide libraries and are also advantageous in yielding high affinity ligands (Devlin et al. 1990; Heinis et al. 2009; Hoess et al. 1994; Luzzago et al. 1993; McLafferty et al. 1993).

A popular strategy of phage display is affinity selection or phage panning with the target immobilized on a plate or bead surface. After blocking of unspecific sites with unrelated proteins or nonionic detergents, the phage display random peptide library is added to the target in large amounts to maximize diversity. Next the unbound phage are removed and the selected phage are eluted either with a solution containing a free target or a competing ligand (specific elution) or using extremes such as low pH, denaturants, high ionic strength, limited proteolysis or sonication. The selected phage can be amplified and selection can be repeated depending on demand. The basic method can be adapted in many various ways to increase the chances of selection of high affinity ligands e.g. by increasing the strength of the washes or by introducing negative screening to eliminate the phage which do not bind to the target. An example of the modifications is described in section 1.8.3.1, which details the invention of the PMCA4 selective inhibitor, caloxin 1c2.

### **1.8. Caloxins –concepts and classification**

Caloxins are extracellular peptide inhibitors, which bind exdoms of PMCA and inhibit their activity. They are obtained by a screening method using phage display. The exdoms of PMCA were chosen as a target since they do not share any significant homology with the other members of P-type ATPases and are therefore unique targets to obtain PMCA specific inhibitors. Moreover, the alternative splicing does not affect the exdom sequences, therefore the obtained caloxin would be expected to inhibit all PMCA splicing variants. The rationale for the development of selective PMCA inhibitors lies in their ability to bind on the extracellular surface to exdoms to alter the conformational changes occurring during the PMCA reaction cycle and thereby modulate the pump activity. The model was predicted based on structural studies of SERCA inhibition by thapsigargin, which binds to helical loops located in the lumen of the SER inhibiting their movement (Toyoshima et al. 2002). In PMCA, such helices would correspond to exdoms. Moreover ouabain, a selective Na<sup>+</sup> pump inhibitor, was also shown to inhibit the pump by binding to one of its extracellular loops (Qiu et al. 2005).

The name of a caloxin contains information about the target and screening method. The first number denotes the number of the exdom used as a screening target. The letter indicates the screening method: a - screening with synthetic peptide as a target, b – screening with synthetic peptide as a target followed by affinity chromatography with the native protein, c- screening by affinity chromatography with native protein using phage library displaying mutated peptide obtained with method b. The second number denotes a serial number obtained within the same category.

**Table 1. Caloxins**

Caloxin	Sequence	Target	Ki ( $\mu\text{M}$ ) *
2a1	VSNSNWPSFPSSGGG-amide	PMCA1 exdom2	400 $\pm$ 100
1a1	ACPWWSPHACGGG	PMCA1 exdom1Y	86 $\pm$ 12
3a1	SVWSATFLSSSPGGGSAK	PMCA exdom3	190 $\pm$ 20
1b1	TAWSEVLHLLSRGGG-amide	PMCA4 exdom1X	46 $\pm$ 5 (PMCA4) 105 $\pm$ 11 (PMCA1)
1b2	HGWINYQSLYAWGGGSK- amide	PMCA4 exdom1Y	31 $\pm$ 2 (PMCA4) 100 $\pm$ 8 (PMCA1)
1c2	TAWSEVLDLLRRGGGSK- amide	PMCA4 exdom1X	2.3 $\pm$ 0.3 (PMCA4) 21 $\pm$ 6 (PMCA1) 40 $\pm$ 10 (PMCA2) 67 $\pm$ 8 (PMCA3)

\*Ki – inhibition constant

### 1.8.1. Series A caloxins

The first PMCA selective inhibitor, caloxin 2a1 (Table 1) was obtained by screening a phage library displaying 12-amino acid random peptides for binding to the synthetic peptide corresponding to the exdom 2 sequence of PMCA1, conjugated to a carrier protein, keyhole limpet hemocyanin (KLH) (Chaudhary et al. 2001). It produced a 50% inhibition of  $\text{Ca}^{2+}$ - $\text{Mg}^{2+}$ -ATPase activity of PMCA in human erythrocyte ghosts at a concentration of  $0.4 \pm 0.1$  mM. Consistent with being an allosteric inhibitor, caloxin 2a1 inhibited the PMCA non-competitively with respect to substrates:  $\text{Ca}^{2+}$ , ATP and calmodulin and it did not inhibit any other tested ATPases. It also inhibited the formation of a  $\text{Ca}^{2+}$ -dependent acylphosphate in a partial reaction of PMCA catalytic cycle. A similar screening protocol with synthetic exdom1 and 3 resulted in affinity selection of caloxins 1a1 and 3a1, respectively (Table 1) (Pande et al. 2005; Pande et al. 2005).

### **1.8.2. Series B caloxins**

Series B caloxins, caloxins 1b1 and 1b2 (see Table 1), were obtained by two-step screening using synthetic PMCA4 exdom1X (N-terminal half of exdom1) or exdom1Y (C terminal half of exdom1), respectively, which was followed by affinity chromatography with PMCA protein purified from erythrocyte ghosts as a target (Pande et al. 2006), Jyoti Pande PhD. thesis). Both caloxins 1b1 and 1b2 had a 10-fold higher affinity than the prototype caloxin 2a1 and showed slight PMCA4 isoform preference. Caloxin 1b1 inhibited the  $\text{Ca}^{2+}$ - $\text{Mg}^{2+}$ -ATPase activity of PMCA in leaky erythrocyte ghosts that express mainly PMCA4 isoform with a inhibition constant ( $K_i$ ) value of  $46 \pm 5 \mu\text{M}$ . It was selective for PMCA, since it did not inhibit SERCA,  $\text{Na}^+$ -pump or  $\text{Mg}^{2+}$ -ATPase. Caloxin 1b1 was slightly selective for PMCA4 since it inhibited the other PMCA isoforms with lower affinity (Table 1). It did not inhibit any other ATPases tested. Caloxin 1b2 also showed slight selectivity toward PMCA4 (Table 1) (Jyoti Pande PhD. Thesis).

### **1.8.3. PMCA isoform selective caloxins**

The existence of more than one PMCA isoform in most cell types emphasizes the need for isoform selective caloxins to study the role of PMCA in physiology. Moreover, several disorders are linked with changes of specific PMCA isoform activity (see section 1.4.7). Therefore, isoform-selective caloxins may help to understand the role of PMCA in various pathologies and may aid in treatment development. However, there are several issues which make this task a challenge.

The first challenge in the invention of isoform-selective caloxins is the identification of the allosteric target, which should differ among PMCA isoforms and to which binding should produce the inhibitory effect. Out of all 5 exdoms, exdom1 is the most divergent among PMCA isoforms (Fig. 3). However, exdom1 is long and it contains a cysteine residue in the middle. It is not known if this cysteine takes part in disulfide bond formation that could alter the exdom conformation. Therefore, exdom1 has been arbitrarily divided into exdom1X (N-terminus part) and 1Y (C-terminus part) around the cysteine. Each half of exdom1 is used as a target to obtain isoform-selective caloxins. This option also opens the possibility to develop bidentate caloxins from caloxins selected for different halves of exdom1 to increase inhibitor affinity and selectivity.

The second challenge is to choose appropriate methods of screening to maximally increase the chances of obtaining isoform-selective caloxins. Series “a” caloxins were obtained by screening a phage library displaying random peptides (12 amino acids) for binding to synthetic exdoms (Pande et al. 2005; Pande et al. 2005). However, the series “a” caloxins have very low affinity for PMCA possibly due to differences between the conformation of the synthetic exdom and the exdom in native protein. The best solution would be to use the native protein as the screening target, however, the exdom specificity would then be lost. Therefore, a two step procedure was introduced in which a random peptide phage display library was first screened for binding to the synthetic peptide and then the selected phage pool was used in affinity chromatography with native PMCA. The new strategy improved the affinity of caloxins by tenfold (Pande et al. 2006). The

future improvements of series B caloxins by mutagenesis yielded the development of the first PMCA4 isoform selective caloxin1c2 (Pande et al. 2008).

#### **8.1.3.1. The invention of first PMCA isoform selective allosteric inhibitor -caloxin 1c2**

Caloxin 1c2 was obtained as a mutant of the previously described caloxin 1b1 (see section 1.8.2) (Pande et al. 2008). It was hypothesized that altering one, two, or three residues in caloxin 1b1 would maintain its ability to inhibit PMCA, but it may improve its affinity and isoform selectivity. For this purpose, a phage display library of caloxin 1b1-like peptides was created and screened by PMCA4-affinity chromatography on a calmodulin-agarose column, yielding caloxin 1c2. Several improvements were also introduced into the screening process including negative screening to eliminate phage bound to calmodulin-agarose and a competition experiment to overcome a bias in the library construction and amplification rate of individual clones. To eliminate a bias, an equal amount of each clone obtained after three rounds of affinity chromatography were made to compete against each other for binding to PMCA4. Caloxin 1c2 differed from the parental caloxin 1b1 in two amino acid residues (Table 1). The mutagenesis resulted in the improvement of inhibitor affinity and selectivity for PMCA4. Caloxin 1c2 inhibited erythrocyte ghost  $\text{Ca}^{2+}$ - $\text{Mg}^{2+}$ -ATPase ( $K_i = 2.3 \mu\text{M}$ ) with a 20-fold higher affinity than that of caloxin1b1. It also inhibited PMCA1 (21  $\mu\text{M}$ ), 2 (40  $\mu\text{M}$ ), and 3 (67  $\mu\text{M}$ ), but with much lower affinities than that for PMCA4. Thus, caloxin 1c2 had a tenfold or greater selectivity for PMCA4 over the other isoforms and it can be considered the first PMCA4 selective allosteric inhibitor. The analysis of the mutants of caloxin 1b1

used in the competition experiment showed that the residue W was crucial. Substitution of W with benzoylphenylalanine decreased the affinity while substitution of K with the same residue had very little effect. Based on mutagenesis and the modification studies, the moiety WSEV(L/V) seems to be key to this inhibition, however the exact binding point still has to be verified.

#### **1.8.4. Applications of caloxins**

Three of the caloxins, caloxins 2a1, 1b1 and 1c2 have proved to be useful tools in understanding PMCA action in various tissues.

Caloxin 2a1 has been used to prove the hypothesis that PMCA countertransports  $\text{Ca}^{2+}$  for proton(s) during PMCA reaction cycle (Makani et al. 2010; Vale-Gonzalez et al. 2007). It was observed that, during synchronous neural activity, the rapid removal of protons from the extracellular space occurs. Caloxin 2a1 inhibited the formation of the extracellular alkaline transient generated upon synchronous activation of hippocampus CA1 pyramidal neurons (Makani et al. 2010). This provided direct evidence that the countertransport of proton(s) by PMCA generates extracellular alkaline shifts observed upon synchronous activation of a neuronal population. Caloxin 2a1 also blocked the intracellular acidification accompanying an increase in  $[\text{Ca}^{2+}]_i$  in cultured mouse cerebellar granule cells induced by phycotoxin or glutamate receptor activation (Vale-Gonzalez et al. 2007). This suggests that the acidification was related to the proton influx that accompanied  $\text{Ca}^{2+}$  removal by PMCA. Caloxin 2a1 also helped in determining the role of PMCA in  $[\text{Ca}^{2+}]_i$  oscillations which are important for signaling in both excitable and non-excitable cells. In HEK293 cells expressing the extracellular  $\text{Ca}^{2+}$  sensing

receptor, PMCA-mediated  $\text{Ca}^{2+}$  extrusion was an essential occurrence of  $[\text{Ca}^{2+}]_i$  oscillations induced by receptor stimulation. The oscillations were eliminated in the presence of caloxin 2a1 (De Luisi et al. 2003). It also inhibited the spontaneous  $[\text{Ca}^{2+}]_i$  oscillations in human bone marrow-derived mesenchymal stem cells, as did the non-selective inhibitor, carboxyeosin (Kawano et al. 2003). Caloxin 2a1 induced a  $[\text{Ca}^{2+}]_i$  transient followed by the return of  $[\text{Ca}^{2+}]_i$  to basal levels but carboxyeosin markedly increased the basal  $[\text{Ca}^{2+}]_i$  before stopping the oscillations. It is consistent with caloxin 2a1 being a selective PMCA inhibitor. An initial increase in  $[\text{Ca}^{2+}]_i$  caused by PMCA inhibition activates other  $\text{Ca}^{2+}$  removing systems such as SERCA and NCX. In contrast, carboxyeosin also inhibits SERCA and the sodium pump. The sodium pump may locally reverse the sodium gradient leading to  $\text{Ca}^{2+}$  influx by NCX in reverse mode. Similar differences in the effects of caloxin 2a1 and carboxyeosin have been observed in mouse embryonic stem cells. Caloxin 2a1 has also been used to study the effect of PMCA inhibition in rat aorta (Chaudhary et al. 2001). Consistent with the inhibition of PMCA in vascular endothelium leading to eNOS activation, caloxin 2a1 produced an endothelium-dependent relaxation that was inhibited by eNOS inhibitor -N(G)-nitro-L-arginine methyl ester.

Caloxin 1b1 was used to study the role of PMCA in coronary artery physiology (Pande et al. 2006). It increased the force of contraction produced by a submaximal concentration of phenylephrine in de-endothelialized rat aortic rings. In cells cultured from pig coronary artery, it caused a greater increase in  $[\text{Ca}^{2+}]_i$  in the SMC than in EC, which is consistent with higher PMCA expression in smooth muscle and with slight

preference toward PMCA4, which is expressed in this tissue at much higher levels compared to endothelium.

Caloxin 1c2 has been used by us and others to study the role of PMCA. In pig coronary artery smooth muscle PMCA4 inhibition by caloxin 1c2 increased the basal tone of the de-endothelialized arteries and increased the  $\text{Ca}^{2+}$  sensitivity of the tissue to produce greater force of contraction at low extracellular  $\text{Ca}^{2+}$  when NCX and SERCA were inhibited (Pande et al. 2008). These results are consistent with the role of PMCA in  $\text{Ca}^{2+}$  extrusion and also with PMCA being a low capacity  $\text{Ca}^{2+}$  extrusion system in smooth muscle. Studies done with caloxin 1c2 in the intestine of caveolin-1 knockout mice revealed the importance of the presence of PMCA4 in intact caveolae in order for proper PMCA4 calcium removal function (El Yazbi et al. 2008). Caloxin 1c2 increased the carbachol-induced contractions in the intestinal longitudinal smooth muscle from the control mice but the effect of caloxin 1c2 was not observed in the tissues from caveolin-1 knockout mice. Thus, caloxin 1c2, which is the first isoform selective PMCA inhibitor, has been proven to be a useful tool in studying PMCA4 physiology.

### **1.9. Problem definition and objectives**

Changes in  $[\text{Ca}^{2+}]_i$  in SMC and EC are pivotal to regulation of coronary tone. However, the role of PMCA in these processes under physiological as well as pathophysiological conditions is not well understood due to lack of selective PMCA inhibitors. Therefore, the major objectives of my thesis were to determine the expression of PMCA isoforms in the smooth muscle and the endothelium of coronary artery and to

invent high affinity caloxins that are specific for the isoforms expressed in these tissues.

Towards these objectives, the proposed study has three Aims.

*Aim1:* Determine distribution of PMCA isoforms in pig coronary artery endothelium and smooth muscle.

*Hypothesis:* Pig coronary artery endothelium and smooth muscle differ in their PMCA isoform expression.

*Rationale:* Vascular SMC and EC belong to two different cell types which serves distinct functions in the organism. SMC are excitable cells which in response to increased  $[Ca^{2+}]_i$  contract and decrease vessel diameter. In response to increase in  $[Ca^{2+}]_i$  EC produce NO which cause vasorelaxation. I propose to compare the total amount of PMCA in the two tissues based on their  $Ca^{2+}$ - $Mg^{2+}$ -ATPase activity levels and in Western blots using antibodies which react with all isoforms of PMCA. I also propose to determine the PMCA isoforms expressed in the two tissues using RT-PCR for mRNA characterization and Western blots using PMCA isoform selective antibodies for protein detection. In initial experiments in Aim 1, it was determined that EC express predominantly PMCA1 and in SMC the major isoform is PMCA4 and that the tissues do not express PMCA2 and PMCA3.

*Aim2:* To invent PMCA 1 selective caloxins.

*Hypothesis:* Exdom1 of PMCA1 can be used as a target to obtain PMCA 1 selective caloxins by screening phage display libraries.

**Rationale:** The preliminary results from Aim 1 suggest a need for PMCA1 selective inhibitors to study PMCA physiology in EC. This Aim would require appropriate targets

and protocols for screening and inhibition assays. I will examine several tissues and select a source containing plasma membranes which are rich in PMCA1 and poor in other PMCA isoforms. This source will be used for further work in Aim 2. The exdom1 of PMCA is the most divergent exdom among PMCA isoforms 1-4 (Fig. 3) and would provide a target to screen for PMCA1 selective caloxins. The exdom1 is long and contains a cysteine in the middle that can produce uncertainties in the conformation by forming disulfide bridge. For invention of PMCA4 selective caloxins, exdom1 was divided around the cysteine into the N-terminal half as exdom1X and the C-terminal half as exdom1Y (Fig. 3). The screening process will be sequential and strategies analogous to those developed for the PMCA4 selective caloxin 1c2. The invented peptides will be tested for PMCA isoform inhibition and for their effects on  $[Ca^{2+}]_i$  in EC.

*Aim3:* To obtain ultra high affinity PMCA4 selective bidentate caloxins.

**Hypothesis:** The caloxins obtained for PMCA4 exdom1X and 1Y can be linked to obtain high affinity PMCA4 selective bidentate caloxins.

**Rationale:** Caloxins have been used to examine PMCA physiology in SMC which are rich in PMCA4. However, more selective and higher affinity caloxins would be more useful. The existing PMCA4 caloxins were invented using either PMCA4 exdom1X (caloxin 1c2) or exdom1Y (caloxin 1b2) as targets. It was considered that the two molecules that bind to proximal sites on the same protein can be optimally linked to make bidentate ligands with a much higher affinity and selectivity (Bouboutou et al. 1984; Hajduk et al. 1997).

## 2. MATERIALS AND METHODS

### 2.1. Materials

Bovine serum albumin (BSA), imidazole, ouabain, NADH, phospho(enol) pyruvate, pyruvate kinase-lactate dehydrogenase from rabbit muscle (~1000 units/ml lactate dehydrogenase; ~700 units/ml pyruvate kinase), ATP (microbial), calmodulin from bovine testes (>40,000 units/mg protein), keyhole limpet hemocyanin, donkey anti-rabbit-HRP antibody, sheep anti-mouse-HRP antibody, mouse monoclonal anti-PMCA4 (JA9) antibody, ovalbumin, phenylmethylsulfonylfluoride, calmodulin-agarose (2.3 mg calmodulin from bovine testes/ml suspension), soyabean phosphatidyl serine, egg yolk phosphatidyl choline, lectin from *Griffonia Simplicifolia*, calpain inhibitor MDL 28170, pluronic acid, probenecid, Tween 20, polyethylene glycol–8000, thapsigargin, glutamine and tetracycline were obtained from Sigma Aldrich (St Louis, MO, USA). New Zealand White rabbits were purchased from Charles River Labs (St. Constant, QC, Canada). Complete EDTA-free protease inhibitor cocktail tablets (broad spectrum of serine and cysteine proteases), dithiothreitol and DNase I were from Roche (Mississauga, ON, Canada). Dulbecco's modified Eagle's medium, gentamicin, amphotericin B, TRIzol reagent, ThermoScript RT-PCR system, Fluo 4/AM, Ca<sup>2+</sup>- and Mg<sup>2+</sup>-free Hanks' balanced salt solution, M-450 epoxy magnetic beads were from Invitrogen (Burlington, ON, Canada). Bradford reagent was obtained from Bio-Rad Laboratories (Hercules, CA). Polyvinylidene fluoride membrane was from Pall Corporation (Port Washington, NY). Cellulose acetate filters (0.45µm) were purchased from Whatman (La Jolla, CA, USA).

Super Signal West Femto Kit was from Pierce Chemical Company (Rockford, IL, USA). GeneRuler 100 bp and 1kb DNA Ladder and PageRuler Prestained Protein Ladder were obtained from Fermentas (Burlington, ON, Canada). Anti-PMCA (5F10) was from Affinity BioReagents (Rockford, IL, USA). Custom made rabbit-polyclonal anti-PMCA1 antibody (raised in rabbit against a PMCA1 specific sequence 8–23 VAYGGVKNSLKEANH, Protein bank P20020) was made by Pacific Immunology (Ramona, CA). AmpliTaq polymerase was purchased from Applied Biosystems (Carlsbad, CA, USA). Klenow fragment, Ph.D-12 library, Phusion High-Fidelity DNA Polymerase, *EagI* and *Acc65I* restriction enzymes, calf intestine alkaline phosphatase, T4 DNA ligase were from NEB (Pickering, ON, Canada). All exdoms synthetic peptides and their conjugates were synthesized commercially by Dalton Chemical Labs (Toronto, ON, Canada). 96 well microtiter plates and 15 ml Falcon tubes were purchased from BD Biosciences (Mississauga, ON, Canada). EZ-10 Spin Column Plasmid DNA kit was from Bio Basic Inc, (Markham, ON, Canada). 96-well UV-transparent microtiter plates and 96-well polystyrene plates were obtained from Corning Inc. (Corning, NY, USA). Bidentate oligonucleotides were synthesized by IDT technologies (Coralville, IA, USA) and by W.M. Keck Facility (Yale University, USA). 1b3-like and 1b2-like oligonucleotides were synthesized by W.M. Keck Facility (Yale University, USA). RNeasy kit, RNase-Free DNase Set, QIAprep Spin Miniprep Kit QIAquick Gel Extraction Kit, MinElute PCR Purification Kit were purchased from QIAGEN Inc. Mississauga, ON, Canada. The non-competent XL1-Blue *E. coli* cells and XL2-Blue MRF<sup>+</sup> Ultracompetent cells were from Stratagene (La Jolla, USA). The synthetic exdom

peptides were synthesized by Dalton Pharma Services (Toronto, ON, Canada). Dr E.E. Escher, Sherbrooke University, Canada, synthesized the two photoreactive derivatives of caloxin 1c2, 3Bpa1c2-biotin and 16Bpa1c2-biotin. All caloxins were synthesized by Anaspec (Fremont, CA, USA). All peptides were greater than 95 % pure by HPLC and verified by mass spectroscopy. All primers were synthesized by MOBIX (McMaster University, Hamilton, Canada). All other chemicals were purchased from the standard commercial sources.

## **2.2. Membrane isolation**

### **2.2.1. Rabbit duodenal mucosa (RDM)**

RDM plasma membrane enriched fraction was isolated, by a previously described method with some modifications (Grover et al. 1985). New Zealand White rabbits were euthanized with sodium pentobarbital (100 mg/kg) and duodenum was immediately dissected and placed in chilled physiological saline solution (in mM: 138 NaCl, 10 Glucose, 10 N-2-hydroxyethylpiperazine-N'-2-ethanesulfonic acid (HEPES), 1 MgCl<sub>2</sub>, 5 KCl, 2 CaCl<sub>2</sub>, pH= 6.4). All steps were carried out at 4°C. The duodenum was dissected open, washed and duodenal mucosa was scraped from the smooth muscle layer. The tissue was homogenized in 7-10 volumes of homogenization buffer (8% sucrose and the following in mM: 100 KCl, 2 dithiothreitol, 1 phenylmethylsulfonylfluoride, 0.5 ethylene glycol-bis(-aminoethyl ether)-N,N,N',N'-tetraacetic acid (EGTA), 0.002 calpain inhibitor MDL 28170) for 3×15 s using a Polytron PT20 at a setting of 4.5. The homogenate was centrifuged at 10,000 × g for 10 min (rotor JA-20) and the supernatant was filtered

through cheese cloth and centrifuged at  $388,000 \times g$  for 45 min (rotor 60.1 TI). The pellet was suspended in water containing 0.5 mM EGTA to burst the microsomes and ensure that calmodulin was removed and centrifuged again at  $388,000 \times g$  for 30 min (rotor 60.1 TI). This pellet was suspended in 8% (w/w) sucrose, layered on top of 32% (w/w) sucrose and centrifuged at  $278,000 \times g$  in a swinging bucket rotor (SW 41 TI) for 2 h. The layer of turbid membranes at the interphase between 8% and 32% sucrose was collected and stored at  $-80^{\circ}\text{C}$  until use.

### **2.2.2. Leaky erythrocyte ghosts**

The leaky human erythrocyte ghosts were prepared as described previously with some modifications (Jarrett et al. 1978). Human blood (200 ml) in acid citrate dextrose (2.5 % trisodium citrate, 1.4 % citric acid, 2 % dextrose, pH=4.5) was centrifuged at  $3,000 \times g$  for 5 min (rotor JA-20). The top clear buffy layer containing platelets and plasma was collected by a person from another lab who routinely works with blood. All following steps were carried out at  $4^{\circ}\text{C}$ . The lower layer of erythrocytes was mixed with 10 volumes of TRIS-HCl (172 mM tris(hydroxymethyl)aminomethane (TRIS), pH=7.6 at  $4^{\circ}\text{C}$ ) and centrifuged at  $4,000 \times g$  for 5 min (rotor JA-14). The clear supernatant was discarded and the step was repeated 3 more times. The red blood cells were mixed with 14 volumes of distilled water and lysed by vigorous shaking for 5 min. Following this step all centrifugation was done at  $14,000 \times g$  for 10 min (rotor JA-14). The red supernatant was carefully removed and a tight and loose pellet was kept. The pellets were washed with 14 volumes of imidazole-EDTA (10 mM imidazole-HCl, 1 mM (ethylenedinitrilo)tetraacetic acid (EDTA), pH=7.0). This step was repeated about 7 times

until the pellet was almost white. Next, tight pellet was discarded and the pale loose pellet was washed two times in 14 volumes of imidazole-HCl (40 mM imidazole-HCl, pH=7) and two times in storage buffer (in mM: 130 KCl, 20 HEPES, 0.5 MgCl<sub>2</sub>, and 2 dithiothreitol). The ghosts were then stored in small aliquots at –80°C.

### **2.2.3. Pig coronary artery smooth muscle membranes**

Pig coronary artery smooth muscle was used for preparing microsomes, as described previously with some modifications (Grover et al. 1985). Pig hearts were obtained from Maple Leaf Pork, Burlington, ON, Canada and transported in chilled physiological saline solution (in mM: 138 NaCl, , 10 Glucose, 10 HEPES, 1 MgCl<sub>2</sub>, 5 KCl, 2 CaCl<sub>2</sub>, pH = 6.4). The left descending coronary artery was dissected with surrounding myocardium, put on metal rod, cleaned from surrounding tissue and flipped inside out. The smooth muscle layer was scraped off, put in the homogenization buffer (see section 2.2.1) on ice, finely chopped and forced through a sieve. All following steps were carried out at 4°C. The tissue was further homogenized using motorized teflon-glass homogenizer (about 3 min, 2000 rpm). The homogenate was centrifuged at 10,000 × g for 10 min (rotor JA-20) and the supernatant was filtered through cheese cloth, incubated with KCl (final concentration 0.7 M) for 15 min and centrifuged at 388,000 × g for 45 min (rotor 60.1 TI) to obtain a microsomal pellet. The pellet was rinsed and suspended in 8% sucrose and stored in small aliquots in -80C. To obtain the plasma membrane fraction the microsomal pellet was suspended in 8% sucrose containing KCl (0.7 M) and incubated on ice for 15 min. Next the microsomes were centrifuged on sucrose density gradient consisting of layers of 60, 40, 28 and 18 % sucrose for 2h at 250000 x g

(swinging bucket rotor TLS 55). The turbid layer between 18 and 28 % sucrose was collected as plasma membrane enriched fraction.

#### **2.2.4 Cultured pig coronary artery endothelium and HEK293 cells**

Pig coronary artery endothelial cells and HEK293 cells were cultured as described in section 2.3. The microsomes were obtained as previously described (Grover et al. 1997). Prior to isolation, cells were cultured on 10 cm Petri dish. The media was removed, the cells were scraped in homogenization buffer (see section 2.2.1) using plastic triangle and homogenized for  $3 \times 5$  s using a Polytron PT20 at a setting of 4.5. The homogenate was centrifuged at  $10,000 \times g$  for 10 min (rotor JA-20). The pellet was discarded and the supernatant was centrifuged at  $388,000 \times g$  for 30 min (rotor TLA 100.4) to obtain microsomal pellet. The pellet was suspended in 8% sucrose. The plasma membrane enriched fraction was obtained with the method described in section 2.2.3 for smooth muscle, however, the KCl incubation step was omitted.

#### **2.3. Pig coronary artery endothelium and HEK293 cell culture**

Pig coronary artery endothelial cells were cultured as described previously (Grover et al. 1997). The arteries were obtained as described in section 2.2.3 and placed in Krebs' solution at room temperature (in mM: NaCl 115.5, KCl 4.6, MgSO<sub>4</sub> 1.2, NaH<sub>2</sub>PO<sub>4</sub> 1.2, CaCl<sub>2</sub> 2.5, NaHCO<sub>3</sub> 22, D-glucose 11.1, bubbled with 95% oxygen and 5% carbon dioxide). The arteries were then dissected open and endothelium was gently removed using a cotton swab and plated in Dulbecco's modified Eagle's medium supplemented with 0.5 mM HEPES (pH =7.4), 2 mM glutamine, 50 mg/l gentamicin,

0.125 mg/l amphotericin B, and 10% fetal bovine serum. After growing to confluence the cells were removed from the plates by trypsinization in  $\text{Ca}^{2+}$ - and  $\text{Mg}^{2+}$ -free Hanks' balanced salt solution containing 0.25% trypsin and 1mM EDTA for 4 min at 37°C and then replated. At the fourth passage, the cells were aliquoted ( $2 \times 10^6$  per aliquot) and stored in liquid nitrogen. When needed, an aliquot of cells was thawed and grown to confluence. The medium was changed after 2 days and cells were used for experiments after 6-10 days. The cell phenotype was verified by Western blot. The cells were positive for endothelial cells markers e-NOS and von Willebrand factor and negative for smooth muscle alpha-actin as reported previously.

The HEK293 cells (gift from Dr. Mike Zhu) were cultured to confluence in Dulbecco's modified Eagle's medium supplemented with 0.5 mM HEPES (pH =7.4), 2 mM glutamine, 50 mg/l gentamicin, 0.125 mg/l amphotericin B, and 10% fetal bovine serum and used for experiments, as previously described (Grover et al. 1997).

#### **2.4. Protein estimation**

Protein estimation was done using Bradford reagent, following manufacturer's instructions. Bovine serum albumin was used to make the standard curve. Absorbance was measured at 595 nm.

#### **2.5. Western blotting**

Specified amounts of membrane proteins were suspended in 6x Laemli SDS sample buffer and used for SDS-polyacrylamide (7.5 %) gel electrophoresis at 80 V. The proteins from the gel were transferred to the polyvinylidene fluoride membrane at 100 V

for 2.5 h using an ice-cold transfer buffer (25 mM TRIS base, 150 mM glycine, 10 % methanol, pH=8.3). All the following steps were performed at room temperature. The membrane was then washed in distilled water and incubated on a rocker in the blocking buffer (3 % skim milk powder in TBS-Tween 20: 10 mM TRIS/HCl, 140 mM NaCl, 0.1 % (v/v) Tween 20, pH=7.5, filtered through 0.45µm cellulose acetate filters) for 1 h. The blocking buffer was also used in steps involving antibody binding and TBS-Tween was used in washing steps. The blot was then incubated with primary antibody for 1h, washed every 15 min for 1h, incubated with horse radish peroxidase (HRP) conjugated secondary antibody for 1 h and washed every 10 min for 1.5 h (see Table 2). The peroxidase activity was visualized with Super Signal West Femto Kit and a LAS3000 mini Luminiscent Image Analyzer (Fujifilm Life Science, Stamford, CT). The molecular mass of the bands was determined using PageRuler Prestained Protein Ladder. The band intensity was quantified with Multi Gauge v 3.0 software (Fujifilm).

**Table 2. Antibodies/proteins and dilutions used for Western blot analysis**

<b>Target Protein</b>	<b>Primary Antibody/Protein</b>	<b>Secondary Antibody (HRP conjugated)</b>
All PMCA isoforms	5F10, mouse-monoclonal 1:1000	Sheep anti-mouse 1:20000
PMCA1	rabbit-polyclonal 1:1000	Donkey anti-rabbit 1: 20000
PMCA4	JA9, mouse-monoclonal 1:1000	Sheep anti-mouse 1:20000

## 2.6. Isolation of fresh EC

Fresh EC were obtained from two pig aortas with *Griffonia Simplicifolia I* lectin coated magnetic beads, as described previously (Davis et al. 2006). The M-450 epoxy magnetic beads were concentrated on a magnet Dynal MPC-S and a Dynal Biotech Sample Mixer was used for stirring (Dynal Biotech. Inc, Lake Success, USA). All steps of magnetic beads coating with *Griffonia Simplicifolia I* lectin were done at 4°C.  $1.2 \times 10^8$  beads were washed two times in 3 ml of 0.1 M sodium borate buffer (pH=9.5) for 2 min and then suspended in 480 µl of borate buffer and 120 µl of 1 mg/ml lectin in phosphate buffered saline solution (in mM: 10 Na-phosphate, 140 NaCl, pH=7.4). The beads were stirred for 24 h, washed for 10, 30 min and 20 h in the phosphate buffered saline solution containing 0.1% bovine serum albumin and then resuspended in 300 µl of the same solution but containing 0.02% sodium-azide. The lectin coated magnetic beads were stored for no more than two weeks at 4°C. Two pig plucks were obtained from Maple Leaf Pork (Burlington, ON) and transported in chilled physiological saline solution (section 2.1.3). The aortas were dissected from plucks and placed immediately in Krebs' solution (see section 2.3) at room temperature. The aortas were dissected open, endothelial cells dislodged using a cotton swab and placed in 8 ml chilled Na-HEPES buffer (in mM: 134 NaCl, 5.4 KCl, 10 glucose, 0.8 MgSO<sub>4</sub>, 20 HEPES, 1.8 CaCl<sub>2</sub>, pH=7.3). 100 µl of lectin coated magnetic beads were washed twice in 1 ml of Na-HEPES buffer to remove sodium-azide. The beads were added to cell suspension, stirred at room temperature for 1 h and washed three times with 3 ml Na-HEPES. Cells isolated by this method were positive for von Willebrand factor and e-NOS.

## **2.7. RNA isolation**

Total RNA from fresh EC and pig brain was isolated with TRIzol reagent, following the manufacturer's instructions. The RNA from fresh EC was isolated while still attached to the beads. The cells were homogenized in TRIzol reagent using a needle (20-gauge) and brain tissue was homogenized using glass-teflon homogenizer. Briefly, the tissue was incubated with the reagent, mixed with chloroform and centrifuged to obtain separation into a lower red phenol-chloroform phase, an interphase, and a colorless upper aqueous phase containing RNA, which was saved for future processing. Next the isopropanol was added and sample was centrifuged to obtain RNA pellet. The pellet was washed in 75% EtOH, dried and resuspended in diethylpyrocarbonate treated water. To make sure that the RNA was properly resuspended the sample was incubated at 55-60°C for 10 min and then aliquoted and stored at -80°C. Total RNA from all other tissues was isolated with the RNeasy kit according to manufacturer's instructions. Briefly, the cultured cells were lysed directly on tissue culture dish and homogenized by passing through the needle (20-gauge) and the tissues were homogenized in lysis buffer for 45 s using a Polytron PT20 at a setting of 4.5 and centrifuged to remove debris. Next, 70% EtOH was added and the solution was applied to a spin column containing silica-gel-based membrane for RNA adsorption. The residual DNA adsorbed to the column was digested with RNase-Free DNase Set by addition of DNase I solution and incubation at room temperature for 15 min. The DNase I was removed from the column during subsequent washes. The RNA was eluted by applying RNase-free water onto the membrane, spun down, aliquoted and stored at -80°C.

## 2.8. RT-PCR

The isolated RNA was reverse transcribed using the ThermoScript RT-PCR system, following instructions of the manufacturer. The RNA isolated with TRIzol reagent was DNase I digested prior to use according to manufacturer's protocol. The sample was incubated with the DNase I for 15 min at room temperature and inactivated by incubation with EDTA (final concentration 8 mM) for 10 min at 65°C. The RNA was reversibly transcribed in the presence of oligo(dT) primers (5 µM), dNTP (1 mM), DTT (5 mM), RNaseOUT (recombinant ribonuclease inhibitor, 2 U/µl), ThermoScript RT (reverse transcriptase, 1.5 U/µl) to obtain cDNA. First RNA was annealed with oligo(dT) primer for 5 min at 65°C and the reverse transcriptase reaction was carried out at 55°C for 1h. The enzyme was heat-inactivated for 10 min at 85°C. To remove RNA, *E. coli* RNase H (0.1 U/µl) was added and sample was incubated at 37°C for 20 min. The sample including all components but reverse transcriptase was saved as a “NO RT” control.

PCR was carried out with AmpliTaq. Primers sequences are given in Table 3. The reaction mixture contained the following in a total volume of 20 µl: 1 µM of each primer, 2.5 mM MgCl<sub>2</sub>, 200 µM of each dNTP, 1 unit of AmpliTaq, 2 µl of 10x PCR buffer and 5 µl of different cDNA dilutions. The PCR conditions were as follows: denaturation at 94°C (40 sec), annealing at 58°C (40 sec) and extension at 72°C (50 sec) for 30 cycles. Water, NO RT and RNA were used as templates for negative controls. PCR products were analyzed by gel electrophoresis using 6.5% polyacrylamide gels and GeneRuler 100

bp DNA Ladder. Gels were stained with ethidium bromide, washed and visualized with KODAK 1D 3.6 camera system.

RT-PCR with primers designed previously for human PMCA1, 2 and 3, gave appropriate products with pig and rabbit brain (Stauffer et al. 1995). Neither primers designed previously for human nor rat PMCA4 worked for pig and rabbit. The PMCA4 sequence from pig was unknown, so the regions with the highest similarity between PMCA4 sequences in human (Genbank accession NM\_001684), rat (NM\_001005871), and mouse (NM\_213616) were chosen to design the new primers. The heart and brain cDNA was used to optimize PCR conditions. Identities of pig PMCA1b and rabbit PMCA4b bands were confirmed by the sequencing of gel-purified PCR products. Pig PMCA4b sequence (deposited in GenBank as accession no. DQ145551) was not previously known, but it has 88% identity with the human PMCA4b (GenBank accession no. NM\_001684). Specificity of the pig PMCA4a was confirmed by RT-PCR with PMCA4a specific primers

## **2.9. Screening Ph.D-12 library for binding to a synthetic exdom (biopanning)**

Biopanning was carried out with some modifications of a previously described procedure (Chaudhary et al. 2001). Ph.D-12 library was screened using the synthetic PMCA1 exdom1X as a target consisting of residues 119-137 (IVSLGLSFYQPPEGDNALC, Protein bank P20020). The peptide was used by itself or as cysteine conjugates with ovalbumin or KLH. The screening was carried out for 3 rounds. Each round of screening consisted of the following steps:

**Table 3. PMCA isoform specific Primers for PCR analysis**

<b>PMCA isoform</b>	<b>5'-3'</b>
PMCA1 (human, bovine, pig, rat, rabbit)	up TAGGCACTTTTGTGGTACAG dn GGCTCTGAATCTTCTATCCTA
PMCA2 (human, bovine, pig)	up AGATCCACGGCGAGCGCAAT dn CGAGTTCTGCTTGAGCGCGG
PMCA3 (human, pig)	up CGAGTTCTGCTTGAGCGCGG dn CTATCCACAGAACAGTGGCTC
PMCA4 human	up CCCAGCCAGCACTATAACCATT dn TGTAGAGAG CTGTCCGACTGG
PMCA4 rat	up TGCAGGTGTCTACCGCAACAT dn GGCAGTCCACGGCATTGTTAT
PMCA4 rabbit	up AGTGCTGTGGTGTCTCTTC dn GTCGTCCTCCTGCTCATCTA
PMCA4 pig, bovine	up CCCAGCCAGCACTATAACCATT dn TGTAGAGAGCTGTCCGACTGG
PMCA4a, human, pig	up CCCAGCCAGCACTATAACCATT dn AAAGAGGCTCCCGTCTGGAAT

Day 1: 20 wells of a 96 well polyvinyl U-bottom microtiter plate were each coated with 200 µl of the target peptide solution (0.1 mg/ml each of the synthetic exdom1X and its KLH conjugate dissolved in sterile phosphate-buffered saline (PBS containing in mM: 137 NaCl, 2.7 KCl, 8 Na<sub>2</sub>HPO<sub>4</sub> and 1.5 KH<sub>2</sub>PO<sub>4</sub>, pH=7.4). Sodium-azide was also added to this solution to a concentration of 1 mM. After coating the wells, the plate was covered with plastic wrap and left overnight at 4°C.

Day2: The target peptide solution was poured off from the wells of the microtiter plate and the wells were blocked for 1h at 4°C with 250 µl of blocking buffer (5 mg/ml BSA in sterile PBS with 1 mM sodium azide). Next the blocking buffer was discarded and the

wells were washed 6x with chilled sterile PBS. All the remaining steps were carried out at room temperature.  $1 \times 10^{12}$  plaque forming units (pfu) of the original phage display peptide library (Ph.D-12) were diluted in 2 ml of a BOK solution (5 mg/ml BSA, 0.5 mg/ml ovalbumin, 0.5 mg/ml KLH, 0.1 mg/ml PMCA4 exdom1X-KLH conjugate, 0.1 mg/ml PMCA4 exdom1X peptide in sterile PBS) and incubated on rotator for 15 min. The PMCA4 exdom1X consists of residues 116-131 (ISLVLSFYRPAGEENEL, GenBank accession no.NM\_001684) and an additional N-terminal cysteine to link the peptide to different proteins. 100  $\mu$ l of the phage solution was then added to each coated well and incubated with rocking for 2 h. After removing the unbound phage the wells were washed extensively with 200  $\mu$ l of the following: quick wash with PBS, 10 min on rocker with BOK, quick wash with PBS, 10 min on rocker with 5% carnation milk in PBS, quick wash with PBS, 10 min with PBS, 10 quick washes with PBS. The phage was eluted for 24h with 100  $\mu$ l of elution buffer (0.1 mg/ml PMCA1 exdom1X-ovalbumin conjugate, 10  $\mu$ g/ml tetracycline in sterile PBS).

Day3: The eluted phage was collected amplified, titered and subjected to the next cycle of screening at a constant input of  $10^{10}$  pfu.

#### **2.10. Assay to determine phage selectivity for the PMCA1 exdom1X target.**

The phage pool selected after 3 rounds of biopanning was tested for binding to PMCA1 exdom1X over binding to PMCA4 exdom1X and KLH alone. The assay was performed in the same manner as biopanning (see section 2.9). The modifications included: BOK solution did not contain any peptides, the wells were coated in triplicates for each target, phage was eluted separately from each well, the preselected phage and the

same amount of Ph.D-12 library was tested for binding at the same time on two different plates. The adsorbents and eluants are given in Table 4.

**Table 4. Adsorbents and eluants used in selectivity test.**

Adsorbent	Eluant
PMCA1 exdom1X and PMCA1 exdom1X-KLH	PMCA1 exdom1X-ovalbumin
PMCA1 exdom1X and PMCA4 exdom1X-KLH	PMCA4 exdom1X-ovalbumin
KLH	Ovalbumin

### 2.11. Phage amplification and precipitation

All culture media and pipette tips were sterilized by autoclaving before use. XL1-Blue *E. coli* non-competent cells were streaked on Luria Broth (LB)-agar-tetracycline (1.5% agar, 10 µg/ml tetracycline in LB: 85.6 mM NaCl, 0.5 % yeast extract, 1 % trypticase peptone) plates and incubated for 16-20 h at 37°C. A single colony of XL1-Blue *E. coli* was allowed to grow in LB-tetracycline (LB with 10 µg/ml tetracycline) for 16-20 h in a shaker (225-250 rpm) at 37°C. The culture was diluted in fresh LB-tetracycline and grown again for 1.5 h and then diluted in an equal volume of LB. The eluted phage suspension was added to the culture (100 µl of phage and 1 ml of bacterial culture per tube) and incubated at 37°C for 4.5 h with shaking. The resulting suspension was centrifuged at 16,000 g for 2 min and the supernatant containing the phage particles was transferred to fresh tube. 300 µl of PEG/NaCl (20 % (w/v) polyethylene glycol–8000, 2.5 M NaCl) was added to precipitate the phage over 16-20 h at 4°C. The

precipitated phage was centrifuged at 16,000 g for 2 h at 4°C, resuspended in LB and the suspension was rotated for 3 h at 4°C. The titer of the phage was determined before use.

### **2.12. Determining phage titers**

Bacterial cells were cultured in 100 ml LB as above, centrifuged at 23,000 g at 4°C for 5 min and then suspended in 6 ml of LB. The LB-agar plates (1.5% agar in LB) were prewarmed to 37°C and the agarose (0.6 % agarose in LB) was melted and equilibrated in a water bath at 48°C. The phage was serially diluted over a wide range in LB. 100 µl cells were placed into 15 ml plastic round bottom Falcon tubes and mixed with 100 µl of the diluted phage. One at a time, 5 ml of 0.6 % agarose at 48°C was added to the tubes with cells-phage mix and the contents were poured onto the prewarmed LB-agar plates. After solidifying, the plates were incubated at 37°C over night. The plaques were counted and phage concentration in pfu/µl was calculated.

### **2.13. Picking phage clones and plasmid isolation**

The phage titers were done the day before. XL-1 blue cells were cultured as described above and then diluted with an equal volume of LB. Each phage clone (plaque) was picked with a new sterile plastic stick (inoculating needles, VWR) from the plate containing no more than 100 plaques per plate to avoid cross-contamination. Each plaque was transferred to a 15 ml sterile Falcon tube containing 500 µl of the cell culture. The individual phage clones were amplified at 37°C with shaking at 250 rpm for 4.5 h. The amplified phage for each clone was centrifuged at 16,000 g for 2 min and the supernatant containing phage particles was transferred to fresh tubes and stored at 4°C. Each phage

suspension obtained above (200  $\mu$ l) was amplified in 1.5 ml of bacterial cells. The amplified phage of each clone was centrifuged at 16,000 g for 2 min and the supernatant was saved for future experiments and stored at 4°C. The bacterial pellet was used for plasmid DNA isolation using QIAprep<sup>®</sup> Spin Miniprep Kit or EZ-10 Spin Column Plasmid DNA kit, following manufacturer's instructions. Briefly, the cells suspended in buffer containing RNase A were lysed under alkaline conditions, neutralized and centrifuged at high speed to remove the debris. Clear lysate was then placed in spin columns for adsorption of the plasmid DNA to the silica resin. After washing the resin with ethanol, the plasmid DNA was eluted with 10 mM TRIS-HCl, pH=8.5 buffer. The plasmid DNA was then sequenced by MOBIX (McMaster University, Hamilton, Canada) using the downstream -96gIII primer (5'-CCCTCATAGTTAGCGTAACG-3').

#### **2.14. Screening the phage using PMCA affinity chromatography**

The phage selected after 3 rounds of screening for binding to synthetic PMCA1 exdom1X peptide (see section 2.9) and the library displaying caloxin 1b3-like peptides were used for affinity chromatography with PMCA isolated from RDM (mostly PMCA1), as previously described (Szewczyk et al. 2010). The library displaying caloxin 1b2-mutants or bidentate peptides was screened using affinity chromatography with erythrocyte ghosts PMCA (mostly PMCA4), as previously described (Pande et al. 2006). In this approach PMCA is immobilized on calmodulin-agarose beads. In the presence of  $Ca^{2+}$ , PMCA binds calmodulin with high affinity through its C-terminal calmodulin binding domain.  $Ca^{2+}$  removal leads to PMCA dissociation from calmodulin and elution.

### **2.14.1 Affinity chromatography with RDM PMCA**

Membranes (4 mg protein, RDM plasma membranes or erythrocyte ghosts) were centrifuged at 500,000 g for 15 min (rotor TLA 100.4) and used for preparation of two separate columns. The pellets were resuspended to obtain a protein concentration of 16 mg/ml in a HEPES buffer containing the following in mM: 130 NaCl, 20 HEPES, 0.5 MgCl<sub>2</sub>, 2 dithiothreitol, 0.1 CaCl<sub>2</sub> at a pH of 7.4 plus a cocktail of protease inhibitors (Complete Mini, EDTA-free). To these suspensions, an equal volume of a HEPES buffer containing 1.6% Triton X-100 was added slowly, mixed by inversion and incubated for 10 min. The suspensions were centrifuged at 500,000 g for 15 min and the supernatants containing solubilized PMCA1 and PMCA4 were retained. A suspension of phosphatidylserine (2 % (w/v) in 1 % Triton X-100) was prepared by sonication on ice and stored under N<sub>2</sub> at -80°C until use. The phospholipid suspension was added to the solubilized PMCA1 and 4 to a final concentration of 0.05 % and allowed to mix by slow rotation at 4°C for 10 min. A bed volume of 800 µl agarose–calmodulin resin was packed into two columns and washed with 3 volumes of wash buffer (HEPES buffer containing 0.4% Triton X-100 and 0.05% phospholipids). The reconstituted membrane was applied separately onto two agarose–calmodulin columns and rotated for 2 h. The unbound flow-through material from the columns was discarded. The columns were washed with 10 ml of the wash buffer. The phage pool selected after 3 rounds of screening for binding to PMCA1 exdom1X synthetic peptide was diluted in 500 µl of wash buffer, applied to the erythrocyte ghost column for negative affinity chromatography to decrease the phage that would bind non-specifically or bind to

PMCA4. After 30 min incubation, the flow-through was collected. Column was washed with another 500  $\mu$ l of wash buffer and the eluate was collected. The two eluates were mixed and applied on a column prepared using RDM and mixed by rotation for 16-20 h at 4°C. The unbound phage particles were removed as flow through and by washing the column with 10  $\times$  2.5 ml of the wash buffer. PMCA with the bound phage was eluted by incubation for 20 min with 400  $\mu$ l of Ca<sup>2+</sup>-free elution buffer (0.4% Triton X-100, 0.05% phosphatidylcholine and the following in mM: 130 NaCl, 20 HEPES, 1 MgCl<sub>2</sub>, 2 dithiothreitol, 5 EGTA, pH=7.4) twice at 37°C. Next, the eluates were pooled and the phage were precipitated over 16-20 h with PEG/NaCl and amplified the next day. The affinity chromatography was repeated two times and the final phage pool was titered and plasmid DNA of individual clones was sequenced. For competition experiments, equal amounts of each unique clone were mixed together and used for affinity chromatography with the protocol described above. The only difference was the introduction of extensive washes. After phage binding to PMCA from the RDM, the phage-PMCA-calmodulin-agarose complex was washed in 10 ml wash buffer for 3 days changing the buffer twice each day.

#### **2.14.2. Affinity chromatography with erythrocyte ghosts PMCA**

The protocol is similar to that described for RDM PMCA (section 2.14.1). The modifications include: 8 mg protein of erythrocyte ghosts was solubilized and applied on a column, negative screening was done with PMCA1 and final screening with PMCA4, instead of phosphatidylcholine a mix of phosphatidylserine and phosphatidylcholine (2 % in 1 % (w/v) Triton X-100) was used throughout the screening process, PMCA was

eluted at room temperature with two times 500 µl elution buffer. The washing steps were also modified. After phage binding to the PMCA, the column was washed with 5 bed volumes of the wash buffer. The contents of the column were transferred to a 50 ml sterile Falcon tube containing 20 ml of wash buffer and rotated for 2 h. The process was repeated 5 times with rotation for 1 h. The phage clones were titered, amplified and sequenced after one round of screening (no amplification was introduced). For screening phage library displaying caloxins 1b2-like peptides, the unique clone sequences obtained from two separate experiments were titered and combined for a round of completion experiment of affinity chromatography with erythrocyte ghosts PMCA, as described above.

#### **2.15. Construction of Ph.D caloxin 1b3-like peptide library.**

A Ph.D library displaying caloxin 1b3-like peptides was constructed with the method previously described (Pande et al. 2008). To construct the Ph.D caloxin 1b3-like peptide library, limited mutagenesis was carried out in the 36 bases that encode 12 amino acids starting from N-terminus. It was computed that retaining 91 % of the original base at each of the 36 base positions and replacing the remainder with equal percent of the other three bases would be optimum. Mutations were made in the minus strand (5'CCACGCATACAAAGACTGATAATTAATCCAACCATG3') of the caloxin 1b3. A mixture of oligonucleotides with partially randomized caloxin 1b3 encoding domain, flanked by conserved bases in the minus strand of the phage DNA (5'CATGTTTCGGCCGAACCTCCACC(N)<sub>36</sub>AGAGTGAGAATAGAAAGGTACCCGGGCATG3') were synthesized. The flanking conserved bases contained the restriction

sites *Acc65I/EagI* required for cloning. The steps involved in the library construction are briefly described below.

### **2.15.1. Synthesis of a duplex from single stranded oligonucleotides**

5 µg of each oligonucleotide was annealed with 4.2 µg of the universal extension primer (5'CATGCCCGGGTACCTTTCTATTCTC3') in a total volume of 50 µl of TE buffer (10 mM TRIS, 1 mM EDTA, pH=8) containing 100 mM NaCl. The annealing reaction mixture was heated to 95°C for 10 min and the tube was then placed in a dish filled with boiled water that was allowed to cool down slowly to approximately 37°C. The annealed duplex was extended by Klenow fragment (5 U/µl) in NEB3 reaction buffer (100 mM NaCl, 50 mM TRIS-HCl, 10 mM MgCl<sub>2</sub>, 1 mM DTT, pH=7.9) containing 0.4 mM each of dNTP in a final reaction volume of 200 µl. The extension reaction was carried out at 37°C for 10 min and then the enzyme was heat-inactivated at 65°C for 15 min. The size of the duplex was determined by 12 % polyacrylamide gel electrophoresis. Molecular masses of the bands were estimated using a GeneRuler 100 bp DNA Ladder.

### **2.15.2. Digestion of the oligonucleotide duplex**

The oligonucleotide duplex was digested with *EagI* and *Acc65I* (12.5 U) in the NEB3 reaction buffer in a final volume of 400 µl at 37°C for 3 h. The digested product was purified using MinElute PCR Purification Kit, according to manufacturer instructions. Briefly, DNA was bound to a silica membrane in spin columns, washed and eluted in 10 mM TRIS/HCl buffer pH=8. The molecular mass and concentration was determined on 12 % polyacrylamide gel using the GeneRuler 100 bp DNA ladder.

### **2.15.3. Preparation of the M13KE vector**

The M13KE vector (5 µg) was digested at 37°C for 3 h with 200 units each of *EagI* and *Acc65I* (50 U) in a total volume of 200 µl of 1x NEB3 reaction buffer with 0.1 mg/ml BSA. The digested DNA was dephosphorylated at 37°C for 1 h by 2.5 units of calf intestine alkaline phosphatase in the same buffer. The alkaline phosphatase was heat-inactivated for 5 min at 65°C. The digested M13KE vector was tested on 1 % agarose buffer. The digested M13KE vector was run on 1% agarose gel (75 V) in TRIS-acetate-EDTA (40 mM TRIS acetate/1 mM EDTA) and gel purified using QIAquick Gel Extraction Kit. Briefly, bands were visualized with ethidium bromide staining on blue light transilluminator and excised from the gel. The agarose gel was dissolved and a solution containing DNA was placed in a spin column for adsorption to silica membrane. After washing, the DNA was eluted in 10 mM TRIS/HCl buffer pH=8. The molecular mass and concentration was determined on agarose gel using the GeneRuler 1 kb DNA ladder.

### **2.15.4. Ligation of digested oligonucleotide duplex into digested M13KE vector**

The ligation was carried out with 400 ng vector, 1.25 molar excess of the insert, 1000 units of T4 DNA ligase in 200 µl volume of 1x ligase reaction buffer (50 mM TRIS-HCl, 10 mM MgCl<sub>2</sub>, 1 mM ATP, 10 mM DTT, 25 µg/ml BSA pH 7.5 at 25°C) for 16 h at 16°C. Next, the ligase was heat-inactivated for 15 min at 65°C.

#### **2.15.5. Transformation of XL2-Blue MRF' ultracompetent cells**

The ligated product was used to transform XL2-BlueMRF' Ultracompetent cells, following the protocol provided by the manufacturer. 600  $\mu$ l of cells were thawed on ice and incubated for 10 min with  $\beta$ -mercaptoethanol (final concentration 0.024 M). Cells were transferred to prechilled 15 ml Falcon polypropylene round bottom tubes (100  $\mu$ l per tube), mixed with 20  $\mu$ l of ligation mixture and incubated on ice for 40 min. Next, the tubes were heat-pulsed in a 42°C water bath for 30 s and incubated on ice for 2 min. The tubes containing the transformed cells were incubated with 0.9ml NZY+ broth (1 % NZ amine, 0.5 % yeast extract, 85.5 mM NaCl, pH 7.5 (NaOH) with 20 mM glucose and 12.5 mM each of MgCl<sub>2</sub> and MgSO<sub>4</sub> added prior to use) at 37°C for 30 min with shaking at 225-250 rpm. The transformation mixture was centrifuged at 16,000 g for 2 min and the supernatant containing the phage was titered using the mid log phase culture of non-competent XL1-Blue cells. Plaques were picked to determine the complexity of the library. The library was amplified once, using XL1-Blue cells. The amplified Ph.D caloxin 1b3-like peptide library was precipitated by addition of PEG/NaCl and resuspended in LB containing 50% glycerol and stored at -20°C.

#### **2.16. Construction of the Ph.D caloxin 1b2-like peptide library**

Ph.D caloxin 1b2-like peptide library was constructed by Jyoti Pande with the method described in section 2.15. The limited mutagenesis was carried out in the 36 bases that encode caloxin 1b2. Mutations were made in the minus strand (5'CCACGCATACAAAGACTGATAATTAATCCAACCATG3') of caloxin 1b2. A mixture of oligonucleotides with partially randomized caloxin 1b2 encoding domain,

flanked by conserved bases in the minus strand of the phage DNA (5'CATGTTTCGGCCGAACCTCCACC(N)<sub>36</sub>AGAGTGAGAATAGAAAGGTACCCGGGCATG3') were synthesized. The flanking conserved bases contained the restriction sites *Acc65I/EagI* required for cloning.

### **2.17. Construction of the phage expressing bidentate peptides**

Different variants of phage displaying bidentate caloxin1c2-caloxin1c4 were constructed. We designed 20 different variants of oligonucleotides encoding for caloxins in different orientations and separated by 0, 1, 2, 3 or 4 GGS repeats to fine-tune the proper distance between them (see Fig. 4). The oligonucleotides flanked by conserved bases containing restriction sites for *EagI* and *Acc65I* in the minus strand of the phage DNA were synthesized. DNA duplexes were prepared from single stranded oligonucleotides. Typically, 1 µg of an oligonucleotide was annealed with 1 µg of the universal extension primer (5'CATGCCCGGGTACCTTTCTATTCTC3') in a total volume of 10 µl of TE buffer (10 mM TRIS, 1 mM EDTA, pH = 8) containing 100 mM NaCl. The annealing reaction was heated to 95°C for 10 min and the tube was then placed in a dish filled with boiled water that was allowed to cool down to approximately 37°C. The annealed duplex was extended by Klenow fragment (5 U/µl) in NEB3 reaction buffer (100 mM NaCl, 50 mM Tris-HCl, 10 mM MgCl<sub>2</sub>, 1 mM DTT, pH=7.9) containing 0.4 mM each of dNTP in a final reaction volume of 40 µl. The extension reaction was carried out at 37°C for 10 min and then the enzyme was heat-inactivated at 65°C for 15 min. The duplex was checked on 12 % polyacrylamide gel. Molecular masses of the

bands were estimated using a GeneRuler 100 bp DNA Ladder. DNA from some of the samples were amplified by PCR using Phusion High-Fidelity DNA Polymerase (0.02 U/ $\mu$ l), following manufacturer's instruction. The PCR mixture contained: upstream and downstream primers (0.5  $\mu$ M, universal extension primer complementary to 3' of minus strand and primer complimentary to 3' of plus strand 5'-CATTTCGGCCGAACCTCCA-3'), 200  $\mu$ M of each of dNTP, 1 ng double stranded oligonucleotides, 1.5 mM MgCl<sub>2</sub>, Phusion™ HF Buffer. The reaction conditions were as follows: denaturation 98°C (5 s), annealing 56°C (20 s), extension 72°C (10 s) for 10 cycles. PCR products were purified on 5% polyacrylamide gel with QIAquick Gel Extraction Kit, according to the instructions of the manufacturer. Briefly, bands were visualized with ethidium bromide staining on a blue light transilluminator and excised from the gel. The gel was finely cut and placed for 30 min at 50°C in diffusion buffer (0.5 M ammonium acetate, 10 mM magnesium acetate, 1mM EDTA, pH=8, 0.1% SDS). Next it was mixed by vortexing, frozen and put again at 50°C for 10 min. The process was repeated three times. The gel with the liquid was placed into a chromatography column (BioRad, USA) and quickly centrifuged to remove any gel pieces. The volume of the recovered supernatant was determined and three volumes of binding buffer were added. The solution was placed in a spin column for adsorption to silica membrane. After washing, the DNA was eluted in 10 mM TRIS-HCl buffer at pH 8. The oligonucleotide duplex (about 0.8  $\mu$ g) was digested with *EagI* and *Acc65I* (12.5 U) in the NEB3 reaction buffer in a final volume of 50  $\mu$ l at 37°C for 3 h. The digested product was purified using MinElute PCR Purification Kit, according to manufacturer's instructions. The molecular

mass and concentration was determined on a 12 % polyacrylamide gel using the GeneRuler 100 bp DNA ladder.

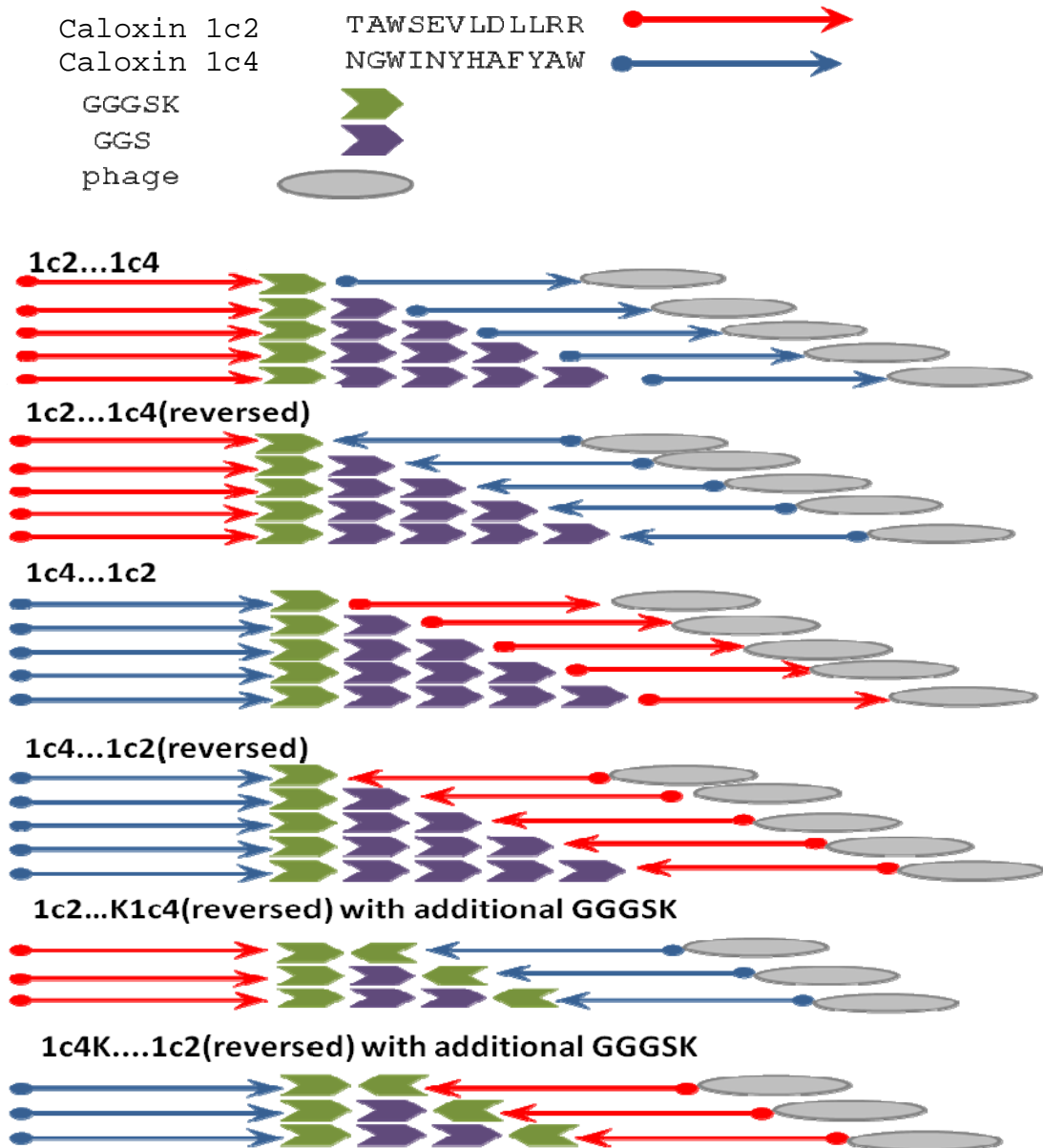


**Fig 4. Bidentate peptides expressed on M13 phage.** Peptide sequences consist of a variable sequence of caloxin 1c2 and 1c4 in two different orientations with variable number of GGS repeats. At C-terminus peptide is linked with phage particle, leaving N-terminus free.

The ligation was carried out with 20 ng vector (for preparation see section 2.15.3), 100 units of T4 DNA ligase in 10  $\mu$ l volume of 1x ligase reaction buffer (50 mM TRIS-HCl, 10 mM MgCl<sub>2</sub>, 1 mM ATP, 10 mM DTT, 25  $\mu$ g/ml BSA pH 7.5 at 25°C) for 16 h at 16°C. Next, the ligase was heat-inactivated for 15 min at 65°C. The ligated product was used to transform XL2-BlueMRF'Ultracompetent cells, following the protocol provided by the manufacturer. The transformed cells were mixed with 100  $\mu$ l XL-1 blue cells suspension and diluted further with bacterial cells and used for titer determination. Plaques were picked from these plates and the phage was amplified and titered before screening.

## **2.20. Coupled enzyme ATPase assay**

In a coupled enzyme ATPase assay, the ADP obtained upon the hydrolysis of ATP is regenerated using the energy of oxidation of NADH. The disappearance of NADH absorbance was measured at 340 nm as previously described but in 96-well UV-transparent microtiter plates using a TECAN Safire Infinite M1000 microplate reader (Chaudary et al. 2001). Ca<sup>2+</sup>-Mg<sup>2+</sup>-ATPase and Mg<sup>2+</sup>-ATPase activities were measured at 37°C under conditions where SERCA, Na<sup>+</sup>-pump and mitochondrial ATPase were inhibited. The membranes were incubated with or without caloxin for 30 min on ice. The basal Mg<sup>2+</sup>-ATPase activity was determined as slope for the disappearance of NADH in a 140  $\mu$ l assay solution (1  $\mu$ g protein, excess pyruvate kinase-lactate dehydrogenase mix, 4 ng/ml calmodulin, 0.015% Triton X-100 and the following in mM: 0.2 ouabain, 1 sodium azide, 0.005 thapsigargin, 100 NaCl, 20 KCl, 6 MgCl<sub>2</sub>, 30 imidazole-HCl (pH 7.0), 0.5

EDTA, 0.5 EGTA, 0.5 ATP, 0.2 NADH, 1 phosphoenol pyruvate). After 30 min, 10  $\mu$ l  $\text{CaCl}_2$  was added to attain a final concentration of 0.55 mM and the disappearance of NADH due to  $\text{Ca}^{2+}$ - $\text{Mg}^{2+}$ -ATPase activity was monitored for another 30 min. The difference in the ATPase activity in saturating (6 mM)  $\text{Mg}^{2+}$  with and without  $\text{Ca}^{2+}$  is defined as the  $\text{Ca}^{2+}$ - $\text{Mg}^{2+}$ ATPase activity of PMCA. The effect of caloxins on PMCA1 and 4 activities was assessed with RDM membranes and erythrocyte ghosts, respectively. PMCA1 isoform is also predominant in endothelial cell membranes; however, its activity was difficult to monitor, due to higher  $\text{Mg}^{2+}$ -ATPase activity. For PMCA2 and 3, microsomes from SF9 insect cells infected with baculoviral vectors expressing PMCA2 and PMCA3 were used. The insect microsomes, prepared by a previously published method, were a gift from Dr. A. Filoteo (Caride et.al. 2001). Triton X-100 is required to suppress high  $\text{Mg}^{2+}$ -ATPase activity or to permeabilize microsomes, however at higher concentrations it also inhibits  $\text{Ca}^{2+}$ - $\text{Mg}^{2+}$ -ATPase activity. The assay for leaky erythrocyte ghosts can be done without Triton X-100 due to low basal  $\text{Mg}^{2+}$ -ATPase activity. RDM membranes contain very high  $\text{Mg}^{2+}$ -ATPase activity, therefore, the optimization of Triton X-100 concentration was done on RDM membranes for each membrane batch. In assays comparing the effect of caloxins on  $\text{Ca}^{2+}$ - $\text{Mg}^{2+}$ ATPase activity of different PMCA isoforms, the concentration of Triton X-100 was kept the same, however the Triton X-100 to protein ratio had to be optimized independently for each membrane preparation. Decreasing the  $\text{Mg}^{2+}$  concentration or changing pH of the buffer within the range of 6.5-7.8 did not increase the difference between basal  $\text{Mg}^{2+}$ -ATPase and  $\text{Ca}^{2+}$ - $\text{Mg}^{2+}$ -ATPase. Due to solubility problems caloxin 1c5 had to be

dissolved in DMSO. DMSO final concentration up to 1.8% did not affect  $\text{Ca}^{2+}$ - $\text{Mg}^{2+}$ -ATPase activity in erythrocyte ghost membranes. Final concentration used in assay did not exceed 0.5%.

### **2.21. $[\text{Ca}^{2+}]_i$ determination in endothelial cells**

$[\text{Ca}^{2+}]_i$  in pig coronary artery endothelial cells was measured using the fluorescent  $\text{Ca}^{2+}$  indicator Fluo 4/AM, as previously described (Szewczyk et al. 2010). Endothelial cells were cultured from pig coronary artery, as described in section 2.2. After passage 4 cells were seeded into 96-well polystyrene plates and cultured until subconfluent. After removing the growth medium, the cells were washed three times with a wash buffer (in mM: 115 NaCl, 25 HEPES, 12 glucose, 5.8 KCl, 2.2  $\text{KH}_2\text{PO}_4$ , 1  $\text{CaCl}_2$ , 0.6  $\text{MgCl}_2$ , 2 probenecid). Next, the cells were incubated in the wash buffer containing fluorescent  $\text{Ca}^{2+}$  indicator Fluo 4/AM (4  $\mu\text{M}$ ) and pluronic acid (0.02%) in the dark for 45 min at room temperature. After dye loading the cells were washed two times with the wash buffer to remove the dye and incubated in it for another 25 min to allow proper dye de-esterification. The wash buffer was then exchanged and the plate was placed in the TECAN Safire microplate reader at 37°C for 5min. Background fluorescence was recorded at an excitation of 485 nm and emission of 525 nm for 2 min and then caloxin (dissolved in ethanol) was added. As a control, the same ethanol was added to some wells (final concentration 0.004%). The caloxin was also added to unloaded cells to determine the effect of caloxin itself on fluorescence intensity. After another 20 min, calibration was carried out. Maximal fluorescence intensity ( $F_{\text{max}}$ ) was determined in the presence of the  $\text{Ca}^{2+}$  ionophore 4-bromo A23187 (6  $\mu\text{M}$  in wash buffer, TefLabs, Austin,

USA) and minimal fluorescence intensity ( $F_{min}$ ) was obtained by addition of 2 mM EGTA to the above. Fluorescence values were expressed as percent of maximum ( $100 \times (F - F_{min}) / (F_{max} - F_{min})$ ). The background fluorescence was subtracted to determine the change in fluorescence with time.

## **2.22. Data Analysis**

The values given are mean  $\pm$  SEM. For non-competitive inhibition by caloxins in the presence of saturating substrates, the data was analyzed by non-linear regression using the equation: percent inhibition =  $100 \times [\text{inhibitor}] / (K_i + [\text{inhibitor}])$ . The curve fitting was done with FigP software (Biosoft Corporation, Ancaster, Ontario). Statistical significance was determined with Student's t-test, ANOVA or Chi-square test using the software GraphPad InStat (San Diego, CA) and values of  $p < 0.05$  were considered to be significant.

### 3. RESULTS

The present study aimed towards developing inhibitors as tools to understand the role of PMCA in coronary artery function. It had three major Aims. Aim 1 was to determine PMCA isoform expression in pig coronary artery EC and SMC, Aim 2 was to obtain a PMCA1 isoform selective caloxin using the N-terminal half of exdom1 (exdom1X) of PMCA1 as a target and Aim 3 was to obtain ultra high affinity PMCA4 isoform selective bidentate caloxins.

#### 3.1. PMCA isoform expression in pig arterial SMC and EC

The goals in this Aim were to determine the relative levels of PMCA activities in SMC and EC and to delineate the PMCA isoforms expressed in the two tissues. PMCA isoform distribution in EC and SMC was analyzed at mRNA and protein levels, using RT-PCR and Western blot analysis, respectively. Moreover, PMCA  $\text{Ca}^{2+}$ - $\text{Mg}^{2+}$ -ATPase activity was compared in those tissues using an enzyme coupled assay. Since EC form a monolayer inside the vessel and the amount of material is very small, freshly isolated EC could be used only to determine PMCA expression at the mRNA level and cultured EC were used in all other experiments.

##### 3.1.1 PMCA mRNA expression

RT-PCR was conducted in RNA isolated from freshly isolated and cultured EC and SMC using primers specific for PMCA1, 2, 3 and 4 (Table 3). In all instances, the primers flanked the cryptic splice site C that lies within the PMCA regulatory domain. The PCR conditions were optimized with brain and heart cDNA. RT-PCR using SMC

and EC gave products only with primers for PMCA1 and PMCA4, no products were observed with PMCA2 and PMCA3 specific primers. Based on RT-PCR results, fresh aortic EC and cultured pig coronary artery EC express PMCA1b and 4b and fresh aortic smooth muscle tissue and cultured pig coronary artery SMC expresses PMCA 1b, 4b and 4a (Fig 5). The exact nature of the observed bands was confirmed by sequencing the DNA extracted from these bands. The following controls gave no PCR products: no reverse transcriptase and no cDNA template (data not shown). Since optimal conditions for PMCA1 and PMCA4 specific primers were identical, co-PCR with both primer sets and with different cDNA dilutions were used to determine which PMCA isoform is expressed in higher amounts at mRNA level (Fig 5). With very dilute cDNA from cultured and fresh EC, only the band for PMCA1b was observed. Using very dilute cDNA from SMC and based on the relative intensities and molecular weights of bands, PMCA4 gene products (a+b) were 60-70% (fresh aortic SMC), 50% (cultured pig coronary artery SMC) and PMCA1 was 30-40% (fresh aortic SMC) and 50% (cultured pig coronary artery SMC). Thus, at mRNA level EC express predominantly PMCA1 and SMC express both PMCA1 and 4.

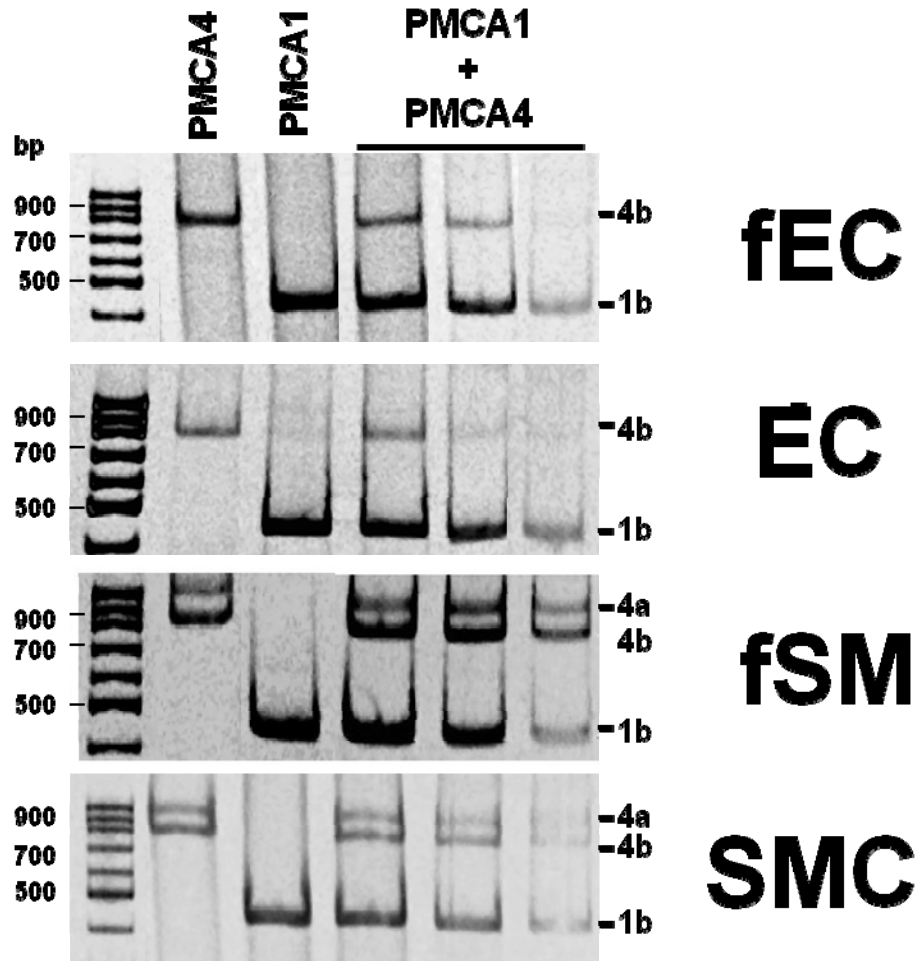


**Fig. 5. PMCA isoform expression in pig vascular tissues examined using RT-PCR.** **fSM:** fresh aortic smooth muscle, **fEC:** freshly isolated endothelial cells from aorta, **EC:** cultured endothelial cells from coronary artery, **SMC:** cultured smooth muscle cells from coronary artery. PMCA4 and PMCA1 specific primers were used separately in the first two lanes and co-PCR with the two primer sets with different cDNA dilutions were conducted for the others. Expected molecular weights for PMCA4a, PMCA4b, and PMCA1b bands are 902, 727, and 429 bp, respectively. The identities of PMCA1b and PMCA4b bands were confirmed by the sequencing of gel-purified PCR products. PMCA1b sequence was identical to that previously published (Genbank accession # NM\_214352). Pig PMCA4b sequence (deposited in Genbank DQ145551) was not previously known but it has 88% identity with the human PMCA4b (Genbank accession NM\_001684). The identity of PMCA4a was confirmed by RT-PCR with PMCA4a specific primers.

### **3.1.2. PMCA protein expression**

The relative abundance of PMCA in pig coronary artery cultured EC and fresh SMC was determined with three different antibodies: an antibody that recognizes all PMCA isoforms, an anti-PMCA1 and an anti-PMCA4. In initial experiments, it was determined that RDM expressed predominantly PMCA1 and the erythrocyte ghosts contained mostly PMCA4. Therefore, RDM and erythrocyte ghosts were used as controls. Fig 6 shows band intensities in Western blots for total PMCA, PMCA1 and PMCA4 expression in 0.5, 1 and 2  $\mu$ g plasma membrane protein of RDM, erythrocyte ghosts, SMC and EC. Based on the relative intensities of the total PMCA bands, it was computed that SMC contain 2.9 times more total PMCA protein than EC (Fig. 7). Analysis of the PMCA1 and PMCA4 data showed that SMC contained 8.4 times more PMCA4 than EC whereas EC contain 4.2 times more PMCA1 (Fig. 7). Since RDM expressed mostly PMCA1 and erythrocyte ghosts contain mostly PMCA4, computations were carried out with the assumption that relative band intensity of total PMCA equals relative band intensity of PMCA1 in RDM and PMCA4 in erythrocyte ghosts. Based on this assumption it was calculated that EC express 78 % PMCA1 and 22 % PMCA4 and SMC express 90 % PMCA4 and 10 % PMCA1 protein. The analysis done on repeating the experiments using membrane preparations from different days were consistent with presented results in that pig coronary artery EC express mainly PMCA1 whereas SMC contain mostly PMCA4.

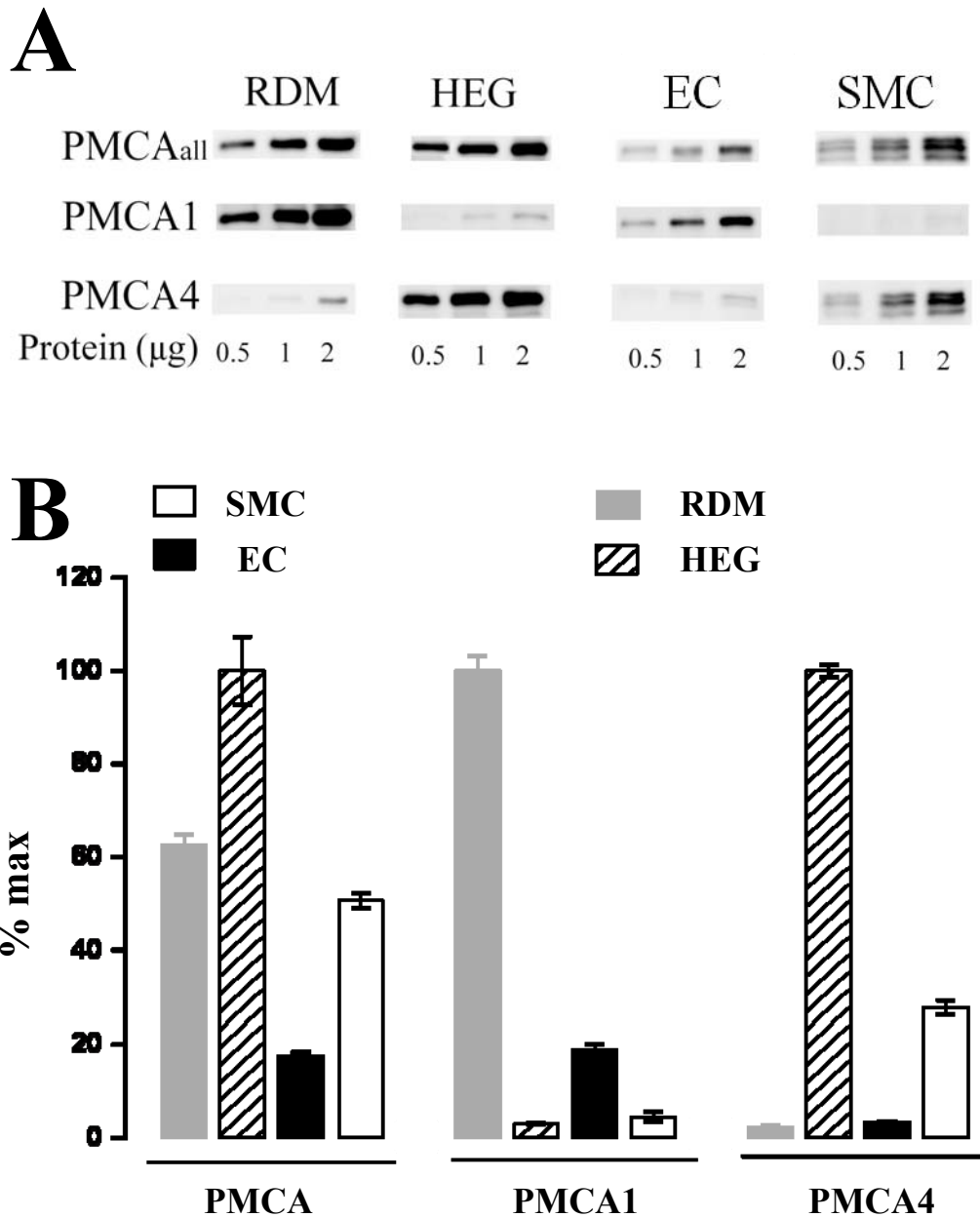


**Fig. 6. PMCA isoform expression analyzed by Western blots.** RDM: rabbit duodenal mucosa; HEG: human erythrocyte ghosts; EC: cultured pig coronary artery endothelial cells; SMC: cultured pig coronary artery smooth muscle cells. **A:** The amount of plasma membrane proteins loaded, primary antibodies used and the tissues are specified. All the lanes from different tissues for each antibody were compared together in one gel. **B:** The relative intensities of bands per μg protein are presented as % maximal value within a group. The values are mean +/- SEM of 3 replicates (Szewczyk et.al. 2010).

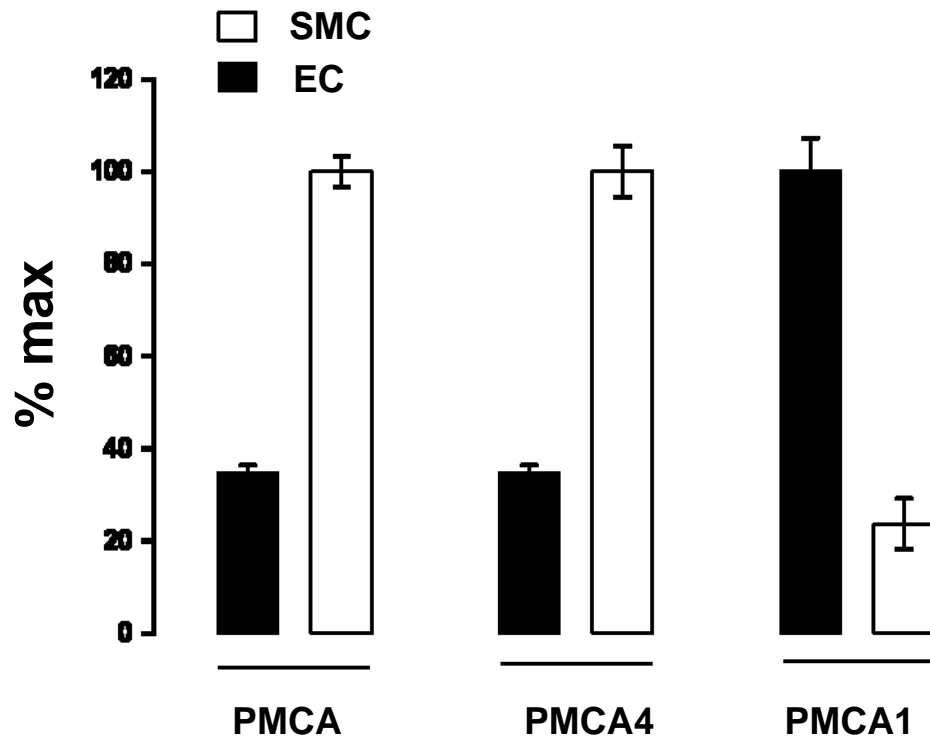


**Fig. 7. Comparison of PMCA isoform expression in pig coronary artery EC and SMC analyzed by Western blots.** EC: cultured pig coronary artery endothelial cells; SMC: cultured pig coronary artery smooth muscle cells. The relative intensities of bands per  $\mu\text{g}$  protein are presented as % maximal value within a group. The values are mean  $\pm$  SEM of 3 replicates.

### 3.1.3. PMCA $\text{Ca}^{2+}$ - $\text{Mg}^{2+}$ -ATPase activity

PMCA  $\text{Ca}^{2+}$ - $\text{Mg}^{2+}$ -ATPase activity was measured in plasma membrane enriched fractions isolated from pig coronary artery fresh SMC and cultured EC as  $\text{Ca}^{2+}$ -stimulated hydrolysis of ATP in a coupled enzyme assay containing calmodulin and the following inhibitors of other ATPases: sodium azide (mitochondrial  $\text{Ca}^{2+}$ -ATPase), ouabain ( $\text{Na}^+$ - $\text{K}^+$ -ATPase) and thapsigargin (SERCA). PMCA activity was 3.66 times lower in EC ( $0.3 \pm 0.1$  nmol/min/mg protein) than in SMC ( $1.1 \pm 0.2$  nmol/min/mg protein). PMCA activity

results are consistent with the values of abundance of total PMCA obtained in Western blots with antibody recognizing all PMCA isoforms (5F10) (Fig. 8). The comparison was done on the same membrane preparation. The activity results are also similar with the values of abundance of total PMCA obtained in Western blots with membrane from different membrane preparations, where SMC contained 2.9 times more total PMCA compared to EC (Fig. 7).

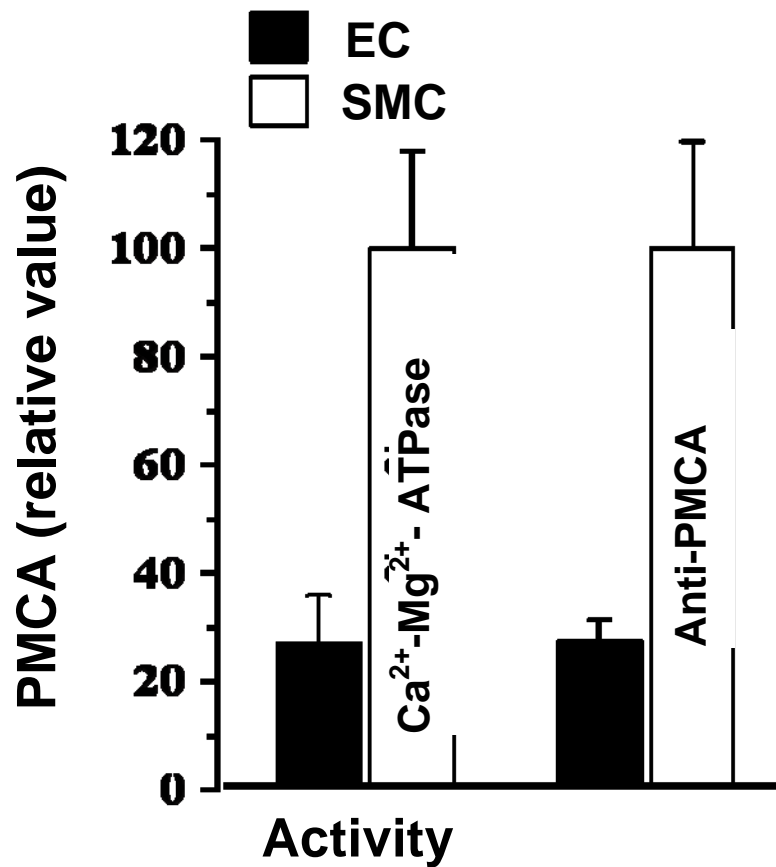


**Fig.8. Relative values of PMCA activity and total PMCA protein abundance in Western blots in pig coronary artery EC and SMC.** The relative value for each parameter was computed taking the mean value in SMC as 100%. PMCA activity in EC was  $0.3 \pm 0.1$  nmol/min/mg protein and in SMC  $1.1 \pm 0.2$  nmol/min/mg protein.

### **3.2. Aim 2: Invention of PMCA1 selective caloxins**

Exdom1 of PMCA is the most divergent between all the PMCA isoforms (see Fig. 3). However, exdom1 is long and contains a cysteine residue that can produce uncertainties in the configuration of the exdom. Therefore, it was divided into exdom1X (N-terminal half) before this cysteine and exdom1Y (C-terminal half) after it. The overall experimental strategy to be used is described in Fig 9. Similar strategies have been used successfully for PMCA4 specific inhibitors.

#### **3.2.1. Tissue selection for PMCA1**

A source rich in PMCA1 and mainly in PMCA1 was required to invent PMCA1 selective caloxins and to assay their inhibitory properties. Such a tissue should also be poor in other PMCA isoforms and be easily obtained in large amounts. A source had to be found. RT-PCR with the primers, flanking cryptic splice site C that lies within PMCA regulatory domain was used to determine the PMCA genes in several cell lines and tissues. Primers for human PMCA isoforms were previously published (Stauffer et al. 1995). Rabbit brain and heart was used to test and optimize conditions for rabbit PMCA isoforms. Neither HEK293 cells nor RDM expressed PMCA2 and PMCA3 mRNA (data not shown). Figure 10 shows the results for RT-PCR using PMCA1 and PMCA4 specific primers in HEK283 and RDM. Controls without reverse transcriptase or those without RNA did not show any bands (data not shown).

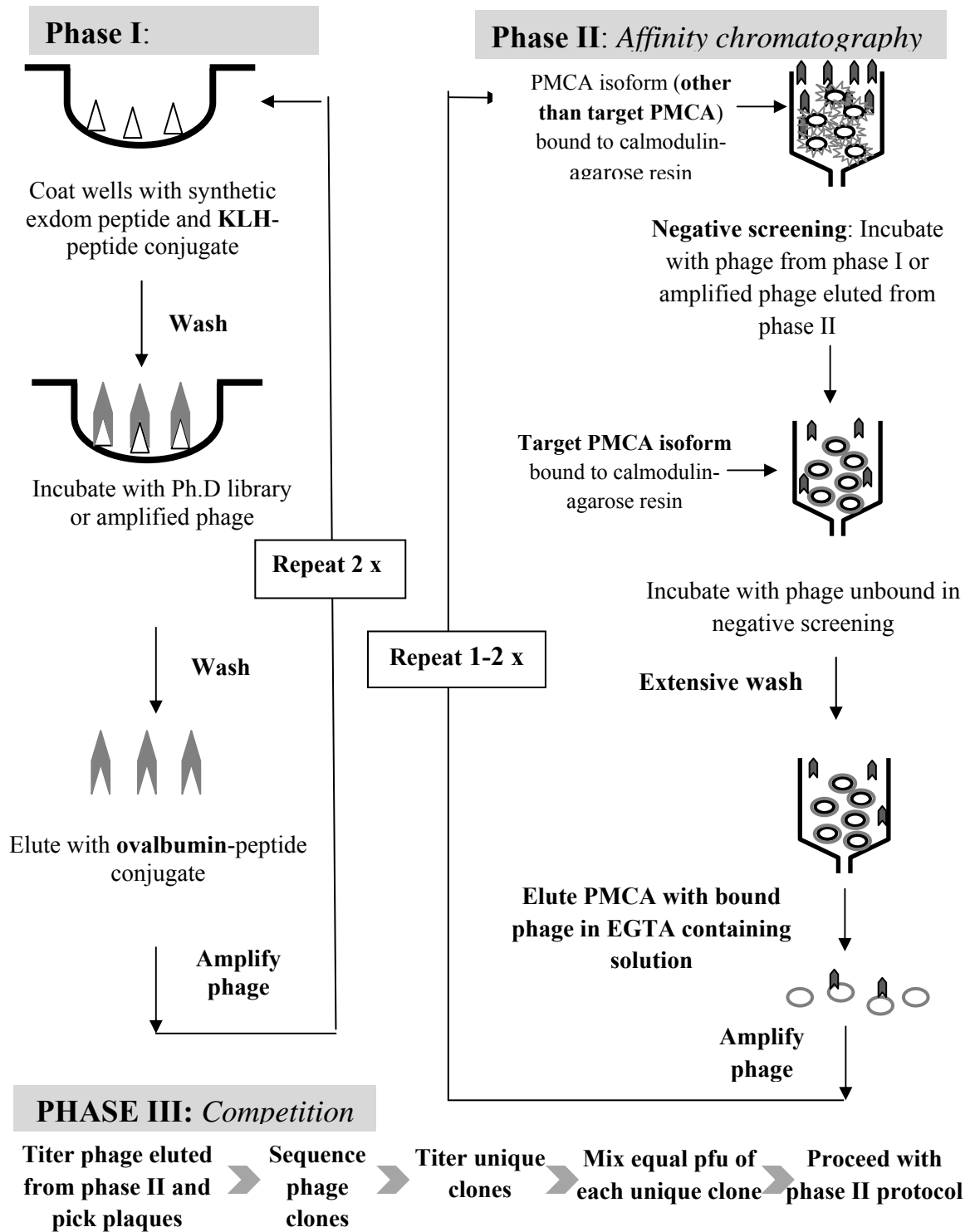


**Fig. 9. Overview of the screening procedure to obtain isoform selective caloxins.** Details are described in Experimental methods (sections 2.9-2.14).

Thus, based on molecular weights, HEK293 cells express PMCA1b and 4b and RDM express PMCA1b, 4b and 4a splice variants. Since the optimal conditions were identical for PCR using PMCA1 and PMCA4 selective primers, co-PCR with primers for both PMCA1 and PMCA4 was carried out for transcripts from HEK293 cells and RDM. Since in both tissues the band corresponding to PMCA1b was predominant it was concluded that RDM and HEK293 cells expressed predominantly mRNA for PMCA1 isoform. To compare PMCA1 isoform abundance at protein levels, Western blots with anti-PMCA1 antibody were done with HEK293 and RDM plasma enriched fraction (Fig. 11). Based on relative band intensities it was computed that RDM expresses much more PMCA1 per  $\mu\text{g}$  protein than HEK293 cells (114 times difference in intensities). Thus, RDM is a rich source for PMCA1. Affinity chromatography experiments require large amounts of membrane fraction (4 mg protein per experiment) and from one rabbit duodenum only 5-7 mg of RDM membrane fraction can be obtained; therefore pig duodenum mucosa was tested for PMCA1 and 4 isoform expression. Compared to rabbit RDM, pig duodenum mucosa contained much less of PMCA 1 and more PMCA4 (data not shown). Pig duodenal mucosa was much harder to dissect from smooth muscle layer, compared to RDM, which would result in higher content of smooth muscle in the collected tissue. The mucosa from other parts of rabbit intestine (duodenum, jejunum, proximal colon, distal colon and caecum) was also analyzed for PMCA1 and 4 content (Fig. 12). RDM and rabbit jejunum contained the highest levels of PMCA1. Based on relative band intensities it was calculated that the PMCA1 to 4 ratio in duodenum and jejunum were similar. Since, RDM expressed the highest levels of PMCA1 compared to other tissues, it

contained low levels of PMCA4 and no detectable mRNA for PMCA2 or PMCA3, it was chosen as the source of PMCA1 for further work in this Aim.

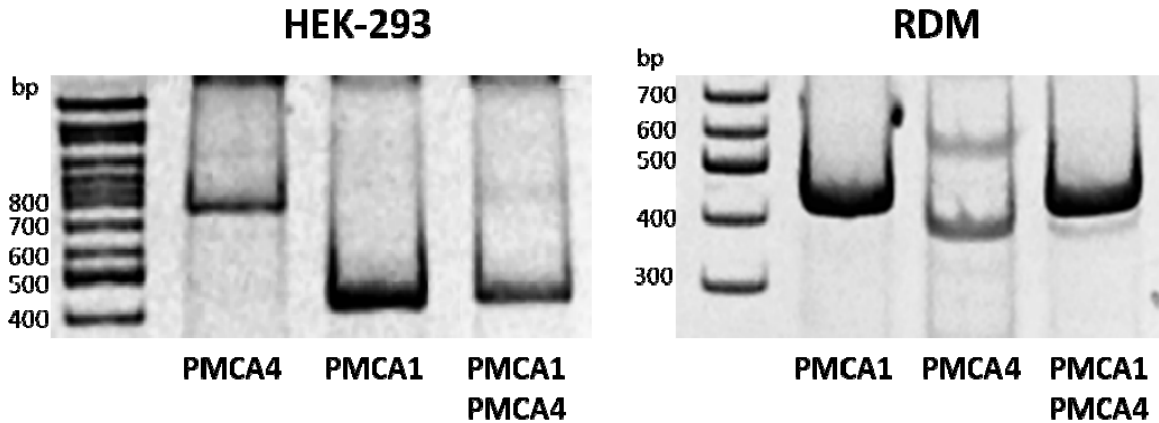


**Fig. 10. PMCA isoform expression in HEK-293 cells and RDM examined using RT-PCR.** Expected sizes for human and rabbit PMCA1b, human PMCA4b, rabbit PMCA4a and rabbit PMCA 4b were 429 bp, 727 bp, 551bp and 376 bp, respectively. RT-PCR for each set of primers was done with the same amount cDNA.

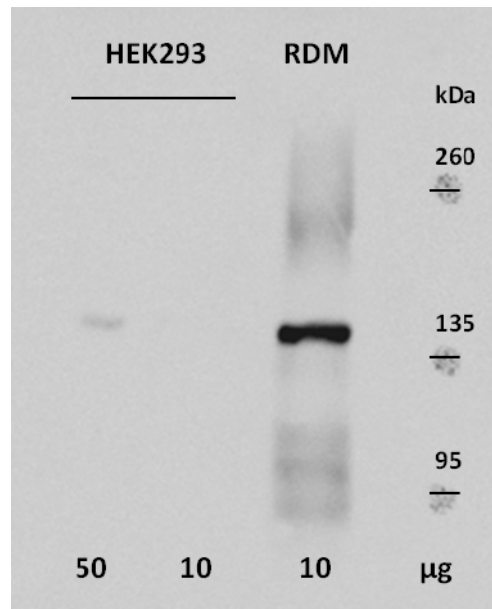


**Fig.11. PMCA1 protein expression in HEK293 and RDM plasma membrane enriched fraction.** The amount of plasma membrane proteins loaded and the tissues are labeled. All the lanes from different tissues were compared together in one gel.

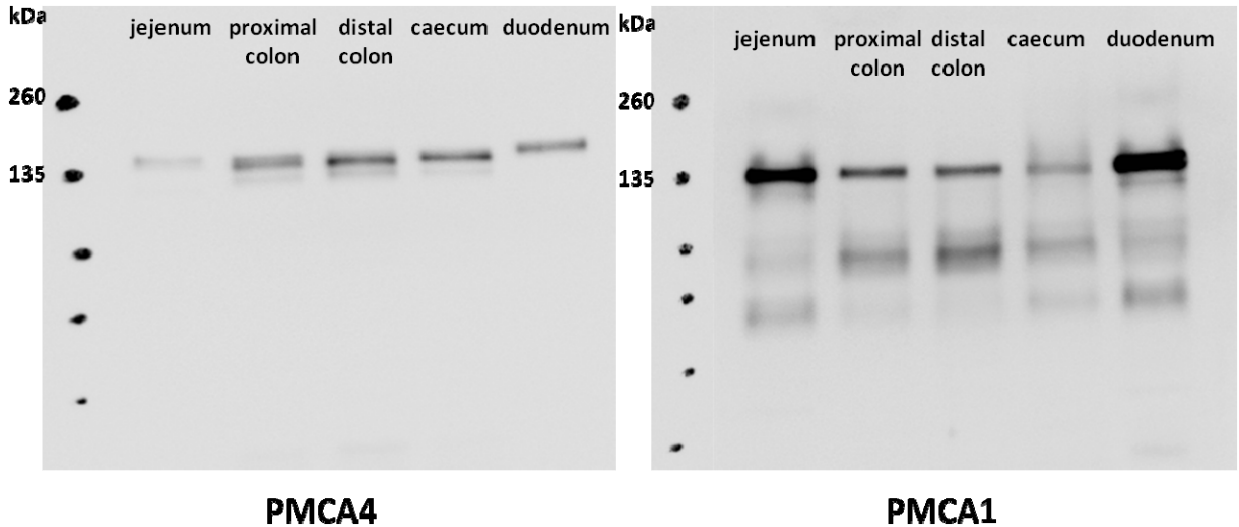


**Fig. 12. PMCA1 and PMCA4 isoform expression in mucosa from different parts of rabbit intestine.** 5  $\mu$ g plasma membrane protein of each tissue was analysed with anti-PMCA1 or anti-PMCA4 antibodies. All samples were compared together in one gel.

PMCA1 is the predominant isoform present in the plasma membrane of RDM (Fig. 6). Therefore, it was also chosen to test caloxins for PMCA1  $\text{Ca}^{2+}$ - $\text{Mg}^{2+}$ -ATPase activity inhibition in a coupled enzyme assay. However, the RDM membranes contained very high basal  $\text{Mg}^{2+}$ -ATPase activity. Several experiments were done to determine how to suppress the basal activity while retaining the  $\text{Ca}^{2+}$ - $\text{Mg}^{2+}$ -ATPase activity (not shown). It was determined that Triton X-100 suppressed the basal activity but at higher concentration it also inhibits  $\text{Ca}^{2+}$ - $\text{Mg}^{2+}$ -ATPase. Due to variability between membrane preparations the optimization of Triton X-100 concentration had to be done on RDM membranes for each membrane batch. Decreasing  $\text{Mg}^{2+}$  concentration or changing pH of the buffer within the range of 6.5-7.8 did not improve PMCA activity. Since EC have PMCA1 as the dominant isoform, attempts were also made to monitor PMCA activity in

the EC membranes. However, basal  $Mg^{2+}$ -ATPase activity was too high compared to PMCA activity and all attempts to optimize conditions failed. Thus, RDM membranes were chosen as a best source for monitoring PMCA1 activity.

### **3.2.2. Phase I: Biopanning**

The synthetic peptide corresponding to PMCA1 residues 119-137 (IVSLGLSFYQPPEGDNALC, Protein bank P20020) was used as a target for screening Ph.D-12 phage library displaying random 12 amino acid peptides. The peptide consists of exdom1X of PMCA1 (residues 121-137) with additional two aminoacids (119-120) of TM1 in the N-terminus. The peptide was used as such or with its cysteine residue conjugated to KLH or ovalbumin. A mixture of peptide and peptide-KLH conjugate was used as a target for trapping the phage while the peptide-ovalbumin conjugate was used for elution. The screening was started with  $1 \times 10^{12}$  pfu of the Ph.D-12 library. The phage was eluted, amplified and the screening was repeated two more times with the constant input of  $1 \times 10^{10}$  pfu. The phage pool selected after three rounds of screening was tested for its selectivity for binding to exdom1X of PMCA1 over exdom1X of PMCA4. The phage population obtained after 3 rounds of panning contained a significantly larger number of phage particles that bound preferentially to the synthetic exdom1X of PMCA1 as compared to synthetic exdom1X of PMCA4 (Fig. 13). Only the selected phage, and not the initial library, showed this preference for binding to exdom1X.

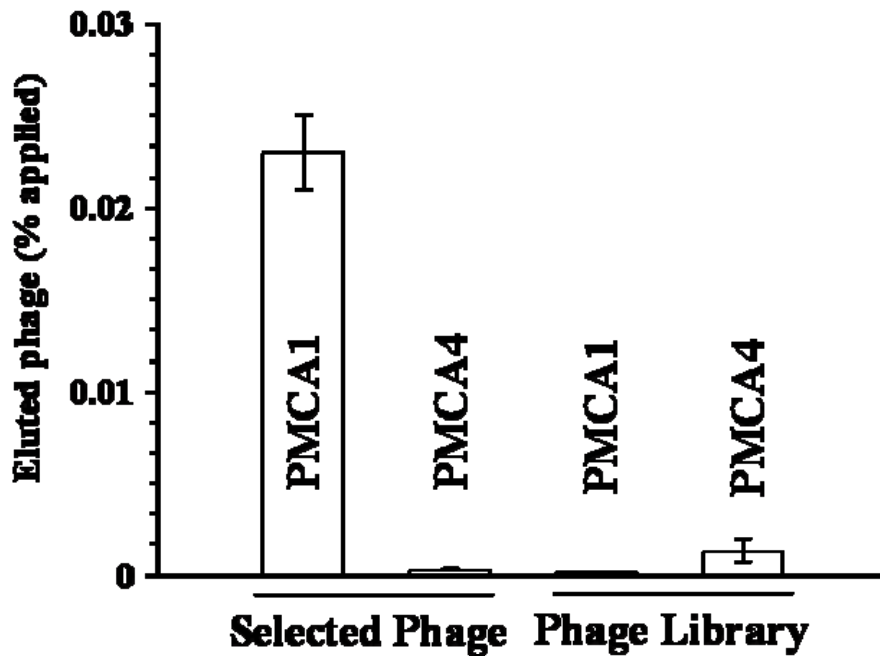


**Fig. 13. Selectivity of phage population obtained upon biopanning.** The data are mean  $\pm$  SEM of a total of 6 replicates from two experiments. The pfu applied/well were  $9.6 \times 10^5$  in the first experiment and  $2.6 \times 10^6$  in the second. Each experiment was conducted in triplicate. The counts for the eluted phage in each experiment were converted to percent applied and pooled. A multiway ANOVA test showed that the group PMCA1-selected phage differed significantly from all the other groups ( $p < 0.05$ ). The three remaining groups did not differ significantly from each other ( $p > 0.05$ ). (Szewczyk et al. 2010)

### 3.2.3. Phase II: Screening by affinity chromatography with RDM PMCA

#### 3.2.3.1. Optimization of affinity chromatography

In preliminary experiments PMCA was purified from RDM on a calmodulin-agarose column with the methods previously described for erythrocyte ghosts PMCA (Pande et al. 2006). However, purification of RDM PMCA was not very efficient with this approach. First, the optimization focused on increasing PMCA binding to the column; however the attempts only marginally improved the efficiency in PMCA purification. The attempts included: prevent calpain cleavage (including calpain inhibitor

in homogenization buffer), ensure that PMCA is free of calmodulin (introducing additional water/EGTA wash during RDM isolation to burst microsomes and chelate  $\text{Ca}^{2+}$ ), increase time for PMCA binding to agarose-calmodulin and removing acidic phospholipid-phosphatidylserine from the protocol. Next, the elution step was analyzed in more detail. The elution of erythrocyte ghost PMCA was carried out at 4°C by applying  $\text{Ca}^{2+}$ -free, EGTA containing elution buffer (100  $\mu\text{l}$  /100  $\mu\text{l}$  resin) two times. Analysis of the eluates showed that with this approach most of RDM PMCA remained on the column. As shown in Fig. 14, increasing the incubation time to 2 h (two times 1 h) at 4°C and introducing sample rotation did not improve elution efficiency. However, increasing the elution temperature to 37°C resulted in a significant increase in amounts of eluted PMCA.

### 3.2.3.2. Screening results

*Experiment 1:* The phage population selected after three rounds of screening for binding to synthetic PMCA1 exdom1X peptide was screened in three cycles of affinity chromatography with RDM PMCA (Fig. 9, Phase II). The phage input in each cycle was  $1 \times 10^{10}$  pfu and the eluate was amplified after the first and the second cycles to attain the large number of pfu needed for the next column. As shown in Table 5 the binding efficiency decreased unexpectedly after the third round of screening.

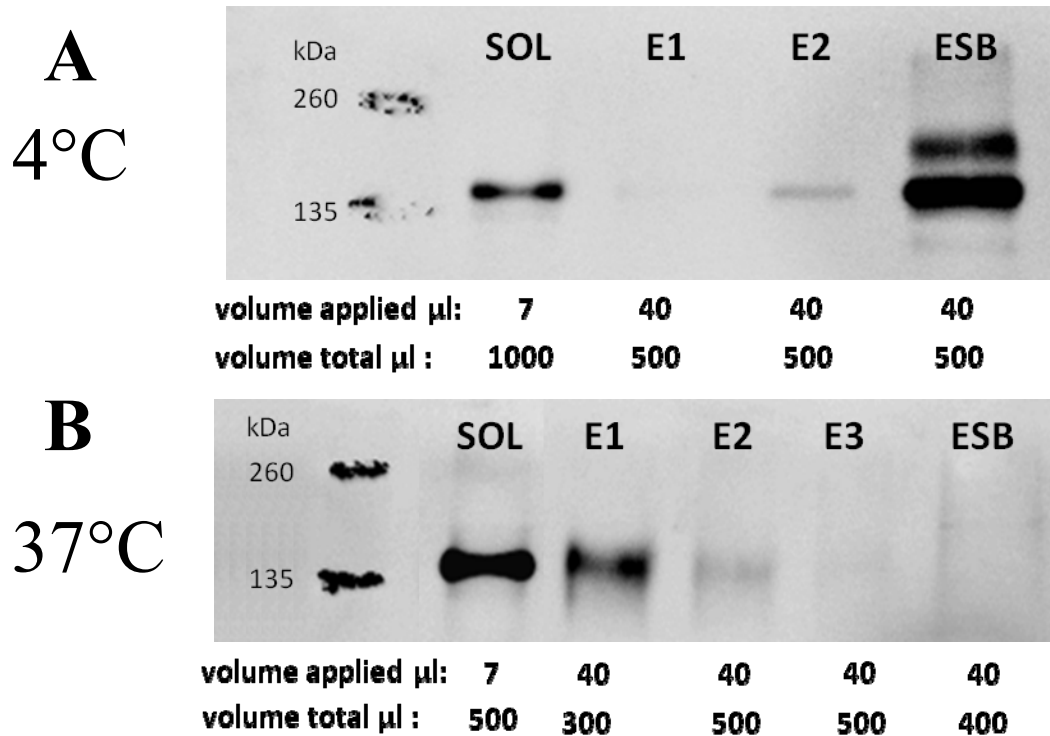


**Fig. 14. Western blot analysis of RDM PMCA1 eluted from calmodulin-agarose column.** Solubilised protein (SOL) was applied on calmodulin-agarose column and rotated for 1h at 4°C. Column was washed with 10 ml of wash buffer. **A.** Resin with PMCA was incubated with elution buffer containing 5 mM EGTA (100  $\mu$ l/100  $\mu$ l beads) for 1h on rotator at 4°C and eluate was collected (**E1**). The process was repeated and all liquid was removed by centrifugation (**E2**). Next 5 x Laemmli sample buffer was added (100  $\mu$ l/100  $\mu$ l beads) to dried beads and incubated for 5 min at 95°C and eluate was collected (**ESB**). **B.** Resin with PMCA was incubated with elution buffer for 30 min at 37°C and eluate was collected (**E1**). The process was repeated twice (**E2**, **E3**). The resin was incubated with 5 x Laemmli sample buffer as described above and **ESB** was collected. The total volumes of collected samples and volumes of samples applied on a gel are shown. The analysis was done with anti-PMCA1 antibody.

**Table 5. Binding efficiency in each round of phase II.**

Round #	Input (pfu)	Output (pfu)	Binding efficiency %	Comments
I	$1 \times 10^{10}$	$2.1 \times 10^5$	0.0021	amplified
II	$1 \times 10^{10}$	$1.6 \times 10^6$	0.0160	amplified
III	$1 \times 10^{10}$	$1.5 \times 10^5$	0.0015	titered and sequenced

Phage eluted after the third round was titered and 190 clones were sequenced. Out of 190 sequenced clones there were 46 unique clones and 109 clones encoded for the variable peptide SVSVG MKPSRP (60% of total). To test the predominant clone for amplification efficiency, the phage population selected after three rounds of screening was amplified four times and 12 clones were sequenced. Out of 12 clones 11 encoded for the variable peptide SVSVG MKPSRP. This indicates that a high amplification efficiency of this phage clone in the three cycles led to its predominance. This may also have been a cause for a reduction in the binding efficiency during consecutive steps. The peptide was also analyzed by program SAROTUP (Scanner And Reporter Of Target-Unrelated Peptides). The program has a database of target unrelated peptides (TUPs) which are likely to bind to other than target components of the screening system (e.g. plastic plates) or have a higher amplification efficiency. The program classified SVSVG MKPSRP as propagation-related TUP, which is repetitively selected from the commercially available Ph.D.-12 library in many labs using completely different targets.

*Experiment 2:* Since the amplification resulted in the enrichment of SVSVG MKPSRP phage,  $1 \times 10^{10}$  pfu of the phage population selected after three rounds of panning was used in two rounds of affinity chromatography with RDM PMCA

without the amplification step in between. DNA from 90 phage clones was sequenced. Out of these there were 66 unique clones (55 differed from the previous affinity chromatography screening) and only 14 encoded the previously observed peptide SVSVG MKPSRP (15%). Nevertheless the predominant clone was still the most abundant clone indicating that it was already enriched during amplifications done in the panning experiment (Fig. 9, phase I).

### **3.2.4. Phase III: Competition experiment**

To rule out selection of phage due to copy-number bias that can arise during library construction, panning and phage amplification, a mixture of equal numbers of 101 unique phage clones selected in phase II were allowed to compete for binding to RDM PMCA during affinity chromatography in two separate experiments. Following the competition, the DNA from 95 clones from each eluate was sequenced. The clones encoding the peptide TIPKWISIIQALR had the highest frequency, those encoding peptide sequence QDWMKLLEVMRK were next (Table 6). The success of the competition experiment is demonstrated by the observation that the previously predominant clone displaying the peptide SVSVG MKPSRP was eliminated in this experiment. The most frequently observed peptide sequences were not identified as TUP artifacts by the program SAROTUP. The variable sequence along with a spacer that connects it to the coat protein in phage was chemically synthesized and designated as caloxin 1b3 (TIPKWISIIQALRGGGSK-amide) and caloxin 1b4 (QDWMKLLEVMRKGGGSK-amide).

**Table 6. Phage clones obtained after competition experiment in affinity chromatography with RDM PMCA. Predominant clones are bolded**

Variable peptide sequence	Clone frequency		
	Competition I	Competition II	% Total (Comp.I + Comp.II)
DKNWDTLRLMTT	7	1	4.2
DPFLLPAADIQK	1	0	0.5
DPNIWPWNLDDN	1	0	0.5
DQNTHQLYQTHS	1	1	1.1
DYFSSPYEQLF	1	0	0.5
EMTERVAVAWQP	1	0	0.5
FAIHTPNPIKTL	1	0	0.5
FHDTFMMPSPAPR	1	1	1.1
FNPLIHTMLSQ	1	0	0.5
FTPFKHWSLPSN	1	0	0.5
GSMSPYVRWYTP	1	1	0.5
LPWPLISHYLRT	2	5	3.7
LSPRSSIHPPPR	1	0	0.5
MSMPTHSHDHAR	2	0	1.1
NNDYIPHQVLL	1	0	0.5
PRPRPPTMLAPT	3	0	1.6
<b>QDWMKLLLEVMRK</b>	<b>23</b>	<b>28</b>	<b>26.8</b>
QYVTVNLTSSER	1	0	0.5
SNNHFSALMSAG	1	0	0.5
SWPLYSRDSGLG	1	0	0.5
<b>TIPKWISIIQALR</b>	<b>39</b>	<b>59</b>	<b>51.6</b>
VSSYYVTKQVSP	1	0	0.5
YPNSTWPTPLY	1	0	0.5
YPPKTMHPDLM	1	0	0.5
YQDYFKMVPGNL	1	0	0.5

### **3.2.5. Inhibition of PMCA $\text{Ca}^{2+}$ - $\text{Mg}^{2+}$ -ATPase activity in coupled enzyme assay by caloxin 1b3 and 1b4**

Caloxin 1b3 and 1b4 were selected for binding to PMCA1 exdom1X followed by affinity chromatography using RDM PMCA which contain mainly PMCA1. RDM plasma membranes were used to test the effect of caloxins on PMCA1 inhibition in a coupled enzyme assay. Typically PMCA activity in the absence of caloxin was 0.05 to 0.1 nmol/min. The difference between the slopes of the NADH absorbance disappearance in the presence and absence of  $\text{Ca}^{2+}$  is the  $\text{Ca}^{2+}$ - $\text{Mg}^{2+}$ ATPase activity of PMCA. As shown in Fig.15 caloxin 1b3 produced 50 % inhibition of PMCA1  $\text{Ca}^{2+}$ - $\text{Mg}^{2+}$ -ATPase activity at a concentration of  $17 \pm 2 \mu\text{M}$  and caloxin 1b4 at a concentration of  $120 \pm 35 \mu\text{M}$ . Since the  $K_i$  value obtained with caloxin 1b3 was significantly smaller, only this peptide was used in further experiments.

Caloxin 1b3 was tested for PMCA isoform selectivity using membranes containing mostly PMCA1, 2, 3 or 4: human erythrocyte ghosts (PMCA4), RDM plasma membrane fraction (PMCA1) and microsomes from SF9 insect cells overexpressing PMCA2 and PMCA3. As shown in Fig.16, caloxin 1b3 inhibited PMCA1 preferentially over PMCA4 since the inhibition of PMCA1 was greater than that of PMCA4 at 15, 25, 50 or 100  $\mu\text{M}$  of this peptide. Based on the data in Fig. 16 the computed  $K_i$  value of caloxin 1b3 for PMCA4 was  $45 \pm 4 \mu\text{M}$ , which is 2.6 times higher than that for PMCA1. The effect of 15, 25 or 50  $\mu\text{M}$  of caloxin 1b3 on PMCA1, 2, 3 and 4 is compared in Fig. 17. At any concentration, the inhibition was significantly greater for PMCA1 than for other PMCA isoforms. Therefore, caloxin 1b3 is first PMCA1 isoform selective caloxin.

Caloxin 1b3 was also PMCA selective in that it had no effect on  $Mg^{2+}$ -ATPase activity when tested in erythrocyte ghosts and RDM membranes at concentrations up to 100  $\mu M$  (Fig.18).

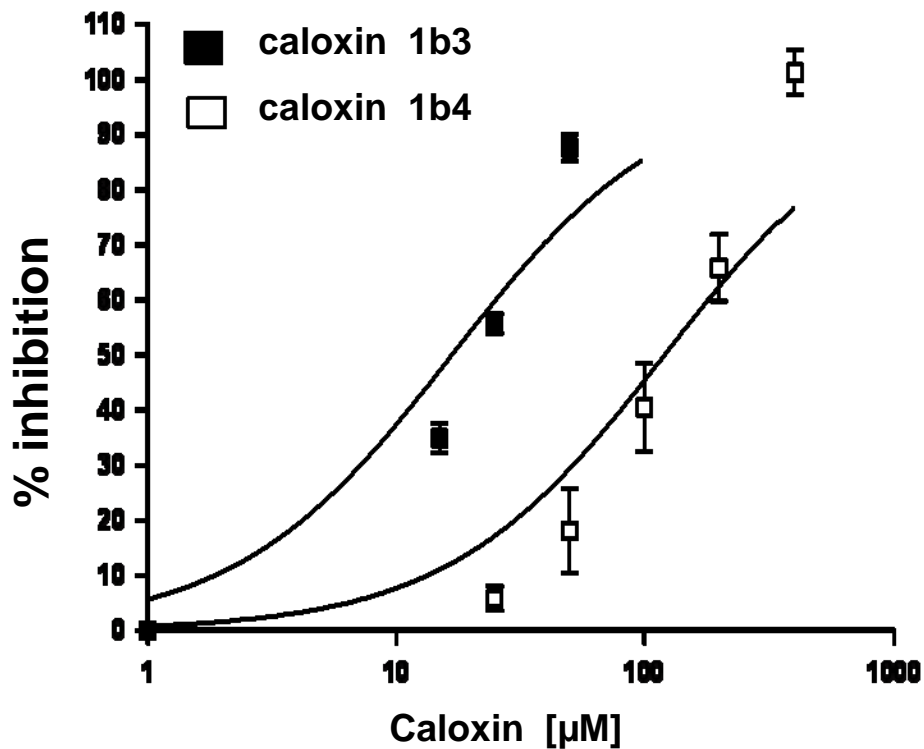


**Fig.15. Caloxin 1b3 and 1b4 inhibition of PMCA activity in rabbit duodenal mucosa measured by coupled enzyme assay.** For each experiment, the data were normalized with the mean value of the  $Ca^{2+}$ - $Mg^{2+}$  ATPase activity in the absence of caloxin taken as 100 %. Each value is the mean  $\pm$  SE of 2-4 experiments done on separate days (n = 6-24). For each day, the data were normalized with the mean value of the activity in the absence of caloxin taken as 100 %. The inhibition constant ( $K_i$ ) of caloxin 1b3 and caloxin 1b4 was calculated to be  $17 \pm 2 \mu M$  and  $120 \pm 35 \mu M$ , respectively.

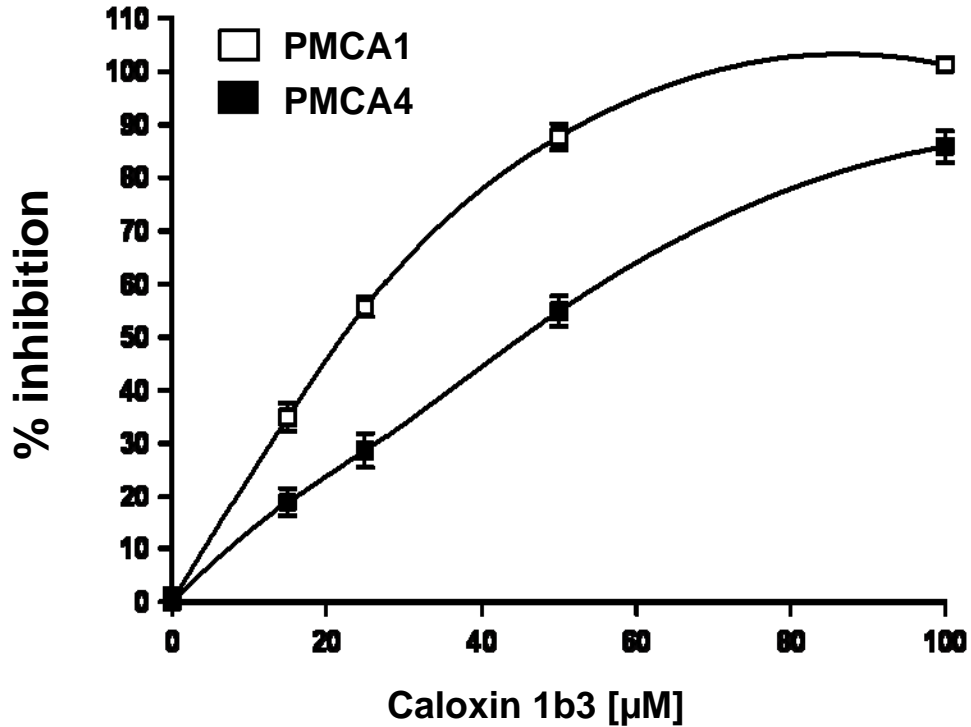


**Fig.16.** The effect of caloxin 1b3 on PMCA activity in rabbit duodenal mucosa (PMCA1) and human erythrocyte ghosts (PMCA4) measured by coupled enzyme assay. The difference between the slopes of the NADH absorbance disappearance in the presence and absence of  $\text{Ca}^{2+}$  is the  $\text{Ca}^{2+}$ - $\text{Mg}^{2+}$ ATPase activity of PMCA. For each experiment, the activity was normalized with the mean value of the  $\text{Ca}^{2+}$ - $\text{Mg}^{2+}$ ATPase in the absence of caloxin 1b3 taken as 100 %. Each value is the mean  $\pm$  SE of 2-4 experiments done on separate days (n=6-24). The data fit best with the  $K_i$  values of  $17 \pm 2 \mu\text{M}$  (PMCA1) and  $45 \pm 4 \mu\text{M}$  (PMCA4).

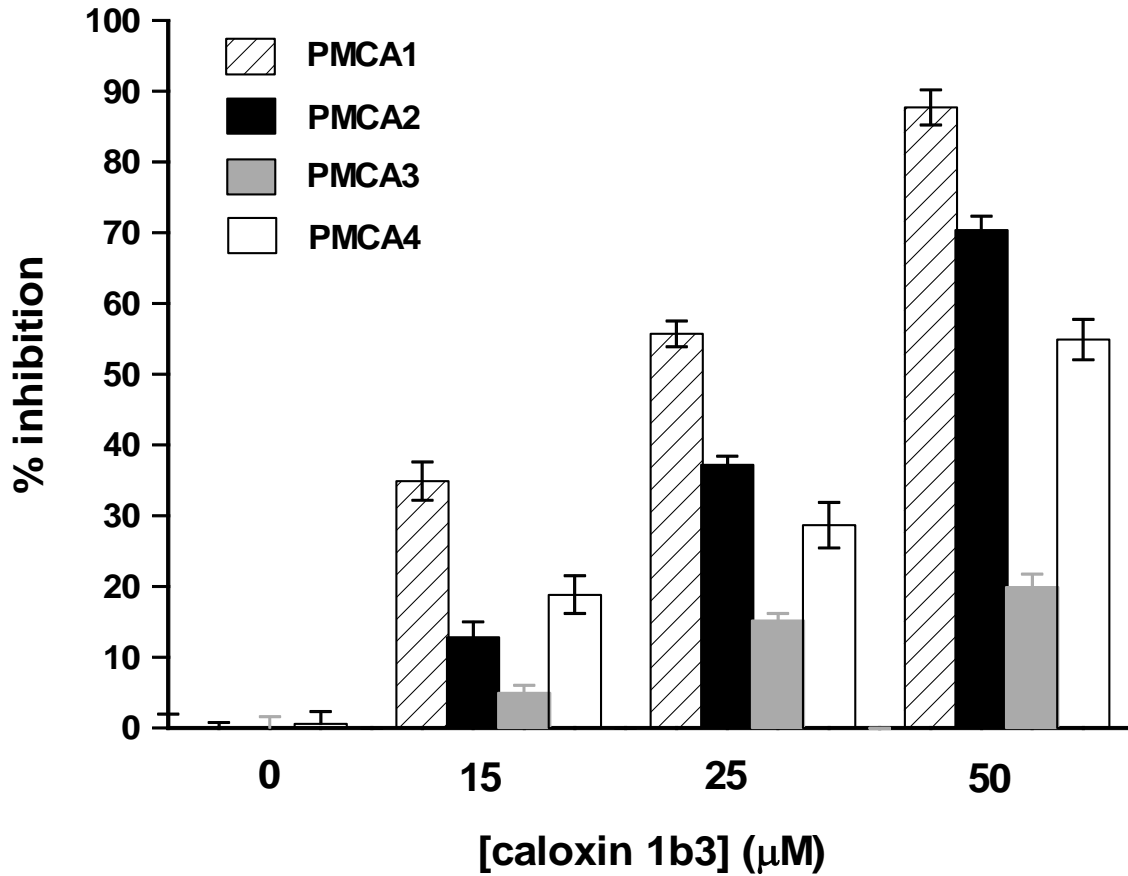


**Fig.17. Caloxin 1b3 inhibition of  $\text{Ca}^{2+}$ - $\text{Mg}^{2+}$  ATPase activity of PMCA1-4 measured in the coupled enzyme assay.** The sources of PMCA isoforms are: PMCA1 (the plasma membrane enriched fraction of RDM), PMCA2 and 3 the plasma membrane enriched fraction of SF9 insect cells overexpressing PMCA isoforms 2 or 3), PMCA4 (leaky human erythrocyte ghosts). Each value is the mean of 2 experiments done on different days. For each day, the data were normalized with the mean value of the activity in the absence of caloxin 1b3 taken as 100 %.

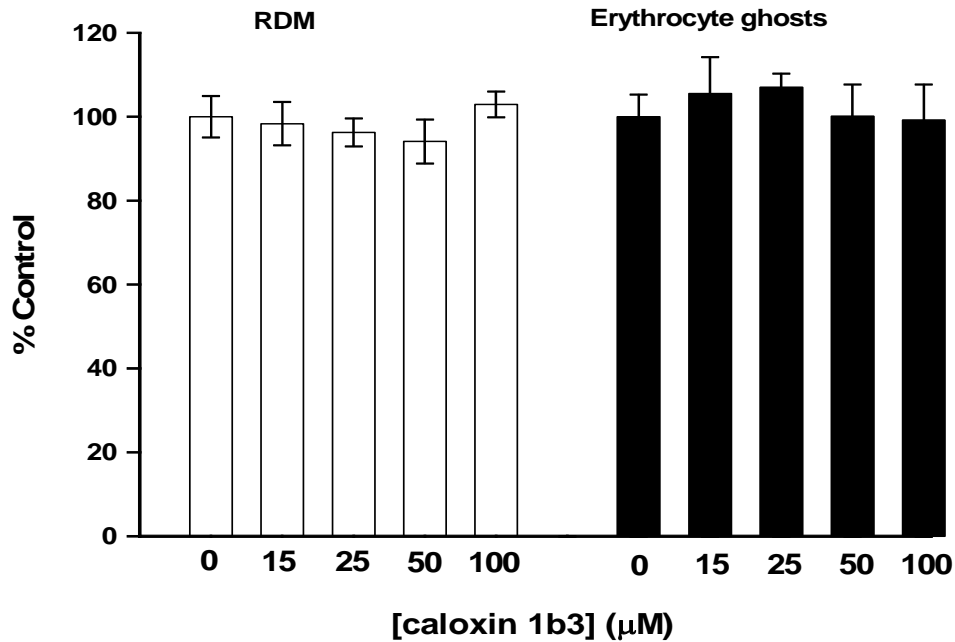


**Fig.18. The effect of caloxin 1b3 on  $Mg^{2+}$ ATPase activity in RDM membranes and human erythrocyte ghosts measured by coupled enzyme assay.** The activity in the absence of caloxin 1b3 was taken as 100 % and the activity in its presence was used to compute the % activity remaining. Each value is the mean  $\pm$  SE of 2-4 experiments done on separate days (n=6-24).

### 3.2.6. Effects of caloxin 1b3 on $[Ca^{2+}]_i$ in endothelium

Pig coronary artery endothelial cells express mostly PMCA1 (Fig. 6). Since caloxin 1b3 showed some PMCA1 isoform specificity, we determined its effects on  $[Ca^{2+}]_i$  in cultured pig coronary artery endothelial cells. Both concentrations (20 and 50  $\mu$ M) increased  $[Ca^{2+}]_i$  in EC with the increase being much greater at 50 (about 20% max) than at 20  $\mu$ M (about 50% max) (Fig.19). The experiments were also done with 0, 3, 10, 50 and 100  $\mu$ M caloxin 1b3 (data not shown). Caloxin 1b3 at concentrations of 0, 3

and 10  $\mu\text{M}$  had no effect on  $[\text{Ca}^{2+}]_i$  and the effects of 50 and 100  $\mu\text{M}$  were similar. For comparison, the effect of Caloxin 1b1 which has a preference for PMCA4 but also inhibits PMCA1 with a relatively lower affinity was also tested. Caloxin 1b1 at 20 and 50  $\mu\text{M}$  had a much smaller effect on  $[\text{Ca}^{2+}]_i$  in EC as compared to caloxin 1b3. This result is consistent with a larger expression of PMCA1 than PMCA4 in EC and the preference of caloxin 1b3 to inhibit PMCA1.

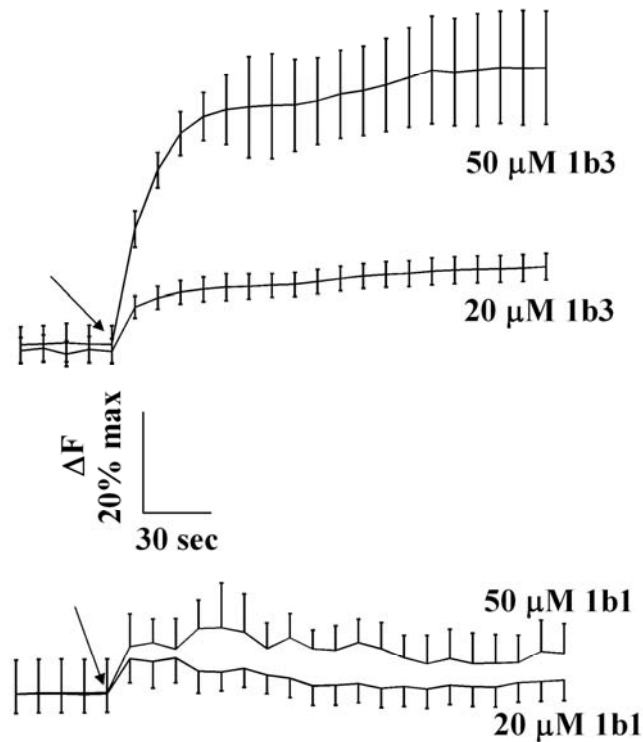


**Fig.19. The effect of caloxins 1b3 and 1b1 on  $[\text{Ca}^{2+}]_i$  in cultured pig coronary artery endothelial cells.**  $\Delta\text{F}$  = change in fluorescence. Arrow indicates the time of addition of caloxin. All the values obtained 20 s after adding the caloxins differed significantly from the baseline values ( $p < 0.05$ ). The values obtained with 20 and 50  $\mu\text{M}$  caloxin1b3 were significantly larger than the corresponding values obtained with caloxin 1b1 ( $p < 0.05$ ). (Szewczyk et al. 2010). The maximal fluorescence was determined with calcium ionophore 4-Br A23187.

### 3.2.7. Mutagenesis of caloxin 1b3

The mixture of 1b3-like oligonucleotides, encoding mutants of the first 12 amino acids of caloxin 1b3 (TIPKWISIIQAL) was used to construct a caloxin 1b3-like peptide phage display library, as described previously (Pande et al. 2008). Limited mutagenesis was used to obtain a library that contained mostly phage displaying peptides with 1, 2 or 3 amino acid changes. To characterize the library, 24 clones were sequenced. Out of the 24 clones, only one sequence was repeated (Table 7). Based on this result and the total number of pfu obtained, the library diversity was calculated to be  $9.6 \times 10^4$ . The statistical analysis showed that there was no difference in the observed frequencies for phage encoding peptides with 0, 1, 2, 3 or >3 amino acid substitutions in the library. The frequencies expected were based on the limited mutagenesis strategy (Table 8). Since the library contained only  $1 \times 10^5$  pfu, it was amplified once (total  $2.2 \times 10^{12}$  pfu obtained) and then  $1 \times 10^9$  pfu were used for screening in one round of affinity chromatography with PMCA protein purified from RDM membranes with extensive washing over 3 days at 4°C (phase II). Out of the 185 sequenced clones, there were 120 unique ones (Table 9). Since amplification may introduce bias due to differential amplification efficiencies of individual phage clones, equal amounts of unique clones were made to compete for binding to PMCA1 in affinity chromatography in three separate experiments (phase III). From each experiment 92-95 clones were sequenced (Table 10). Two clones with the highest frequency were chosen for peptide synthesis (SISKWFSIIQALGGGSK, TISKWISIVQALGGGSK). Since the parental caloxin 1b3 contained an additional 13<sup>th</sup> amino acid, arginine, variants containing R were also synthesized

(SISKWFSIIQALRGGGSK, TISKWISIVQALRGGGSK). However, the parental caloxin 1b3 inhibited RDM  $\text{Ca}^{2+}$ - $\text{Mg}^{2+}$ -ATPase (PMCA1) with higher affinity than any of the mutants (data not shown). Thus, caloxin 1b3 was the best PMCA1 selective caloxin obtained in this work.

AIPKWISIGQAL	TIPKWINIIHAS	TIPKRVTIIPAL	TIPKWSSIIQAL
SFPTSISITQAL	TIPKWISFIQAS	TIPKSISIIQAL	TIPKWSSIIQPL
SIPKWISIIPAF	TIPKWISIIQAL	TIPKWISSIQEL	TIPKYISIIQAL
TIPEGMSSIRAL	TIPKWISIIQAL	TIPKWLSIIQAL	TIPRWFSTIEAM
TIPKCINIMQAL	TIPKWISINQAI	TNPKWSSITQGV	TIQKWISIIQAL
TIPKCISNTQAL	TIPKWISMSQAL	TPKGISIIQAL	TLPKWNSIIQAL

**Table 7. Testing small-scale caloxin 1b3-like peptide library.** The library was constructed by retaining 91 % of the original bases and replacing the remainder with 3 % of the other three bases in the caloxin 1b3 encoding oligonucleotide. A total of 24 phage clones were sequenced. The parent caloxin 1b3 (TIPKWISIIQAL) showed two times, whereas all other clones showed only once. The amino acids substituted in the caloxin 1b3-like peptides are bolded.

Number of amino acid substitutions	Expected frequency	Observed frequency
0	2	2
1	5	6
2	7	7
3	5	4
>3	5	5

**Table 8. Characterization of the Ph.D caloxin 1b3-like peptide library.** A total of 24 phage clones from the Ph.D caloxin 1b3-like peptide library were sequenced. Shown is the expected and observed frequency of phage clones encoding peptides with a given number of amino acid substitutions. Chi square value test showed that the two distributions are not significantly different (Chi squared equal 0.417 with 4 degrees of freedom,  $p > 0.1$ )

Sequence	Freq.	Sequence	Freq.	Sequence	Freq.
TIPKWISIIQAL original	25	TIPKWIS <b>FM</b> QVL	1	TIPRWI <b>IYN</b> QAL	1
<b>A</b> IPKGIS <b>MF</b> QAL	1	TIPKWISIIHAL	3	TIPRWINI <b>I</b> NAL	2
<b>A</b> IPKRISIIQAD	1	TIPKWISIIKAL	1	TIPRWISIIQAL	1
<b>A</b> IPKWINIIQAL	1	TIPKWISIIQAM	2	TIP <b>SW</b> VSIIQRL	2
<b>A</b> ITK <b>W</b> NSIIQAL	1	TIPKWISIIQAS	2	TIP <b>TG</b> FSIIQAL	1
<b>A</b> SPN <b>W</b> TS <b>L</b> IQAL	1	TIPKWISIIQAV	4	TIP <b>TW</b> FS <b>NN</b> QAL	1
<b>I</b> IPKW <b>V</b> SMVQAL	1	TIPKWISIIQSL	1	TIP <b>TW</b> IGIIQAL	1
<b>I</b> NPKWIRNIQAL	1	TIPKWISIMQAL	3	TIP <b>TW</b> ISIIQAL	1
<b>N</b> IPKWISIIQAL	2	TIPKWISINQAL	6	TIP <b>TW</b> IS <b>RPQGF</b>	1
<b>N</b> IPKWISIIQAM	1	TIPKWISIRQAL	1	TIP <b>TW</b> TSIIQAL	1
<b>N</b> S <b>P</b> E <b>W</b> FSIIQAL	1	TIPKWISISQAL	2	TIS <b>KW</b> ISIMQAL	1
<b>S</b> IPKWISIIQAL	1	TIPKWISITQAF	1	TIS <b>KW</b> ISIVQAL	1
<b>S</b> IPKWISINQAL	2	TIPKWISITQAL	1	<b>TLP</b> KW <b>TR</b> ITQAL	1
<b>S</b> IPNWISII <b>R</b> AL	1	TIPKWISIVQAL	2	<b>TL</b> PPWIGVIQTL	1
<b>S</b> ISK <b>W</b> FSIIQAL	1	TIPKWIS <b>K</b> IESS	1	<b>TM</b> AKWISIIQAL	1
<b>S</b> MPKWISIIHAL	1	TIPKWIS <b>L</b> MQAL	1	<b>TN</b> AKWISIIQAL	3
<b>S</b> MPKWISIIQAL	1	TIPKWIS <b>M</b> IQAL	1	<b>TNG</b> KWISIIQAL	1
<b>S</b> NQKWISIIQAF	1	TIPKWIS <b>S</b> IQAL	1	<b>TNP</b> KWISIIQAL	4
<b>T</b> FPKWDSIIQAL	1	TIPKWIS <b>T</b> IQAL	2	<b>TNP</b> KW <b>NN</b> IIQEL	1
<b>T</b> FPRWISINQSL	1	TIPKWIS <b>TN</b> QAL	1	<b>TNP</b> KW <b>S</b> SMIQAL	1
<b>T</b> IHK <b>W</b> TNIRQAL	2	TIPKWLSIIQAL	1	<b>TN</b> PTWIS <b>FN</b> QAL	1
<b>T</b> I <b>P</b> E <b>W</b> ISITQAL	3	TIPKWLSIIQAV	1	<b>TSP</b> KWINIIQAL	1
TIP <b>K</b> CIN <b>VI</b> QEL	1	TIPKWLSITQAW	2	<b>TSP</b> KWISIIQAL	2
TIP <b>K</b> CISIDQAL	1	TIPKWLS <b>LN</b> QAL	1	<b>TSP</b> KWISIMQAL	1
TIP <b>K</b> GISIIQAL	2	TIPKWLS <b>NI</b> QAF	2	<b>TSP</b> KW <b>IT</b> IIQAL	1
TIP <b>K</b> LIS <b>VI</b> QAL	1	TIPKWMSITQAL	1	<b>TSP</b> KWNSIIQAV	1
TIP <b>K</b> LMSNIQAL	1	TIPKW <b>M</b> STTQAL	1	<b>TSP</b> KW <b>S</b> IIQAV	1
TIP <b>K</b> LTSIIQAM	1	TIPKWNSIIQAL	2	<b>TSP</b> QWMSIIQAL	1
TIP <b>K</b> QISINQTL	1	TIPKWNSIIQAV	1	<b>TTP</b> KWISII <b>HGL</b>	1
TIP <b>K</b> RISIIQAF	2	TIPKW <b>TR</b> IIQAF	1	<b>TTP</b> KWISIIQAL	2
TIP <b>K</b> RISIIQAL	1	TIPKW <b>TR</b> IIQAL	1	<b>TTP</b> NWISIIKAL	1
TIP <b>K</b> RMSINQAL	1	TIPKW <b>T</b> SIIQAL	3	<b>TTP</b> NWMSNI <b>HAW</b>	1
TIP <b>K</b> SINIIQAL	1	TIPKW <b>T</b> SNIQAL	2	<b>TTP</b> QWNSIIQAL	1
TIP <b>K</b> SISIIQAL	2	TIP <b>M</b> W <b>T</b> STN <b>Q</b> AL	1	<b>TTP</b> RSISII <b>P</b> AL	1
TIP <b>K</b> SISM <b>K</b> AL	1	TIP <b>N</b> SISIIQAL	1	<b>TVP</b> KL <b>NN</b> IIQAI	1
TIP <b>K</b> SNRLIQAL	1	TIPNWISIIQAL	2	<b>TVP</b> KWINI <b>R</b> AL	1
TIP <b>K</b> STSIFQAL	1	TIPNWIS <b>V</b> THAL	1	<b>TVP</b> KWISIIQAL	1
TIPKW <b>I</b> ISQAL	1	TIP <b>Q</b> WISIIQAL	1	<b>TVP</b> KWISITQAL	1
TIPKWINI <b>P</b> AL	1	TIP <b>Q</b> WLSIIQAP	1	<b>TVP</b> KWLSIIQAL	1
TIPKW <b>I</b> PMIQAW	1	TIPRW <b>S</b> IIQAL	1	<b>TYP</b> KWNSIIQAL	1

**Table 9. Phage clones selected after 1 round of screening of the caloxin 1b3-like peptide library. Amino acids different from the original sequence are bolded.**

Sequence	Frequency (% total in a group)			
	Competition I	Competition II	Competition III	% total (I+II+III)
TIPKWISIIQAL	2.3	0.0	1.1	1.3
<b>A</b> IPKWINI <b>I</b> QAL	1.2	0	1.1	0.9
<b>A</b> ITK <b>W</b> NSIIQAL	2.3	2.1	0	1.7
<b>N</b> IPKWISIIQAL	1.2	3.2	1.1	2.1
<b>S</b> IPKWISIIQAL	2.3	2.1	1.1	2.1
<b>S</b> ISK <b>W</b> FSIIQAL	5.8	33.0	53.2	36.1
<b>S</b> MPKWISII <b>H</b> AL	2.3	1.1	0	1.3
<b>S</b> NQKWISIIQ <b>A</b> F	2.3	1.1	0	1.3
TIPKWIS <b>I</b> MQAL	3.5	1.1	0	1.8
TIPKW <b>L</b> SIIQAL	4.7	1.1	0	2.3
TIPKW <b>T</b> RII <b>R</b> AL	2.3	2.1	0	1.7
TIPR <b>W</b> HSIIQAL	1.2	5.3	0	2.5
TIPR <b>W</b> ISIIQAL	1.2	3.2	0	1.7
TISK <b>W</b> IS <b>I</b> MQAL	3.5	4.3	5.3	5.1
TISK <b>W</b> IS <b>I</b> VQAL	3.5	6.4	23	12.9
<b>T</b> MAKWISIIQAL	0.0	8.5	4.2	5
<b>T</b> NAKWISIIQAL	4.7	5.3	2.1	4.7
<b>T</b> NGKWISIIQAL	3.5	4.3	2.1	3.9
<b>T</b> SPKWISIIQAL	3.5	3.2	0	2.6
<b>T</b> SPKW <b>I</b> TIIQAL	0	1.1	0	0.4
<b>T</b> VPKWISIIQAL	2.3	1.1	0	1.3
<b>T</b> VPKWINI <b>R</b> AL	3.5	7.4	2.1	5.1
<b>T</b> YPKWNSIIQAL	2.3	1.1	1.1	1.8

**Table. 10. Characterization of the phage clones selected after competition experiments.** Equal number ( $1 \times 10^5$  competition I and  $1 \times 10^8$  competition II and III) of each of the 120 phage clones selected in the first screening were allowed to compete for binding to RDM PMCA in affinity chromatography. 92-96 clones from each separate experiment were sequenced. Amino acids different from the original sequence are bolded. The amount of the phage is specified in the column. Highlighted sequences were chosen for caloxin synthesis.

### **3.3. Aim 3: The invention of ultra high affinity PMCA4 selective bidentate caloxins**

For the initial work, the PMCA4 exdom1 was divided into an N-terminal half exdom1X and a C-terminal half exdom1Y (Fig. 3). Caloxin 1b1 and 1b2 were developed for binding PMCA4 exdom1X and 1Y, respectively. The goal was to use these caloxins to link them optimally to obtain a bidentate caloxin that would bind to both exdom1X and exdom1Y. Before this optimization, limited mutagenesis was carried out to improve caloxins 1b1 and 1b2. Limited mutagenesis of caloxin 1b1 has already been carried out to obtain caloxin1c2, which also had higher selectivity for PMCA4 over other PMCA isoforms compared to caloxin 1b1. The corresponding higher selectivity peptide by mutagenesis of caloxin 1b2 had not been invented. The overall strategy consisted of two steps. Step 1 was to improve caloxin 1b2 affinity by limited mutagenesis. Step 2 was to link caloxin1c2 and the caloxin1b2 mutant to obtain ultrahigh affinity and PMCA4 selective bidentate caloxins.

#### **3.3.1. Caloxin 1b2 mutagenesis**

A Ph.D caloxin 1b2-like peptide library was constructed to contain mainly phage displaying peptides with 1, 2 or 3 amino acid substitutions. To characterize the library, DNA from 24 clones was sequenced. Out of the 24 sequenced clones, 4 did not contain any inserts and there were 18 unique clones (Table 11). The constructed 1b2-library contained  $4.2 \times 10^7$  pfu. Based on the results presented in Table 11 and the initial titer of the library, the library had a diversity of  $3.1 \times 10^7$  pfu. Statistical analysis showed that there was no difference ( $p > 0.05$ ) in the observed and the expected frequencies of the peptides with 0, 1, 2, 3 or  $>3$  amino acid substitutions in the library (Table 12).

HGW <b>TH</b> YQSLYAW	HGWTNYQSL <b>S</b> AW	HGWINYQ <b>T</b> LYAW	HGGINY <b>H</b> SLYVW
<b>Q</b> GWNNYQSLYAW	HGWNN <b>N</b> QSLYAW	HGWINYQ <b>P</b> LYAW	<b>H</b> FWSNYQ <b>S</b> FYAW
<b>Q</b> GWINYQ <b>P</b> LYAW	HGWI <b>Y</b> YQSMYW	HGWIN <b>H</b> QSLYA	<b>H</b> FWSNYQ <b>S</b> FYAW
HGW <b>V</b> TYQSLYAW	HGWI <b>T</b> DPSLY <b>A</b> L	HGSINYQ <b>S</b> MYAW	<b>D</b> VRINYQSLYAW
HGW <b>T</b> SFQSLYAW	HGWINYRSL <b>H</b> AW	HGLNYQSLYAW	

**Table 11. Testing Ph.D caloxin 1b2-like peptide library diversity.** A total of 24 phage clones from the Ph.D caloxin 1b2-like peptide library were sequenced. Amino acids different from caloxin1b2 (HGWINYQSLYAW) are bolded. One sequence showed two times and 4 clones had no insert.

No. of substitutions	Observed Frequency	Expected Frequency
0	0	2
1	4	5
2	9	6
3	5	4
>3	1	2

**Table 12. Characterization of Ph.D caloxin 1b2-like peptide library.** Shown is the expected and observed frequency of 19 phage clones encoding peptides with a given number of amino acid substitutions. Chi square value test showed that the two distributions are not significantly different ( $p > 0.1$ , Chi squared equals 4.450 with 4 degrees of freedom).

The Ph.D caloxin 1b2-like peptide library was amplified once and then used for screening in one round of affinity chromatography with PMCA protein purified from human erythrocyte membranes (Fig. 9) in two separate experiments using different input of different amounts of phage (Table 13). From each experiment 95 clones were

sequenced. Out of 190 sequenced clones there were 105 unique clones of which 15 clones encoded caloxin1b2 (Table 14).

**Table 13. Phage binding efficiency in each experiment of phase II.**

Exp.	Input (pfu)	Output (pfu)	Binding efficiency %
I	$1.20 \times 10^{11}$	$4.9 \times 10^4$	0.00004
II	$1.50 \times 10^9$	$5.2 \times 10^3$	0.00035

### 3.3.1.3. Phase III: Competition of phage clones selected in phase II

The degeneracy in the codons for individual amino acids and the differential amplification efficiency of the phage expressing different peptides can lead to bias in the copy number of a given phage clone. Thus, to ensure the selection of phage based on its binding affinity to PMCA, equal pfu of each of the 105 phage clones were allowed to compete in one round of affinity chromatography using PMCA protein purified from human erythrocyte membranes. The experiment was conducted two times and a total of 84 clones (42 from each experiment) were sequenced. Out of the 105 different clones that were present in the original phage mix, 45 unique clones were identified at the end of both experiments (Table 15). The sequence encoding caloxin 1b2 did not show after the competition experiment. Of these, the following sequences had the highest frequency: HDWIDYQSLYAW, HGWITYKSLYAW, NGWINYHAFYAW, and QGGINYQFFYAW. None of the sequences were classified as target unrelated protein when analyzed with program SAROTUP.

**Table 14. Phage clones obtained in Phase II screening of caloxin 1b2-like peptide library.**

HGWINYQSLYAW	HGRINNQSLYAW	HGWTNNQSLYAW	HVWSNYQTLYPW
HDWINYQSLYAW	HGRINYQSLNAW	HNWSNYQSLYAW	NVWINSKSLYAW
HGGINYQSLYAW	HGRINYQSLYAS	HSWINYQSLYQW	<b>QAWITYQSLYAW</b>
HGSINYQSLYAW	HGRINYQTLYAW	HSWNNYQSLYAW	<b>QGWFFNYQSSYAW</b>
HGWHNYQSLYAW	HGSINYQSFYAW	HSWVNYQSLYAW	<b>QGWISYQSLYAS</b>
HGWI <b>EY</b> QSLYAW	HGSINYQSLNAW	QGSINYQSLYAW	<b>HAGINYP</b> SLDAW
HGWI <b>KY</b> QSLYAW	HGSINYQTLYAW	QGWINYQSLYAR	<b>HARINYQSFYTW</b>
HGWIN <b>S</b> QSLYAW	HG <b>SL</b> NYQSLYAW	QGWINYQSWYAW	HGGINY <b>HPL</b> NAW
HGWINYQSLDAW	HG <b>ST</b> NYQSLYAW	<b>DGR</b> INKQSLAAW	HG <b>GL</b> NY <b>HSL</b> HAW
HGWINYQSL <b>HAW</b>	HG <b>WF</b> NY <b>PS</b> LYAW	<b>DGWF</b> NYQSSYAW	HG <b>WFNS</b> Q <b>SFHAW</b>
HGWINYQSLYAR	HGWI <b>HY</b> QSLYAR	<b>HAWT</b> NYQSLYAS	HGWIDYQSL
HGWINYQSLYAS	HGWINY <b>HSLY</b> TW	HG <b>AS</b> NYQSWYAW	HGWIN <b>NP</b> PLYVS
HGWINYQSLY <b>EW</b>	HGWINYQ <b>SFY</b> AS	HGG <b>IK</b> QSLYAW	HGWINYQ
HGWINYQSLY <b>TW</b>	HGWINYQSL <b>SS</b>	HGG <b>INN</b> QSSYAW	HGWNNY <b>QPSYAG</b>
HGWINYQ <b>S</b> VYAW	HGWINYQSLY <b>KG</b>	HGSINYQ <b>SSHAW</b>	<b>LGR</b> TNYQSLY <b>SW</b>
HGWINYQ <b>T</b> LYAW	HGWINYQ <b>S</b> MY <b>SW</b>	HG <b>WF</b> NYQSL <b>HPW</b>	<b>NGW</b> INY <b>HAFYAW</b>
HG <b>WV</b> NYQSLYAW	HGWINYQ <b>SSYAL</b>	HGWINY <b>HSLYEL</b>	<b>QGG</b> INY <b>QFFYAW</b>
<b>QGW</b> INYQSLYAW	HGWINYQ <b>SSYAR</b>	HGWINYQ <b>S</b> MY	<b>QGL</b> IN <b>HQT</b> LYAW
<b>ESW</b> INYQSLYAW	HGWINYQ <b>SSYAW</b>	HGWINYR <b>SLHAL</b>	<b>QGW</b> FFNY <b>HSMYAW</b>
<b>HAW</b> INYQSL <b>HAW</b>	HGWINYQ <b>TLYAR</b>	HG <b>WISY</b> QSL <b>SSW</b>	<b>QGW</b> INYR <b>SFYAL</b>
<b>HDW</b> IDYQSLYAW	HG <b>WITY</b> KSLYAW	HG <b>WKS</b> Y <b>HSLYAW</b>	<b>YGW</b> SNNQ <b>SWYAW</b>
<b>HDW</b> INYQSLNAW	HG <b>WMK</b> YQSLYAW	HG <b>WL</b> NYKSLYAR	<b>HDW</b> MDY <b>ESLYGW</b>
<b>HDW</b> INYQSLY <b>PW</b>	HG <b>WMN</b> YQSLYAR	HG <b>WN</b> NDQSLYAR	HG <b>RIY</b> D <b>N</b> SLNAR
HGGINYQ <b>ALYAW</b>	HG <b>WMN</b> YQSLY <b>TW</b>	HG <b>WY</b> QSLNAW	HG <b>SV</b> ND <b>H</b> SLY <b>SW</b>
HGGINYQ <b>S</b> MYAW	HG <b>WS</b> NYQSLYAS	HS <b>WNK</b> YQSLYAW	<b>NGW</b> INYQ <b>S</b>
HG <b>L</b> INY <b>PS</b> LYAW	HG <b>WS</b> NYRSLYAW	H <b>VW</b> INYR <b>STYAW</b>	<b>GW</b> INY <b>HS</b>
			<b>DGG</b> INYQ <b>S</b> MY <b>TR</b>

Note: The amino acids different from the parent caloxin 1b2 sequence are bolded.

Sequence	Frequency	p
<b>QGG</b> IN <b>YQFF</b> YAW (mut4)	9	0.0000001
HDWID <b>YQ</b> SLYAW (mut1)	8	0.000001
HGW <b>ITYK</b> SLYAW (mut2)	4	0.007
<b>NGW</b> IN <b>YHAF</b> YAW (mut3)	4	0.007
HDW <b>IN</b> Y <b>Q</b> SL <b>YPW</b>	3	0.04
<b>QGW</b> IS <b>YQ</b> SL <b>YAS</b>	3	0.04
HGWID <b>YQ</b> SL	3	0.04
HDW <b>MDY</b> ESLY <b>GW</b>	3	0.04

**Table 15. Frequencies of clones (mutants of caloxin 1b2) selected in competition experiment for binding to PMCA4.** A total of 84 clones were sequenced. With 115 possibilities and 84 sequences, selected, the probability ( $p = \frac{1}{\text{Combin}_j^n} \cdot (r^j) \cdot (1/r^j) \cdot ((r-1)/r)^{(n-j)}$ ) for a sequence to appear more than two times will be  $< 0.05$ . These sequences are shown. The sequences that appeared only once or twice ( $p > 0.05$ ) are not shown. Mutated amino acids are shown are bolded. The highlighted clones selected for peptide synthesis differ in 2, 4 or 5 amino acids from caloxin 1b2.

#### 3.3.1.4. Inhibition of PMCA by mutants of caloxin 1b2.

Based on sequences in Table 15, the peptides caloxin mut1, 2, 3 and 4 were synthesized. First, the effects of 25  $\mu\text{M}$  of each caloxin, including caloxin1b2 on PMCA  $\text{Ca}^{2+}$ - $\text{Mg}^{2+}$  ATPase in leaky human erythrocyte ghosts were tested (Fig. 20). At 25  $\mu\text{M}$  the inhibition  $\text{Ca}^{2+}$ - $\text{Mg}^{2+}$  ATPase activity of PMCA was maximum with caloxin mut3. Caloxin mut2 showed similar inhibition to the parental caloxin 1b2 and caloxins mut1 and mut4 barely inhibited PMCA activity. Thus, caloxin mut3 was the only mutant which had higher affinity than parental caloxin 1b2. Consistent with the previous nomenclature, caloxin mut3 was renamed as a c series caloxin (caloxin 1c4). To determine  $K_i$ , the effects of different concentrations of caloxin 1c4 on PMCA  $\text{Ca}^{2+}$ - $\text{Mg}^{2+}$  ATPase in leaky human erythrocyte ghosts were tested (Fig. 21). Caloxin 1c4 had five times higher affinity for PMCA4 ( $K_i = 5.7 \pm 1.1 \mu\text{M}$ ) than caloxin 1b2 ( $K_i = 31 \pm 2 \mu\text{M}$ ).

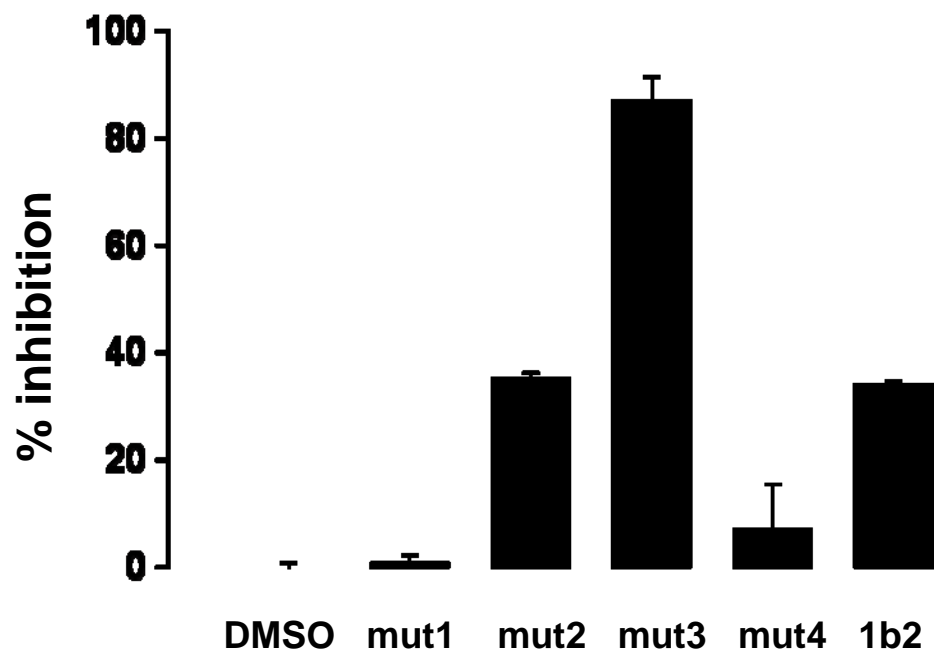


**Fig. 20. PMCA4 inhibition by 25  $\mu$ M the caloxin1b2 mutant peptides.** The values are mean  $\pm$  SEM of a total of 12 replicates from one experiment. All caloxins were tested at the same time. Caloxin mut3 had to be dissolved in DMSO and hence the same DMSO concentration was used for all caloxins and the control. Final DMSO concentration in the assay did not exceed 0.5%. This DMSO concentration had no effect on  $\text{Ca}^{2+}$ - $\text{Mg}^{2+}$  ATPase activity of PMCA in erythrocyte ghosts.

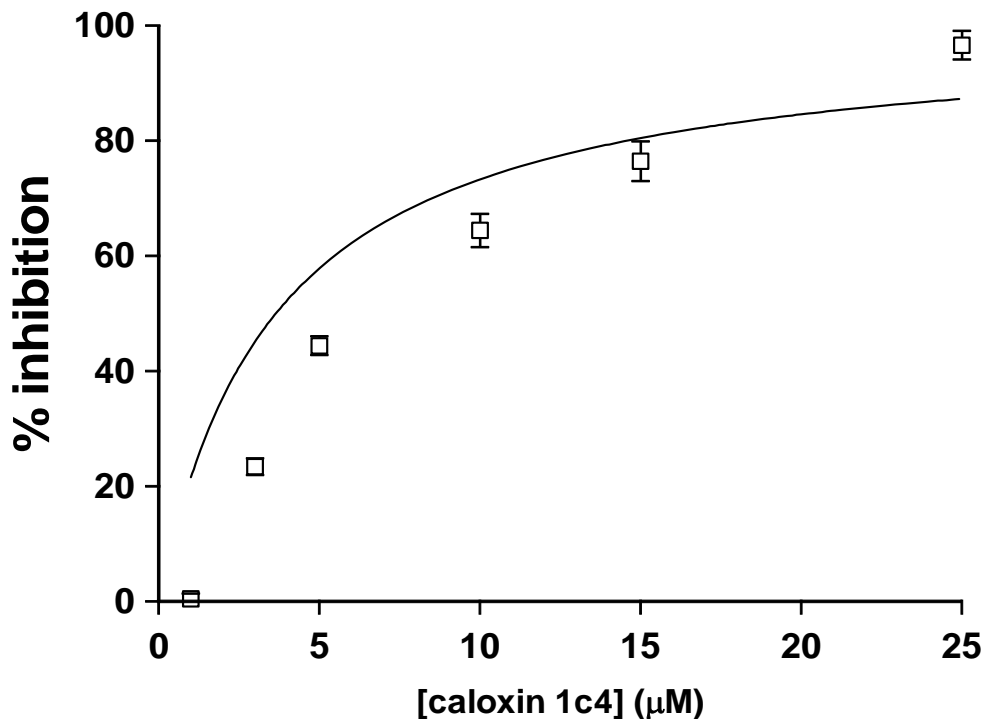


**Fig. 21. Caloxin 1c4 concentration dependence of inhibition of PMCA4.** PMCA activity was measured in a coupled enzyme assay with human erythrocyte ghosts. The activity in the absence of any peptide was taken as 100 % and the decrease in the activity in its presence was used to compute the % inhibition. The values are mean  $\pm$  SEM of a total of 12-24 replicates from experiments on two separate days. The data fit best with the  $K_i$  value of  $5.7 \pm 1.1 \mu\text{M}$ .

### 3.3.1. The invention of bidentate caloxins.

The exdom1X and 1Y were used as targets to screen the Ph.D libraries to obtain high affinity caloxins that bind to the N and C-terminal half of the exdom1 of PMCA4, caloxin 1c2 and caloxin 1c4. It was hypothesized that a bidentate caloxin that binds both exdom1X and 1Y would have much higher affinity and PMCA4 isoform

selectivity. Since we do not know exact binding sites and orientation of caloxin binding to its target the strategy was to create phage displaying different variants of peptides with caloxins in different orientation and separated various distance between them (Fig. 4).

### **3.3.2.1. Preliminary results with bidentate caloxin 1c2-1b2.**

Preliminary experiments were conducted using caloxins 1c2 and 1b2. The first issue was to choose appropriate linkers. Polyethylene glycols (PEG) are commonly used as linkers between proteins and oligonucleotides due to their flexibility, water solubility and relatively low cost of synthesis. To determine the effect of polyglycosylation on inhibitory properties of the caloxins, two caloxins with six PEG repeats were synthesized, caloxin 1c2P6 (TAWSEVLGLLRRGGG(PEG)<sub>6</sub>) and caloxin 1b2P6 (HGWINYQSLYAWGGG(PEG)<sub>6</sub>). The polyglycosylation abolished the inhibitory properties of the two caloxins (data not shown). The peptide linkers (GGG repeats) were tested next. GGS should not affect caloxin affinity since the caloxin variable sequence was originally the peptide displayed on phage particle, followed by a short spacer (GGGS), which continued into the wild type pIII coat. Furthermore, most of the caloxins used in our work contain a GGGS in the N-terminal domain.

Caloxins 1c2 and 1b2 were linked together through  $\epsilon$ -amino group of caloxin 1c2 (H-TAWSEVLGLLRRGGGSK(KSGGGWAYLSQYNIWGH-NH<sub>2</sub>)). The effects of 0.1, 0.3, 1 and 3  $\mu$ M of bidentate caloxin on PMCA Ca<sup>2+</sup>-Mg<sup>2+</sup>ATPase in leaky human erythrocyte ghosts were tested (Fig. 22). Caloxin 1c2-1b2 inhibited human erythrocyte ghosts PMCA (mainly PMCA4) with  $K_i = 1.15 \pm 0.27 \mu$ M. Thus, linking two caloxins obtained for binding to different parts of PMCA4 exdom1 resulted in an inhibitor with

two times higher affinity for PMCA4 than caloxin 1c2 and almost thirty times higher affinity than caloxin 1b2. This preliminary experiment showed that linking the two caloxins in this orientation but with linkers of optimum length could yield in a very high affinity bidentate caloxin.

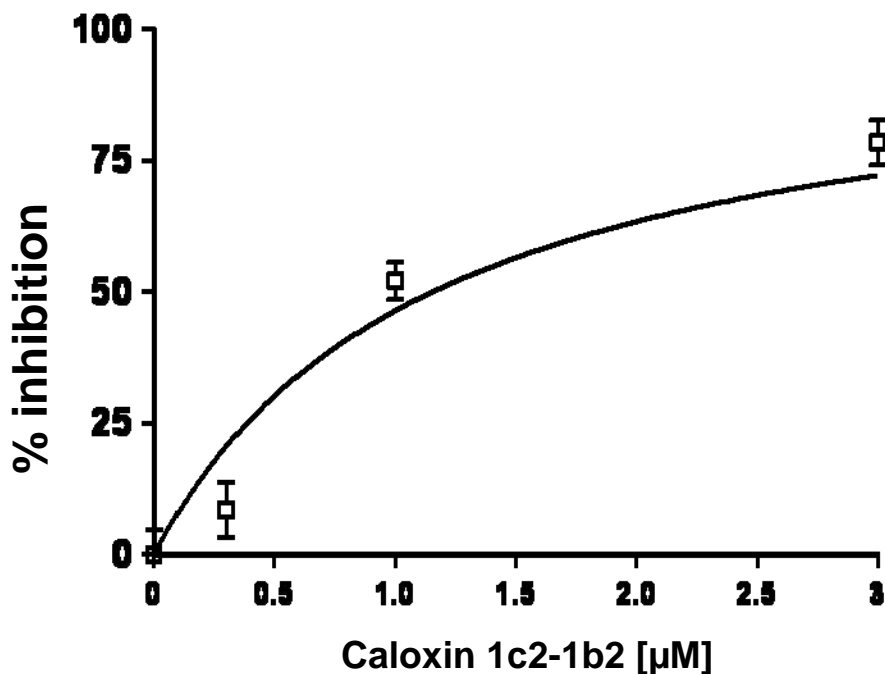


**Fig. 22. Inhibition of PMCA activity in leaky human erythrocyte ghosts by the bidentate caloxin 1c2-1b2.** The activity in the absence of any peptide was taken as 100 % and the decrease in the activity in its presence was used to compute the % inhibition. The values are mean  $\pm$  SEM of a total of 6-12 replicates from experiments on one day. All the concentrations were tested at the same time. The data fit best with the  $K_i$  value of  $1.15 \pm 0.27 \mu\text{M}$ .

### **3.3.2.2. Bidentate caloxin 1c2-1c4 using M13 phage display library.**

Since we do not know the exact binding sites and orientation of caloxin binding to its target we designed 26 different variants of oligos, where caloxins are in different orientations and are separated by 0,1,2,3 or 4 GGS repeats to fine-tune the proper distance between them (Fig. 4). The strategy was to produce different phage clones displaying each of 26 variants. Prior to insertion in the M13 vector the sequences of the synthetic oligonucleotides were confirmed. Despite many attempts, only 11 clones displaying individual peptides could be constructed (Table 16), all other phage clones contained either truncated or mutated sequences. The non-mutated clones were amplified, titered and their sequences were verified by sequencing. Out of 11 clones 5 clones mutated during amplification (Table 16).

Equal amounts of 6 clones expressing bidentate peptides together with 23 mutated clones were mixed and used in a competition experiment (Table 11). The phage mixture was applied on two columns, one containing erythrocyte ghosts PMCA bound to a calmodulin-agarose resin (Col.A) and another containing only calmodulin-agarose (Col.B) as a negative control. The experiment was repeated three times with different phage input. However, the phage binding to both columns was similar (Table 17).

**Table 16. Sequences of bidentate peptides.**

Bidentate peptide	Sequence	Note
1c2(0)1c4	TAWSEVLDLLRRGGGSKNGWINHAFYAW	*
1c2(1)1c4	TAWSEVLDLLRRGGGSKGGSNGWINHAFYAW	**
1c2(2)1c4	TAWSEVLDLLRRGGGSKGGSNGWINHAFYAW	
1c2(3)1c4	TAWSEVLDLLRRGGGSKGGSNGWINHAFYAW	
1c2(4)1c4	TAWSEVLDLLRRGGGSKGGSNGWINHAFYAW	
1c2(0)1c4(reversed)	TAWSEVLDLLRRGGGSKWAYFAHNIWGN	*
1c2(1)1c4(reversed)	TAWSEVLDLLRRGGGSKGGSWAYFAHNIWGN	**
1c2(2)1c4(reversed)	TAWSEVLDLLRRGGGSKGGSWAYFAHNIWGN	
1c2(3)1c4(reversed)	TAWSEVLDLLRRGGGSKGGSWAYFAHNIWGN	
1c2(4)1c4(reversed)	TAWSEVLDLLRRGGGSKGGSWAYFAHNIWGN	
1c4(0)1c2	NGWINHAFYAWGGGSKTAWSEVLDLLRR	**
1c4(1)1c2	NGWINHAFYAWGGGSKGGSTAWSEVLDLLRR	**
1c4(2)1c2	NGWINHAFYAWGGGSKGGSSTAWSEVLDLLRR	**
1c4(3)1c2	NGWINHAFYAWGGGSKGGSSTAWSEVLDLLRR	**
1c4(4)1c2	NGWINHAFYAWGGGSKGGSSTAWSEVLDLLRR	*
1c4(0)1c2(reversed)	NGWINHAFYAWGGGSKRRLLDLVESWAT	
1c4(1)1c2(reversed)	NGWINHAFYAWGGGSKGGSRRLLDLVESWAT	
1c4(2)1c2(reversed)	NGWINHAFYAWGGGSKGGSRRLLDLVESWAT	
1c4(3)1c2(reversed)	NGWINHAFYAWGGGSKGGSRRLLDLVESWAT	
1c4(4)1c2(reversed)	NGWINHAFYAWGGGSKGGSRRLLDLVESWAT	
1c2(0)K1c4(reversed)	TAWSEVLDLLRRGGGSKKSGGGWAYFAHNIWGN	
1c2(1)K1c4(reversed)	TAWSEVLDLLRRGGGSKGSKSGGGWAYFAHNIWGN	
1c2(2)K1c4(reversed)	TAWSEVLDLLRRGGGSKGSKSGGGWAYFAHNIWGN	
1c4(0)K1c2(reversed)	NGWINHAFYAWGGGSKKSGGRRRLLDLVESWAT	
1c4(1)K1c2(reversed)	NGWINHAFYAWGGGSKGSKSGGRRRLLDLVESWAT	
1c4(2)K1c2(reversed)	NGWINHAFYAWGGGSKGSKSGGRRRLLDLVESWAT	

\* peptides which could be originally displayed on a phage particle

\*\* phage clones used in competition experiment

**Table 17. Binding efficiency in each of competition experiments of phage displaying bidentate peptides.**

Experiment	Input pfu	Output pfu	
		Col. A with PMCA	Col. B
I	$2.90 \times 10^9$	$8.1 \times 10^8$	$6.6 \times 10^8$
II	$2.9 \times 10^8$	$1.30 \times 10^6$	$2.1 \times 10^6$
III*	$2.9 \times 10^6$	1286	928

\*In the third experiment the columns were washed extensively for 2 days.

## 4.0. DISCUSSION

The major findings of this work are the differences in the PMCA isoforms in smooth muscle and endothelium of pig coronary artery, invention of a PMCA1 selective caloxin, the role of exdom1 in the PMCA reaction cycle and the effect of PMCA inhibition in endothelial cells. This work also led to technological advances in phage display. The Discussion focuses on scientific importance of each of these aspects.

### 4.1. Differences in the PMCA isoforms in smooth muscle and endothelium

Pig coronary artery smooth muscle and endothelium differ in PMCA expression. First, smooth muscle contains much higher levels of PMCA protein and activity. Second, both tissues expressed mRNA only for PMCA1 and 4. Endothelium expressed predominantly mRNA for PMCA1 (splice variant 1b) and low levels of PMCA4 (4b), whereas smooth muscle expressed PMCA4 (4a and 4b) and lower levels of PMCA1 (1b). Immunoblotting analysis confirmed the predominance of the PMCA4 isoform in smooth muscle and PMCA1 isoform in endothelium. The PMCA variants expressed in these tissues differ in their affinity for calmodulin and regulation. PMCA4a which is expressed in smooth muscle, has lower affinity for calmodulin and can be activated and deactivated much faster than PMCA4b. The calmodulin binding affinity may influence how fast the pump activity can be decreased during  $\text{Ca}^{2+}$  transients. PMCA1b and PMCA4b have been suggested to have similar affinities for calmodulin. Calmodulin dependence of the ATPase activity of PMCA1b is similar to that of PMCA4b, or possibly marginally greater (Guerini et al. 2003). However, the observation on elution of PMCA in the present study

suggests a pronounced difference. PMCA1b was much more difficult to elute from a calmodulin-agarose column upon  $\text{Ca}^{2+}$  depletion with EGTA than was PMCA4, which cannot be explained by only slight differences in calmodulin affinity. PMCA isoforms also differ in their regulation. PMCA1b can be activated by PKA phosphorylation (James et al. 1989). Although both PMCA4b and 4a are substrates for PKC phosphorylation, the phosphorylation of the 4b variant leads to pump activation by relieving autoinhibition, while it has no effect on 4a activity (Verma et al. 1996). All PMCA are also substrates for calpain degradation, however, calpain may activate PMCA4 by removing the calmodulin binding domain, leaving a constitutively active fragment, while PMCA1 is fully degraded by this protease (Guerini et al. 2003). Another difference in the regulation is based on the reports that PMCA4b contains a PDZ binding domain, which allows it to interact with various proteins such as nNOS (expressed in smooth muscle) or other clustering and scaffolding proteins which may influence its specific localization (Oceandy et al. 2007).

The results on the level of PMCA expression in vascular smooth muscle and endothelium together with the literature on NCX and SERCA expression provided an insight into the relationship between the expression of  $\text{Ca}^{2+}$  lowering systems and cell function (Szewczyk et al. 2007). The two cell types differ in regulation of  $[\text{Ca}^{2+}]_i$  since smooth muscle expresses mostly high affinity, tightly regulated calcium extrusion systems (PMCA and SERCA2b), while endothelium expresses high levels of low affinity calcium extrusion pathways (NCX). SMC are contractile cells in which contraction occurs in response to chemical stimuli or stretch. Increased resistance to fatigue and long periods of contraction are unique properties of smooth muscle. A state of continual

contraction supports vasomotor tone and prevents blood pressure from dropping dramatically. Therefore, the contractile process has to be tightly regulated. Different forms of  $\text{Ca}^{2+}$  signaling have been identified in smooth muscle. First, a global increase in cytosolic  $[\text{Ca}^{2+}]_i$  which controls smooth muscle contractility through the activation of the myosin light-chain kinase. Another form of  $\text{Ca}^{2+}$  signaling reported in vascular SMC consists of propagating waves or local  $[\text{Ca}^{2+}]_i$  oscillations (Lee et al. 2002; Wray et al. 2010). These  $[\text{Ca}^{2+}]_i$  waves or oscillations result from intracellular  $\text{Ca}^{2+}$  release through  $\text{IP}_3\text{R}$  and/or  $\text{RyR}$ . Vascular SMC have been shown to produce calcium oscillations that may initiate from different loci within the cell. Moreover, separate regions within a single cell can sustain independent  $[\text{Ca}^{2+}]_i$  oscillations ((Mahoney et al. 1993; Wray et al. 2010). SMC contain few specialized regions, usually adjacent to the superficially located SER, where a local increase in  $[\text{Ca}^{2+}]_i$  (calcium sparks) occurs spontaneously or in response to stimuli. It was demonstrated that the sparks are most likely involved in relaxation of tone via activation of  $\text{Ca}^{2+}$ -activated large-conductance potassium channels (Bolton 2006; Wray et al. 2010). In order to spatially and temporally regulate  $[\text{Ca}^{2+}]_i$ , there have to be critical regulation  $\text{Ca}^{2+}$  transporting systems. In addition to PMCA, smooth muscle expresses high levels of SERCA2b, which can also be regulated by various proteins such as phospholamban and calmodulin dependent kinase (Brini et al. 2009; Wu et al. 2001). Smooth muscle also expresses NCX, but at lower levels than in endothelium, and its inhibitor phospholemman (Philipson et al. 2002; Szewczyk et al. 2007; Wu et al. 2001). The specific localization and type of  $\text{Ca}^{2+}$  extrusion systems may be important for regulation of differential  $\text{Ca}^{2+}$  oscillations within a cell. Smooth muscle is rich in SER

which runs along the longitudinal axis of the cell (Wray et al. 2010). It is suggested that SERCA localized in the peripheral SER may interact with plasma membrane ion channels and modulate near membrane calcium oscillations, whereas in the central SER, SERCA is more involved in contraction regulation. Therefore, SERCA localized in different parts of SER may be differentially regulated. The region where SER is close to caveolae may form a functional unit affecting  $\text{Ca}^{2+}$  signaling. Those microdomains were shown to have higher  $[\text{Ca}^{2+}]_i$  than the bulk cytoplasm and act as a barrier or buffer to the free diffusion of  $\text{Ca}^{2+}$  in this domain (McCarron et al. 2006). It has been suggested that PMCA4b and NCX may localize in caveolae. In such elevated  $\text{Ca}^{2+}$  regions NCX may also contribute to  $\text{Ca}^{2+}$  homeostasis despite its low  $\text{Ca}^{2+}$  affinity. Caveolae also contain nNOS which may interact with PMCA4b through the PDZ domain and therefore influence NO production (Bauser-Heaton et al. 2008; El Yazbi et al. 2008). However, the exact PMCA isoform localization has not been well determined. It would be interesting to determine if the fast acting PMCA4a isoform has a specific localization within the cell e.g. in places where fast response to increased  $[\text{Ca}^{2+}]_i$  is required. Therefore, the expression of a variety of high affinity, tightly regulated  $\text{Ca}^{2+}$  removal systems in smooth muscle is consistent with cyclical control of excitation-contraction and inhibition-relaxation coupling.

Endothelium expresses high levels of NCX and lower levels of the high affinity  $\text{Ca}^{2+}$  extrusion systems PMCA and SERCA2b (Szewczyk et al. 2007). In contrast to smooth muscle, endothelium does not express the NCX inhibitor phospholemman and contains low  $\text{Ca}^{2+}$  affinity SERCA3 which is not affected by phospholamban (Grover et

al. 1997; Szewczyk et al. 2007). EC are paracrine cells which, in response to an increase in  $[Ca^{2+}]_i$ , release endothelium-derived relaxing factors (NO, prostacyclin, hyperpolarisation factors) or constricting factors (e.g. endothelin-1) (Flammer et al. 2010). However, even without any stimulation, EC constantly produce low levels of NO. This is important, since NO has anti-atherogenic properties. It was observed that the basal NO production was significantly lower in atherosclerotic human coronary arteries than in normal arteries (Chester et al. 1990). Decreased basal NO production was correlated with increased circulating and tissue endothelin-1 observed in patients with coronary artery disease (Lerman et al. 1991) and acute coronary syndromes (Wieczorek et al. 1994). NO production depends on  $[Ca^{2+}]_i$  levels, since eNOS is activated upon  $Ca^{2+}$ -calmodulin binding (Duran et al. 2010). It is possible that low levels of high affinity calcium extrusion systems are important for maintenance of  $[Ca^{2+}]_i$  sufficient for basal eNOS activity in EC. Thus, low levels of high affinity  $Ca^{2+}$  extrusion systems and high levels of NCX in endothelium are consistent with a gradual  $Ca^{2+}$  dependent regulation of eNOS near the cell surface.

#### **4.2. Invention of a PMCA1 selective caloxin**

The present study resulted in the development of the PMCA1 selective inhibitor caloxin 1b3. Caloxin 1b3 was selected for binding to exdom1X of PMCA1. The exdom1 was previously used to obtain PMCA4 selective caloxin 1c2, which confirms the utility of this allosteric site in the invention of inhibitors for different PMCA isoforms (Pande et al. 2008). Caloxin 1b3 was invented by the method of screening using phage display system, similar to that developed for PMCA4-selective inhibitors (Pande et al. 2006). It

mostly differed in the nature of the target used: synthetic exdom1X of PMCA1 (instead of PMCA4) for panning and PMCA (mostly PMCA1) protein purified from RDM (instead of erythrocyte ghosts) for affinity chromatography. This indicates that the methods developed for inventing the PMCA4-selective caloxin can be similarly used to obtain caloxins selective for other PMCA isoforms. The comparison of the inhibitory effects of caloxin 1b3 on  $\text{Ca}^{2+}$ - $\text{Mg}^{2+}$ -ATPase activity of various PMCA isoforms, showed that this inhibitor had a higher affinity for PMCA1 as compared to PMCA2, 3 or 4. Thus, caloxin 1b3 is the first ever reported inhibitor which is selective for PMCA1 over all the other PMCA isoforms.

#### **4.2.1. Physiological and pathophysiological implications**

PMCA1 is a ubiquitously expressed isoform. However, the role of PMCA1 in physiology and pathophysiology is difficult to study since a) PMCA1 gene knock-out in the mice model is embryolethal, b) the presence of a heterozygous PMCA1 mutation in mice did not cause major defects and c) there are problems with overexpression of this isoform (Guerini et al. 2003; Okunade et al. 2004; Prasad et al. 2007). Most tissues express PMCA1 together with other PMCA isoforms, therefore, PMCA1 selective inhibitors may be useful in studying the role of this isoform in cell calcium homeostasis and signaling. PMCA1 is the predominant PMCA isoform expressed in pig coronary EC. Preliminary experiments with caloxin 1b3 showed that PMCA1 inhibition in EC led to an increase in  $[\text{Ca}^{2+}]_i$  up to about 50-60 %. It is consistent with the endothelium expressing high levels of NCX which would prevent a further increase in  $[\text{Ca}^{2+}]_i$ . Thus, caloxin 1b3

may be used to study the role of PMCA1 on different aspects of endothelial physiology such as NO or endothelin-1 production. Since smooth muscle expresses predominantly PMCA4, the effect of PMCA1 inhibition in endothelium on coronary artery contractility may also be determined. Since an increase in  $[Ca^{2+}]_i$  in endothelium leads to NO production, one would expect that PMCA1 inhibition may result in vasodilation.

PMCA1 is also expressed in all parts of the intestine, where it is implicated to play a role in secretion of absorbed  $Ca^{2+}$ . Based on the literature, rat and rabbit duodenum express the highest levels of PMCA1 mRNA and the present study confirmed this information at the protein level (Freeman et al. 1995; Howard et al. 1993). This was possible due to obtaining new anti-PMCA1 antibodies, since commercial antibodies did not work well in pig tissue. Therefore, a PMCA1 selective caloxin may help in understanding the role of PMCA in mucosal physiology and in states where  $Ca^{2+}$  absorption from intestine is affected.

There are several pathologies associated with altered PMCA1 activity and expression, such as cancerogenesis, improper neurite extension or cataract formation (Brandt et al. 1996; Eakin et al. 1995; Lee et al. 2002; Saito et al. 2006). Moreover, PMCA1 is very important for embryonic development since its gene knock-out leads to embryo death, possibly because it is the only PMCA isoform expressed at the early stages of embryogenesis (Zacharias et al. 1999). Interestingly, other  $Ca^{2+}$  extrusion systems could not compensate for the loss of this isoform, which often occurs when other PMCA isoforms are removed. Therefore, the use of a PMCA1 selective caloxin may help in understanding the basis of PMCA1 importance in embryolethality. It is possible that

inhibitors specific for PMCA1 will become useful tools to study the role of PMCA in physiology and pathophysiology and will become the basis for the invention of new therapeutical approaches.

#### **4.2.2. Role of exdom1 in PMCA reaction cycle**

The role of exdoms in the reaction cycle of PMCA pumps has been recognized only recently. In the past, exdoms were considered to be too short to play a role in the reaction cycle of the pump other than connecting the transmembrane helices. Major evidence for a possible role of exdoms comes from crystallography of the skeletal muscle SERCA (Toyoshima et al. 2000; Toyoshima et al. 2002). In this pump, several exdoms are in close proximity and form the extracellular lip of a  $\text{Ca}^{2+}$  channel needed for the pump action. Dissociation (or binding) of  $\text{Ca}^{2+}$  accompanies dramatic rearrangements of six (TM1–TM6) out of ten transmembrane helices. The SERCA pump inhibitor thapsigargin binds to the luminal loops and prevents the movements of the TM domains, which result in SERCA inhibition. Because luminal loops in SERCA correspond to exdoms in PMCA, it suggests that the exdoms also play a role in the function of PMCA. The rearrangements are not limited to the loops constituting the low affinity  $\text{Ca}^{2+}$  binding sites (TM4–TM6, TM8) and appear to be quite complicated: TM1 and TM2 move upwards (+z direction, towards the cytoplasm) whereas TM3 and TM4 shift downwards, both up to about 5 Å units. TM1 is unique in that it also shows a large lateral movement within the membrane. The large movements of TM1 and TM2 laterally and in the z direction would require conformational changes in exdom1. Further support for the importance of exdom1 movements in the P-type ATPases comes from the mechanism of

inhibition of the Na<sup>+</sup> pump activity by ouabain, which also binds to the extracellular loop connecting the TM 1/2 (Keenan et al. 2005).

Caloxins 1b3 and 1c4 along with the previously invented caloxins 1a1, 1b1, 1b2 and 1c2 were all obtained for binding to exdom1 (Chaudhary et al. 2001; Pande et al. 2005; Pande et al. 2006; Pande et al. 2008). The inhibitory effects of these caloxins on PMCA activity confirm the important role of exdom1 and TM1-TM2 movements in the PMCA reaction cycle. As described above, the TM domain 1 undergoes movements, which are important for cation translocation in both SERCA and sodium pump (Einholm et al. 2007). The key residues found in TM1 of SERCA are also conserved in PMCA, indicating that similar changes in TM1 may occur during the PMCA reaction cycle. The TM2 domain is connected on an intracellular site with the actuator domain, which plays an important role in pump dephosphorylation. Thus, caloxins may restrict the movement of TM1 and TM2 in PMCA resulting in either preventing Ca<sup>2+</sup> translocation or PMCA dephosphorylation. Caloxin 1b1 and 1a1, obtained for binding to exdom1X caused an increase in the amount of acylphosphate formed during the reaction cycle of PMCA which may be the result of immobilization of the actuator domain, which in turn resulted in locking PMCA in the phosphorylated state (Pande et al. 2005; Pande et al. 2006). This is in contrast to the decrease in the acylphosphate formation by caloxin 2a1 (exdom 2 based) and no effect on the level of acylphosphate by caloxin 3a1 (exdom 3 based) (Chaudhary et al. 2001; Pande et al. 2005). Thus, caloxins binding to the different exdoms of PMCA may affect different conformational states of the pump.

### **4.3. Advances in biotechnology**

The present study took advantage of recent advances in biotechnology and also provided novel concepts in phage display. Even though these concepts were used for PMCA, they would be useful to phage display of various targets.

#### **4.3.1. Phage contamination related propagation**

Selection of non-specifically binding phage (TUP) is a common problem in phage display. This study used a recently developed method to detect such sequences. To ensure that selected peptides do not display TUPs properties, each predominant clone was checked by the program SAROTUP, which contains a database of phage clones reported to have a higher ability to bind to background (e.g. plastic) or higher rate of amplification.

To avoid the selection of non-specific binding phage, this study introduced the concept of negative affinity chromatography. The importance of negative affinity chromatography was evident from the ability to select caloxins 1b3 and 1c4. Perhaps, it was even more important when calmodulin-Sepharose without PMCA was used as a parallel control for the selection of the phage displaying bidentate caloxins. If it were not for the negative control affinity chromatography, several phage would have been selected, sequenced and used unnecessarily for peptide synthesis.

Phage contamination may also result from higher amplification rates of some phage species. To avoid this, the concept of phage competition had been introduced previously in our lab (Pande et al. 2008). This work demonstrated the importance of this competition step and established its usefulness in the phage display technology.

#### **4.3.2. Differentiating between closely related targets**

A common problem in phage display is distinction between related targets. Many protein families are encoded by different genes, and each gene product is distributed in a tissue dependent manner and may be regulated differently. Most inhibitors used in literature cannot distinguish between different isoforms of the proteins. For example, the commonly used SERCA inhibitors like thapsigargin act on SERCA1, 2 and 3. This work advances the technology by using allosteric targets and developing screening methods to distinguish between them. The contribution of this work to resolving this issue is evident from the ability to invent PMCA isoform selective caloxins. Protein sequences in the catalytic sites of all PMCA isoforms are fairly conserved. Even though the allosteric site exdom1 shows the maximum divergence between PMCA1, 2, 3, and 4, there is some identity in the exdom1 sequences between different isoforms. Concepts to deal with this issue were developed for the panning and the PMCA-affinity chromatography steps. During panning, the wells were covered with the PMCA1 exdom1X peptide and then the phage to be applied was mixed with the corresponding PMCA4 peptide. This allowed for a preferential selection of PMCA1 binding phage. In the affinity chromatography step, negative affinity chromatography was carried out using PMCA4 protein and the chromatography with the PMCA1 rich preparation followed. The limited mutagenesis method developed previously in our lab can also be used to develop inhibitors with greater isoform specificity.

### **4.3.3. Bidentate inhibitors**

Compounds which act on more than one site can yield higher affinity inhibitors (Bouboutou et al. 1984; Hajduk et al. 1997). The concept introduced in this work was that peptides that bind to different allosteric sites on the same protein can be linked to form a bidentate inhibitor. However, the proximity of the binding sites and orientation of the inhibitor binding is often not known. In this work, inhibitors based on exdom1X (caloxin 1c2) and exdom1Y (caloxin 1b2 or 1c4) sites of PMCA4 were known. Two strategies were developed. The strategy used for the initial experiments showed that linking the exdom1X and exdom1Y based inhibitors through their GGGSK terminal domains produced a bidentate caloxin with a marginally greater affinity. However, the proximity of the binding sites and relative orientation of the inhibitors when bound was not known. It was considered that in the absence of such information phage display could be used to invent the bidentate caloxins. The strategy included the creation of phage clones displaying one of the variants of bidentate peptide and using them in a competition experiment to select the ligand which would bind with highest affinity to PMCA4. A series of oligonucleotides were synthesized to generate the needed M13 phage species. However, the phage clones obtained were truncated and unstable. This is possibly because the inserted sequences encoded 29-41 amino acid residues. Whereas some workers have used M13 containing up to 38 amino acid residue inserts, others suggest that only shorter peptides can be displayed (Cabilly 1999; Kay et al. 1993). A typical M13 phage display library contains only 7-12 residues in this domain. The present work proved that displaying longer peptides caused the phage to be unstable. Whether, the

instability is more with certain peptides than with others with similar length is not clear. However, M13 phage are used most commonly due to several advantages. They do not lyse bacteria during phage production, which simplifies the intermediate phage purification steps between rounds of panning, since a simple polyethylene glycol precipitation step is sufficient to separate the phage from almost all contaminating cellular proteins. An alternative is to include the inserts in the pVIII capsid protein of the M13 phage instead of pIII coat protein which is commonly used. However, the use of the pVIII capsid protein leads to the display of a larger number of peptides per phage which in turn leads to the selection of very low affinity peptides. Alternatively, one can use T7 phage which is lytic (Molek et al. 2011). Larger peptides at low valency can be displayed using this phage. In short, the present work showed that the creation of bidentate caloxins is feasible and second that M13 phage are not appropriate for display of very long peptides.

#### **4.4. Conclusions and future directions**

Coronary artery smooth muscle and endothelium differ in their PMCA isoform expression: PMCA1 > PMCA4 in endothelium and PMCA4 > PMCA1 in smooth muscle. Therefore, caloxins selective for PMCA1 and 4 can be used to understand the physiology and pathophysiology of the two cell types. Caloxin 1b3 was invented here and shown to raise  $[Ca^{2+}]_i$  levels in endothelial cells to a greater extent than the PMCA4 selective caloxin 1b1. A PMCA4 selective caloxin was previously developed. In this work and previously, exdoms 1X and 1Y have been shown as appropriate targets to

develop isoform selective caloxins. Preliminary data also show that the selectivity and the affinity of such inhibitors can be improved further by developing bidentate caloxins.

Future work on caloxins may lead to several different directions. One is the development of bidentate caloxins which are more selective for PMCA1 and PMCA4. Another is the use of these caloxins in contractility studies to understand the role of PMCA in healthy arteries and those exposed to oxidative stress which results from ischemia-reperfusion. PMCA1 selective caloxins may also lead to a new class of therapeutic drugs for hypertension. Therapeutic use of the PMCA selective inhibitors can be made either by tissue specific expression of the invented peptides or by high throughput screening to invent non-peptide drugs with appropriate delivery systems. Caloxins may also find wider applicability. For example, PMCA1 selective inhibitors may help in understanding the role of PMCA1 in processes underlying NO production by endothelium,  $\text{Ca}^{2+}$  absorption by mucosa, embryonal development, neurite extension, cancer and cataract formation. PMCA4 specific caloxins may be used to study the interaction of PMCA4 and nNOS in smooth muscle and in cardiac cells as well as the importance of PMCA4 in sperm motility, hypertension, platelet maturation and cancer. It is anticipated that PMCA isoform specific caloxins will become a useful research and therapeutic class of drugs.

## 5. REFERENCES

- Adamo, H. P., A. K. Verma, M. A. Sanders, R. Heim, J. L. Salisbury, E. D. Wieben, and J. T. Penniston. 1992. Overexpression of the Erythrocyte Plasma Membrane Ca<sup>2+</sup> Pump in COS-1 Cells. *Biochem.J.* 285 ( Pt 3): 791-797.
- Albert, A. P., A. S. Piper, and W. A. Large. 2005. Role of Phospholipase D and Diacylglycerol in Activating Constitutive TRPC-Like Cation Channels in Rabbit Ear Artery Myocytes. *J.Physiol* 566, no. Pt 3: 769-780.
- Andersen, J. P., B. Vilsen, E. Leberer, and D. H. MacLennan. 1989. Functional Consequences of Mutations in the Beta-Strand Sector of the Ca<sup>2+</sup>(+)-ATPase of Sarcoplasmic Reticulum. *J.Biol.Chem.* 264, no. 35: 21018-21023.
- Apell, H. J. 2004. How Do P-Type ATPases Transport Ions? *Bioelectrochemistry* 63, no. 1-2: 149-156.
- Armesilla, A. L., J. C. Williams, M. H. Buch, A. Pickard, M. Emerson, E. J. Cartwright, D. Oceandy, M. D. Vos, S. Gillies, G. J. Clark, and L. Neyses. 2004. Novel Functional Interaction Between the Plasma Membrane Ca<sup>2+</sup> Pump 4b and the Proapoptotic Tumor Suppressor Ras-Associated Factor 1 (RASSF1). *J.Biol.Chem.* 279, no. 30: 31318-31328.
- Baggaley, E., S. McLarnon, I. Demeter, G. Varga, and J. I. Bruce. 2007. Differential Regulation of the Apical Plasma Membrane Ca<sup>2+</sup> -ATPase by Protein Kinase A in Parotid Acinar Cells. *J.Biol.Chem.* 282, no. 52: 37678-37693.
- Basu, A. and U. C. Chaturvedi. 2008. Vascular Endothelium: the Battlefield of Dengue Viruses. *FEMS Immunol.Med.Microbiol.* 53, no. 3: 287-299.
- Bauser-Heaton, H. D., J. Song, and H. G. Bohlen. 2008. Cerebral Microvascular NNOS Responds to Lowered Oxygen Tension Through a Bumetanide-Sensitive Cotransporter and Sodium-Calcium Exchanger. *Am.J.Physiol Heart Circ.Physiol* 294, no. 5: H2166-H2173.
- Benhar, I. 2001. Biotechnological Applications of Phage and Cell Display. *Biotechnol.Adv.* 19, no. 1: 1-33.
- Bhalla, R. C., R. V. Sharma, and M. B. Aqel. 1987. Molecular Mechanisms Underlying Increased Contractility to Norepinephrine Stimulation in SHR Vascular Smooth Muscle. *Prog.Clin.Biol.Res.* 245: 277-288.
- Bohr, D. F., C. A. Bruner, F. S. Lamb, and R. C. Webb. 1988. Physiology of Vascular Smooth Muscle in Relation to Hypertension. *Acta Physiol Scand.Suppl* 571: 15-24.
- Bolton, T. B. and P. Pacaud. 1992. Voltage-Dependent Calcium Channels of Smooth Muscle. *Jpn.J.Pharmacol.* 58 Suppl 2: 251P-257P.
- Bolton, T. B. 2006. Calcium Events in Smooth Muscles and Their Interstitial Cells; Physiological Roles of Sparks. *J.Physiol* 570, no. Pt 1: 5-11.
- Bottger, V. and A. Bottger. 2009. Epitope Mapping Using Phage Display Peptide Libraries. *Methods Mol.Biol.* 524: 181-201.

Bouallegue, A., G. B. Daou, and A. K. Srivastava. 2007. Endothelin-1-Induced Signaling Pathways in Vascular Smooth Muscle Cells. *Curr.Vasc.Pharmacol.* 5, no. 1: 45-52.

Bouboutou, R., G. Waksman, J. Devin, M. C. Fournie-Zaluski, and B. P. Roques. 1984. Bidentate Peptides: Highly Potent New Inhibitors of Enkephalin Degrading Enzymes. *Life Sci.* 35, no. 9: 1023-1030.

Boyer, C., J. J. Art, C. J. Dechesne, J. Lehouelleur, J. Vautrin, and A. Sans. 2001. Contribution of the Plasmalemma to Ca<sup>2+</sup> Homeostasis in Hair Cells. *J.Neurosci.* 21, no. 8: 2640-2650.

Bozulic, L. D., M. T. Malik, D. W. Powell, A. Nanez, A. J. Link, K. S. Ramos, and W. L. Dean. 2007. Plasma Membrane Ca(2+) -ATPase Associates With CLP36, Alpha-Actinin and Actin in Human Platelets. *Thromb.Haemost.* 97, no. 4: 587-597.

Brandt, P. C., J. E. Siskin, R. L. Neve, and T. C. Vanaman. 1996. Blockade of Plasma Membrane Calcium Pumping ATPase Isoform I Impairs Nerve Growth Factor-Induced Neurite Extension in Pheochromocytoma Cells. *Proc.Natl.Acad.Sci.U.S A* 93, no. 24: 13843-13848.

Bratkovic, T. 2009. Progress in Phage Display: Evolution of the Technique and Its Applications. *Cell Mol.Life Sci.*

Bredeston, L. M. and H. P. Adamo. 2004. Loss of Autoinhibition of the Plasma Membrane Ca(2+) Pump by Substitution of Aspartic 170 by Asparagin. A Ctivation of Plasma Membrane Calcium ATPase 4 Without Disruption of the Interaction Between the Catalytic Core and the C-Terminal Regulatory Domain. *J.Biol.Chem.* 279, no. 40: 41619-41625.

Brini, M. and E. Carafoli. 2009. Calcium Pumps in Health and Disease. *Physiol Rev.* 89, no. 4: 1341-1378.

Brini, M. and E. Carafoli. 2011. The Plasma Membrane Ca<sup>2+</sup> ATPase and the Plasma Membrane Sodium Calcium Exchanger Cooperate in the Regulation of Cell Calcium. *Cold Spring Harb.Perspect.Biol.* 3, no. 2.

Buch, M. H., A. Pickard, A. Rodriguez, S. Gillies, A. H. Maass, M. Emerson, E. J. Cartwright, J. C. Williams, D. Oceandy, J. M. Redondo, L. Neyses, and A. L. Armesilla. 2005. The Sarcolemmal Calcium Pump Inhibits the Calcineurin/Nuclear Factor of Activated T-Cell Pathway Via Interaction With the Calcineurin A Catalytic Subunit. *J.Biol.Chem.* 280, no. 33: 29479-29487.

Burette, A., J. M. Rockwood, E. E. Strehler, and R. J. Weinberg. 2003. Isoform-Specific Distribution of the Plasma Membrane Ca<sup>2+</sup> ATPase in the Rat Brain. *J.Comp Neurol.* 467, no. 4: 464-476.

Burritt, J. B., M. T. Quinn, M. A. Jutila, C. W. Bond, and A. J. Jesaitis. 1995. Topological Mapping of Neutrophil Cytochrome b Epitopes With Phage-Display Libraries. *J.Biol.Chem.* 270, no. 28: 16974-16980.

Busse, R. and I. Fleming. 2006. Vascular Endothelium and Blood Flow. *Handb.Exp.Pharmacol.*, no. 176 Pt 2: 43-78.

Cabilly, S. 1999. The Basic Structure of Filamentous Phage and Its Use in the Display of Combinatorial Peptide Libraries. *Mol.Biotechnol.* 12, no. 2: 143-148.

Cantley, L. C., Jr., L. Josephson, R. Warner, M. Yanagisawa, C. Lechene, and G. Guidotti. 1977. Vanadate Is a Potent (Na,K)-ATPase Inhibitor Found in ATP Derived From Muscle. *J.Biol.Chem.* 252, no. 21: 7421-7423.

Carafoli, E. and M. Zurini. 1982. The Ca<sup>2+</sup>-Pumping ATPase of Plasma Membranes. Purification, Reconstitution and Properties. *Biochim.Biophys.Acta* 683, no. 3-4: 279-301.

Carafoli, E. 1987. Intracellular Calcium Homeostasis. *Annu.Rev.Biochem.* 56: 395-433.

Carafoli, E. 1991. Calcium Pump of the Plasma Membrane. *Physiol Rev.* 71, no. 1: 129-153.

Carafoli, E. and T. Stauffer. 1994. The Plasma Membrane Calcium Pump: Functional Domains, Regulation of the Activity, and Tissue Specificity of Isoform Expression. *J.Neurobiol.* 25, no. 3: 312-324.

Carafoli, E. 1997. Plasma Membrane Calcium Pump: Structure, Function and Relationships. *Basic Res.Cardiol.* 92 Suppl 1: 59-61.

Carafoli, E. and M. Brini. 2000. Calcium Pumps: Structural Basis for and Mechanism of Calcium Transmembrane Transport. *Curr.Opin.Chem.Biol.* 4, no. 2: 152-161.

Carafoli, E., L. Santella, D. Branca, and M. Brini. 2001. Generation, Control, and Processing of Cellular Calcium Signals. *Crit Rev.Biochem.Mol.Biol.* 36, no. 2: 107-260.

Carafoli, E. 2002. Calcium Signaling: a Tale for All Seasons. *Proc.Natl.Acad.Sci.U.S A* 99, no. 3: 1115-1122.

Carafoli, E. 2003. Historical Review: Mitochondria and Calcium: Ups and Downs of an Unusual Relationship. *Trends Biochem.Sci.* 28, no. 4: 175-181.

Carafoli, E. 2004. Calcium-Mediated Cellular Signals: a Story of Failures. *Trends Biochem.Sci.* 29, no. 7: 371-379.

Caride, A. J., A. R. Penheiter, A. G. Filoteo, Z. Bajzer, A. Enyedi, and J. T. Penniston. 2001. The Plasma Membrane Calcium Pump Displays Memory of Past Calcium Spikes. Differences Between Isoforms 2b and 4b. *J.Biol.Chem.* 276, no. 43: 39797-39804.

Carmen, S. and L. Jermutus. 2002. Concepts in Antibody Phage Display. *Brief.Funct.Genomic.Proteomic.* 1, no. 2: 189-203.

Casares, N., F. Rudilla, L. Arribillaga, D. Llopiz, J. I. Riezu-Boj, T. Lozano, J. Lopez-Sagaseta, L. Guembe, P. Sarobe, J. Prieto, F. Borrás-Cuesta, and J. J. Lasarte. 2010. A Peptide Inhibitor of FOXP3 Impairs Regulatory T Cell Activity and Improves Vaccine Efficacy in Mice. *J.Immunol.* 185, no. 9: 5150-5159.

Chaabane, C., S. Dally, E. Corvazier, R. Bredoux, R. Bobe, B. Ftouhi, A. Raies, and J. Enouf. 2007. Platelet. *J.Thromb.Haemost.* 5, no. 10: 2127-2135.

Chaudhary, J., M. Walia, J. Matharu, E. Escher, and A. K. Grover. 2001. Caloxin: a Novel Plasma Membrane Ca<sup>2+</sup> Pump Inhibitor. *Am.J.Physiol Cell Physiol* 280, no. 4: C1027-C1030.

Chester, A. H., G. S. O'Neil, S. Moncada, S. Tadjkarimi, and M. H. Yacoub. 1990. Low Basal and Stimulated Release of Nitric Oxide in Atherosclerotic Epicardial Coronary Arteries. *Lancet* 336, no. 8720: 897-900.

Chesterman, C. N. 1988. Vascular Endothelium, Haemostasis and Thrombosis. *Blood Rev.* 2, no. 2: 88-94.

Chicka, M. C. and E. E. Strehler. 2003. Alternative Splicing of the First Intracellular Loop of Plasma Membrane Ca<sup>2+</sup>-ATPase Isoform 2 Alters Its Membrane Targeting. *J.Biol.Chem.* 278, no. 20: 18464-18470.

Cho, W. J. and E. E. Daniel. 2005. Proteins of Interstitial Cells of Cajal and Intestinal Smooth Muscle, Colocalized With Caveolin-1. *Am.J.Physiol Gastrointest.Liver Physiol* 288, no. 3: G571-G585.

Choquette, D., G. Hakim, A. G. Filoteo, G. A. Plishker, J. R. Bostwick, and J. T. Penniston. 1984. Regulation of Plasma Membrane Ca<sup>2+</sup> ATPases by Lipids of the Phosphatidylinositol Cycle. *Biochem.Biophys.Res.Commun.* 125, no. 3: 908-915.

Cioffi, D. L., C. Barry, and T. Stevens. 2010. Store-Operated Calcium Entry Channels in Pulmonary Endothelium: the Emerging Story of TRPCS and Orail. *Adv.Exp.Med.Biol.* 661: 137-154.

Clausen, J. D., B. Vilsen, D. B. McIntosh, A. P. Einholm, and J. P. Andersen. 2004. Glutamate-183 in the Conserved TGES Motif of Domain A of Sarcoplasmic Reticulum Ca<sup>2+</sup>-ATPase Assists in Catalysis of E2/E2P Partial Reactions. *Proc.Natl.Acad.Sci.U.S A* 101, no. 9: 2776-2781.

Coats, P. 2003. Myogenic, Mechanical and Structural Characteristics of Resistance Arterioles From Healthy and Ischaemic Subjects. *Clin.Sci.(Lond)* 105, no. 6: 683-689.

Consigny, P. M. 1991. Vascular Smooth Muscle Contraction and Relaxation: Pathways and Chemical Modulation. *J.Vasc.Interv.Radiol.* 2, no. 3: 309-317.

Dai, J. M., K. H. Kuo, J. M. Leo, C. van Breemen, and C. H. Lee. 2006. Mechanism of ACh-Induced Asynchronous Calcium Waves and Tonic Contraction in Porcine Tracheal Muscle Bundle. *Am.J.Physiol Lung Cell Mol.Physiol* 290, no. 3: L459-L469.

Danias, P. G. 2002. Correlation of Coronary Artery Anatomy With Myocardial Perfusion Maps. *J.Nucl.Cardiol.* 9, no. 2: 238-239.

Daniel, E. E., A. El Yazbi, and W. J. Cho. 2006. Caveolae and Calcium Handling, a Review and a Hypothesis. *J.Cell Mol.Med.* 10, no. 2: 529-544.

Darby, P. J., C. Y. Kwan, and E. E. Daniel. 2000. Caveolae From Canine Airway Smooth Muscle Contain the Necessary Components for a Role in Ca(2+) Handling. *Am.J.Physiol Lung Cell Mol.Physiol* 279, no. 6: L1226-L1235.

Davis, K. A., S. E. Samson, K. Best, K. K. Mallhi, M. Szewczyk, J. X. Wilson, C. Y. Kwan, and A. K. Grover. 2006. Ca<sup>2+</sup>-Mediated Ascorbate Release From Coronary Artery Endothelial Cells. *Br.J.Pharmacol.* 147, no. 2: 131-139.

Dawson, A. P. 1997. Calcium Signalling: How Do IP<sub>3</sub> Receptors Work? *Curr.Biol.* 7, no. 9: R544-R547.

De Luisi, A. and A. M. Hofer. 2003. Evidence That Ca(2+) Cycling by the Plasma Membrane Ca(2+)-ATPase Increases the 'Excitability' of the Extracellular Ca(2+)-Sensing Receptor. *J.Cell Sci.* 116, no. Pt 8: 1527-1538.

Dean, W. L., D. Chen, P. C. Brandt, and T. C. Vanaman. 1997. Regulation of Platelet Plasma Membrane Ca<sup>2+</sup>-ATPase by CAMP-Dependent and Tyrosine Phosphorylation. *J.Biol.Chem.* 272, no. 24: 15113-15119.

DeMarco, S. J. and E. E. Strehler. 2001. Plasma Membrane Ca<sup>2+</sup>-ATPase Isoforms 2b and 4b Interact Promiscuously and Selectively With Members of the Membrane-Associated Guanylate Kinase Family of PDZ (PSD95/Dlg/ZO-1) Domain-Containing Proteins. *J.Biol.Chem.* 276, no. 24: 21594-21600.

DeMarco, S. J., M. C. Chicka, and E. E. Strehler. 2002. Plasma Membrane Ca<sup>2+</sup> ATPase Isoform 2b Interacts Preferentially With Na<sup>+</sup>/H<sup>+</sup> Exchanger Regulatory Factor 2 in Apical Plasma Membranes. *J.Biol.Chem.* 277, no. 12: 10506-10511.

Devlin, J. J., L. C. Panganiban, and P. E. Devlin. 1990. Random Peptide Libraries: a Source of Specific Protein Binding Molecules. *Science* 249, no. 4967: 404-406.

Di Leva, F., T. Domi, L. Fedrizzi, D. Lim, and E. Carafoli. 2008. The Plasma Membrane Ca<sup>2+</sup> ATPase of Animal Cells: Structure, Function and Regulation. *Arch.Biochem.Biophys.* 476, no. 1: 65-74.

Di Leva, F., T. Domi, L. Fedrizzi, D. Lim, and E. Carafoli. 2008. The Plasma Membrane Ca<sup>2+</sup> ATPase of Animal Cells: Structure, Function and Regulation. *Arch.Biochem.Biophys.* 476, no. 1: 65-74.

Dick, G. M. and J. D. Tune. 2010. Role of Potassium Channels in Coronary Vasodilation. *Exp.Biol.Med.(Maywood.)* 235, no. 1: 10-22.

Dora, K. A. 2010. Coordination of Vasomotor Responses by the Endothelium. *Circ.J.* 74, no. 2: 226-232.

Duncker, D. J. and D. Merkus. 2004. Regulation of Coronary Blood Flow. Effect of Coronary Artery Stenosis. *Arch.Mal Coeur Vaiss.* 97, no. 12: 1244-1250.

Dunham, P. B. and R. B. Gunn. 1972. Adenosine Triphosphatase and Active Cation Transport in Red Blood Cell Membranes. *Arch.Intern.Med.* 129, no. 2: 241-247.

Duran, W. N., J. W. Breslin, and F. A. Sanchez. 2010. The NO Cascade, ENOS Location, and Microvascular Permeability. *Cardiovasc.Res.* 87, no. 2: 254-261.

Dzau, V. J. and G. H. Gibbons. 1991. Endothelium and Growth Factors in Vascular Remodeling of Hypertension. *Hypertension* 18, no. 5 Suppl: III115-III121.

Eakin, T. J., M. C. Antonelli, E. L. Malchiodi, D. G. Baskin, and W. L. Stahl. 1995. Localization of the Plasma Membrane Ca(2+)-ATPase Isoform PMCA3 in Rat Cerebellum, Choroid Plexus and Hippocampus. *Brain Res.Mol.Brain Res.* 29, no. 1: 71-80.

Einholm, A. P., J. P. Andersen, and B. Vilsen. 2007. Roles of Transmembrane Segment M1 of Na<sup>+</sup>,K<sup>+</sup>-ATPase and Ca<sup>2+</sup>-ATPase, the Gatekeeper and the Pivot. *J.Bioenerg.Biomembr.* 39, no. 5-6: 357-366.

El Yazbi, A. F., W. J. Cho, R. Schulz, and E. E. Daniel. 2008. Calcium Extrusion by Plasma Membrane Calcium Pump Is Impaired in Caveolin-1 Knockout Mouse Small Intestine. *Eur.J.Pharmacol.* 591, no. 1-3: 80-87.

El Yazbi, A. F., W. J. Cho, J. Cena, R. Schulz, and E. E. Daniel. 2008. Smooth Muscle NOS, Colocalized With Caveolin-1, Modulates Contraction in Mouse Small Intestine. *J.Cell Mol.Med.* 12, no. 4: 1404-1415.

Elshorst, B., M. Hennig, H. Forsterling, A. Diener, M. Maurer, P. Schulte, H. Schwalbe, C. Griesinger, J. Krebs, H. Schmid, T. Vorherr, and E. Carafoli. 1999. NMR Solution Structure of a Complex of Calmodulin With a Binding Peptide of the Ca<sup>2+</sup> Pump. *Biochemistry* 38, no. 38: 12320-12332.

Elwess, N. L., A. G. Filoteo, A. Enyedi, and J. T. Penniston. 1997. Plasma Membrane Ca<sup>2+</sup> Pump Isoforms 2a and 2b Are Unusually Responsive to Calmodulin and Ca<sup>2+</sup>. *J.Biol.Chem.* 272, no. 29: 17981-17986.

Enyedi, A., M. Flura, B. Sarkadi, G. Gardos, and E. Carafoli. 1987. The Maximal Velocity and the Calcium Affinity of the Red Cell Calcium Pump May Be Regulated Independently. *J.Biol.Chem.* 262, no. 13: 6425-6430.

Enyedi, A., A. K. Verma, R. Heim, H. P. Adamo, A. G. Filoteo, E. E. Strehler, and J. T. Penniston. 1994. The Ca<sup>2+</sup> Affinity of the Plasma Membrane Ca<sup>2+</sup> Pump Is Controlled by Alternative Splicing. *J.Biol.Chem.* 269, no. 1: 41-43.

Enyedi, A., A. K. Verma, A. G. Filoteo, and J. T. Penniston. 1996. Protein Kinase C Activates the Plasma Membrane Ca<sup>2+</sup> Pump Isoform 4b by Phosphorylation of an Inhibitory Region Downstream of the Calmodulin-Binding Domain. *J.Biol.Chem.* 271, no. 50: 32461-32467.

Enyedi, A., N. L. Elwess, A. G. Filoteo, A. K. Verma, K. Paszty, and J. T. Penniston. 1997. Protein Kinase C Phosphorylates the "a" Forms of Plasma Membrane Ca<sup>2+</sup> Pump Isoforms 2 and 3 and Prevents Binding of Calmodulin. *J.Biol.Chem.* 272, no. 44: 27525-27528.

Faddy, H. M., C. E. Smart, R. Xu, G. Y. Lee, P. A. Kenny, M. Feng, R. Rao, M. A. Brown, M. J. Bissell, S. J. Roberts-Thomson, and G. R. Monteith. 2008. Localization of Plasma Membrane and Secretory Calcium Pumps in the Mammary Gland. *Biochem.Biophys.Res.Commun.* 369, no. 3: 977-981.

Falchetto, R., T. Vorherr, J. Brunner, and E. Carafoli. 1991. The Plasma Membrane Ca<sup>2+</sup> Pump Contains a Site That Interacts With Its Calmodulin-Binding Domain. *J.Biol.Chem.* 266, no. 5: 2930-2936.

Falchetto, R., T. Vorherr, and E. Carafoli. 1992. The Calmodulin-Binding Site of the Plasma Membrane Ca<sup>2+</sup> Pump Interacts With the Transduction Domain of the Enzyme. *Protein Sci.* 1, no. 12: 1613-1621.

Falk, R. H. and J. I. Leavitt. 1991. Digoxin for Atrial Fibrillation: a Drug Whose Time Has Gone? *Ann.Intern.Med.* 114, no. 7: 573-575.

Ficarella, R., F. Di Leva, M. Bortolozzi, S. Ortolano, F. Donaudy, M. Petrillo, S. Melchionda, A. Lelli, T. Domi, L. Fedrizzi, D. Lim, G. E. Shull, P. Gasparini, M. Brini, F. Mammano, and E. Carafoli. 2007. A Functional Study of Plasma-Membrane Calcium-Pump Isoform 2 Mutants Causing Digenic Deafness. *Proc.Natl.Acad.Sci.U.S.A* 104, no. 5: 1516-1521.

Fill, M. and J. A. Copello. 2002. Ryanodine Receptor Calcium Release Channels. *Physiol Rev.* 82, no. 4: 893-922.

Filoteo, A. G., N. L. Elwess, A. Enyedi, A. Caride, H. H. Aung, and J. T. Penniston. 1997. Plasma Membrane Ca<sup>2+</sup> Pump in Rat Brain. Patterns of Alternative Splices Seen by Isoform-Specific Antibodies. *J.Biol.Chem.* 272, no. 38: 23741-23747.

Flammer, A. J. and T. F. Luscher. 2010. Three Decades of Endothelium Research: From the Detection of Nitric Oxide to the Everyday Implementation of Endothelial Function Measurements in Cardiovascular Diseases. *Swiss.Med.Wkly.* 140: w13122.

Freeman, T. C., A. Howard, B. S. Bentsen, S. Legon, and J. R. Walters. 1995. Cellular and Regional Expression of Transcripts of the Plasma Membrane Calcium Pump PMCA1 in Rabbit Intestine. *Am.J.Physiol* 269, no. 1 Pt 1: G126-G131.

Fujimoto, T. 1993. Calcium Pump of the Plasma Membrane Is Localized in Caveolae. *J.Cell Biol.* 120, no. 5: 1147-1157.

Gallagher P.,G., Z., Zhang , J.,S., Morrow and B.,G., Forget. 2004. Mutation of a highly conserved isoleucine disrupts hydrophobic interactions in the alpha beta spectrin self-association binding site. *Lab Invest.* 84:229-34

Ghislain, M., A. Schlessler, and A. Goffeau. 1987. Mutation of a Conserved Glycine Residue Modifies the Vanadate Sensitivity of the Plasma Membrane H<sup>+</sup>-ATPase From Schizosaccharomyces Pombe. *J.Biol.Chem.* 262, no. 36: 17549-17555.

Glusa, E. and F. Markwardt. 1988. Studies on Thrombin-Induced Endothelium-Dependent Vascular Effects. *Biomed.Biochim.Acta* 47, no. 7: 623-630.

Gros, R., T. Afroze, X. M. You, G. Kabir, R. Van Wert, W. Kalair, A. E. Hoque, I. N. Mungrue, and M. Husain. 2003. Plasma Membrane Calcium ATPase Overexpression in Arterial Smooth Muscle Increases Vasomotor Responsiveness and Blood Pressure. *Circ.Res.* 93, no. 7: 614-621.

Grover, A. K., S. E. Samson, and R. M. Lee. 1985. Subcellular Fractionation of Pig Coronary Artery Smooth Muscle. *Biochim.Biophys.Acta* 818, no. 2: 191-199.

Grover, A. K. and S. E. Samson. 1986. Pig Coronary Artery Smooth Muscle: Substrate and PH Dependence of the Two Calcium Pumps. *Am.J.Physiol* 251, no. 4 Pt 1: C529-C534.

Grover, A. K. and S. E. Samson. 1997. Peroxide Resistance of ER Ca<sup>2+</sup> Pump in Endothelium: Implications to Coronary Artery Function. *Am.J.Physiol* 273, no. 4 Pt 1: C1250-C1258.

Grover, A. K., S. E. Samson, and C. M. Misquitta. 1997. Sarco(Endo)Plasmic Reticulum Ca<sup>2+</sup> Pump Isoform SERCA3 Is More Resistant Than SERCA2b to Peroxide. *Am.J.Physiol* 273, no. 2 Pt 1: C420-C425.

Guerini, D. and E. Carafoli. 1996. The Targeting of the Plasma Membrane Calcium Pump in the Cell. *Biosci.Rep.* 16, no. 2: 129-137.

Guerini, D., B. Pan, and E. Carafoli. 2003. Expression, Purification, and Characterization of Isoform 1 of the Plasma Membrane Ca<sup>2+</sup> Pump: Focus on Calpain Sensitivity. *J.Biol.Chem.* 278, no. 40: 38141-38148.

Gunaratne, H. J., A. T. Neill, and V. D. Vacquier. 2006. Plasma Membrane Calcium ATPase Is Concentrated in the Head of Sea Urchin Spermatozoa. *J.Cell Physiol* 207, no. 2: 413-419.

Gutterman, D. D. 1999. Adventitia-Dependent Influences on Vascular Function. *Am.J.Physiol* 277, no. 4 Pt 2: H1265-H1272.

Hajduk, P. J., R. P. Meadows, and S. W. Fesik. 1997. Discovering High-Affinity Ligands for Proteins. *Science* 278, no. 5337: 497,499.

Hammes, A., S. Oberdorf-Maass, T. Rother, K. Nething, F. Gollnick, K. W. Linz, R. Meyer, K. Hu, H. Han, P. Gaudron, G. Ertl, S. Hoffmann, U. Ganten, R. Vetter, K. Schuh, C. Benkwitz, H. G. Zimmer, and L. Neyses. 1998. Overexpression of the Sarcolemmal Calcium Pump in the Myocardium of Transgenic Rats. *Circ.Res.* 83, no. 9: 877-888.

Hao, L., J. L. Rigaud, and G. Inesi. 1994. Ca<sup>2+</sup>/H<sup>+</sup> Countertransport and Electrogenicity in Proteoliposomes Containing Erythrocyte Plasma Membrane Ca-ATPase and Exogenous Lipids. *J.Biol.Chem.* 269, no. 19: 14268-14275.

Hecker, M., T. Dambacher, and R. Busse. 1992. Role of Endothelium-Derived Bradykinin in the Control of Vascular Tone. *J.Cardiovasc.Pharmacol.* 20 Suppl 9: S55-S61.

Heinis, C., T. Rutherford, S. Freund, and G. Winter. 2009. Phage-Encoded Combinatorial Chemical Libraries Based on Bicyclic Peptides. *Nat.Chem.Biol.* 5, no. 7: 502-507.

Haeseleer F., Y. Imanishi, I. Sokal, S. Filipek and K. Palczewski .2002. Calcium-binding proteins: intracellular sensors from the calmodulin superfamily. *Biochem Biophys Res Commun.* 290:615-23

Heyliger, C. E., A. Prakash, and J. H. McNeill. 1987. Alterations in Cardiac Sarcolemmal Ca<sup>2+</sup> Pump Activity During Diabetes Mellitus. *Am.J.Physiol* 252, no. 3 Pt 2: H540-H544.

Hill, J. K., D. E. Williams, M. LeMasurier, R. A. Dumont, E. E. Strehler, and P. G. Gillespie. 2006. Splice-Site A Choice Targets Plasma-Membrane Ca<sup>2+</sup>-ATPase Isoform 2 to Hair Bundles. *J.Neurosci.* 26, no. 23: 6172-6180.

Hill, J. K., D. E. Williams, M. LeMasurier, R. A. Dumont, E. E. Strehler, and P. G. Gillespie. 2006. Splice-Site A Choice Targets Plasma-Membrane Ca<sup>2+</sup>-ATPase Isoform 2 to Hair Bundles. *J.Neurosci.* 26, no. 23: 6172-6180.

Hirota, S. and L. J. Janssen. 2007. Store-Refilling Involves Both L-Type Calcium Channels and Reverse-Mode Sodium-Calcium Exchange in Airway Smooth Muscle. *Eur.Respir.J.* 30, no. 2: 269-278.

Hoenderop, J. G., B. Nilius, and R. J. Bindels. 2005. Calcium Absorption Across Epithelia. *Physiol Rev.* 85, no. 1: 373-422.

Hoess, R. H., A. J. Mack, H. Walton, and T. M. Reilly. 1994. Identification of a Structural Epitope by Using a Peptide Library Displayed on Filamentous Bacteriophage. *J.Immunol.* 153, no. 2: 724-729.

Howard, A., S. Legon, and J. R. Walters. 1993. Human and Rat Intestinal Plasma Membrane Calcium Pump Isoforms. *Am.J.Physiol* 265, no. 5 Pt 1: G917-G925.

Iino, M., H. Kasai, and T. Yamazawa. 1994. Visualization of Neural Control of Intracellular Ca<sup>2+</sup> Concentration in Single Vascular Smooth Muscle Cells in Situ. *EMBO J.* 13, no. 21: 5026-5031.

Iino, M. and M. Tsukioka. 1994. Feedback Control of Inositol Trisphosphate Signalling Bycalcium. *Mol.Cell Endocrinol.* 98, no. 2: 141-146.

Inoue, R., T. Okada, H. Onoue, Y. Hara, S. Shimizu, S. Naitoh, Y. Ito, and Y. Mori. 2001. The Transient Receptor Potential Protein Homologue TRP6 Is the Essential Component of Vascular Alpha(1)-Adrenoceptor-Activated Ca(2+)-Permeable Cation Channel. *Circ.Res.* 88, no. 3: 325-332.

Ishida, M. and B. C. Berk. 1997. Angiotensin II Signal Transduction in Vascular Smooth Muscle Cells: Role of Tyrosine Kinases. *Keio J.Med.* 46, no. 2: 61-68.

Jacobsen, J. C., C. Aalkjaer, H. Nilsson, V. V. Matchkov, J. Freiberg, and N. H. Holstein-Rathlou. 2007. A Model of Smooth Muscle Cell Synchronization in the Arterial Wall. *Am.J.Physiol Heart Circ.Physiol* 293, no. 1: H229-H237.

James, P., T. Vorherr, J. Krebs, A. Morelli, G. Castello, D. J. McCormick, J. T. Penniston, A. De Flora, and E. Carafoli. 1989. Modulation of Erythrocyte Ca<sup>2+</sup>-ATPase by Selective Calpain Cleavage of the Calmodulin-Binding Domain. *J.Biol.Chem.* 264, no. 14: 8289-8296.

James, P. H., M. Pruschy, T. E. Vorherr, J. T. Penniston, and E. Carafoli. 1989. Primary Structure of the CAMP-Dependent Phosphorylation Site of the Plasma Membrane Calcium Pump. *Biochemistry* 28, no. 10: 4253-4258.

Jani, M., H. Tordai, M. Trexler, L. Banyai, and L. Patthy. 2005. Hydroxamate-Based Peptide Inhibitors of Matrix Metalloprotease 2. *Biochimie* 87, no. 3-4: 385-392.

Jarrett, H. W. and J. T. Penniston. 1978. Purification of the Ca<sup>2+</sup>-Stimulated ATPase Activator From Human Erythrocytes. Its Membership in the Class of Ca<sup>2+</sup>-Binding Modulator Proteins. *J.Biol.Chem.* 253, no. 13: 4676-4682.

Johns, A., P. Leijten, H. Yamamoto, K. Hwang, and C. van Breemen. 1987. Calcium Regulation in Vascular Smooth Muscle Contractility. *Am.J.Cardiol.* 59, no. 2: 18A-23A.

Jones, S., A. Solomon, D. Sanz-Rosa, C. Moore, L. Holbrook, E. J. Cartwright, L. Neyses, and M. Emerson. 2010. The Plasma Membrane Calcium ATPase Modulates Calcium Homeostasis, Intracellular Signaling Events and Function in Platelets. *J.Thromb.Haemost.* 8, no. 12: 2766-2774.

Kadam, A. P. and A. Sahu. 2010. Identification of Complin, a Novel Complement Inhibitor That Targets Complement Proteins Factor B and C2. *J.Immunol.* 184, no. 12: 7116-7124.

Kawano, S., K. Otsu, S. Shoji, K. Yamagata, and M. Hiraoka. 2003. Ca(2+) Oscillations Regulated by Na(+)-Ca(2+) Exchanger and Plasma Membrane Ca(2+) Pump Induce Fluctuations of Membrane Currents and Potentials in Human Mesenchymal Stem Cells. *Cell Calcium* 34, no. 2: 145-156.

Kay, B. K., N. B. Adey, Y. S. He, J. P. Manfredi, A. H. Mataragnon, and D. M. Fowlkes. 1993. An M13 Phage Library Displaying Random 38-Amino-Acid Peptides As a Source of Novel Sequences With Affinity to Selected Targets. *Gene* 128, no. 1: 59-65.

Keenan, S. M., R. K. DeLisle, W. J. Welsh, S. Paula, and W. J. Ball, Jr. 2005. Elucidation of the Na<sup>+</sup>, K<sup>+</sup>-ATPase Digitalis Binding Site. *J.Mol.Graph.Model.* 23, no. 6: 465-475.

Kehoe, J. W. and B. K. Kay. 2005. Filamentous Phage Display in the New Millennium. *Chem.Rev.* 105, no. 11: 4056-4072.

Kennedy, B. G. and N. J. Mangini. 1996. Plasma Membrane Calcium-ATPase in Cultured Human Retinal Pigment Epithelium. *Exp.Eye Res.* 63, no. 5: 547-556.

Kessler, F., R. Falchetto, R. Heim, R. Meili, T. Vorherr, E. E. Strehler, and E. Carafoli. 1992. Study of Calmodulin Binding to the Alternatively Spliced C-Terminal Domain of the Plasma Membrane Ca<sup>2+</sup> Pump. *Biochemistry* 31, no. 47: 11785-11792.

Kim, E., S. J. DeMarco, S. M. Marfatia, A. H. Chishti, M. Sheng, and E. E. Strehler. 1998. Plasma Membrane Ca<sup>2+</sup> ATPase Isoform 4b Binds to Membrane-Associated Guanylate Kinase (MAGUK) Proteins Via Their PDZ (PSD-95/Dlg/ZO-1) Domains. *J.Biol.Chem.* 273, no. 3: 1591-1595.

Kip, S. N. and E. E. Strehler. 2003. Characterization of PMCA Isoforms and Their Contribution to Transcellular Ca<sup>2+</sup> Flux in MDCK Cells. *Am.J.Physiol Renal Physiol* 284, no. 1: F122-F132.

Kirichok, Y., G. Krapivinsky, and D. E. Clapham. 2004. The Mitochondrial Calcium Uniporter Is a Highly Selective Ion Channel. *Nature* 427, no. 6972: 360-364.

Kozel, P. J., R. A. Friedman, L. C. Erway, E. N. Yamoah, L. H. Liu, T. Riddle, J. J. Duffy, T. Doetschman, M. L. Miller, E. L. Cardell, and G. E. Shull. 1998. Balance and Hearing Deficits in Mice With a Null Mutation in the Gene Encoding Plasma Membrane Ca<sup>2+</sup>-ATPase Isoform 2. *J.Biol.Chem.* 273, no. 30: 18693-18696.

Kralios, A. C., F. A. Kralios, F. L. Anderson, and M. Leonard. 1998. Coronary Venous Hypertension Prevents the Formation of the Electrophysiological Arrhythmogenic Substrate of Acute Ischemia in the Dog: Salutary Effects of Preserved Myocardial Hydration. *J.Mol.Cell Cardiol.* 30, no. 2: 255-268.

Kristan, K., T. Bratkovic, M. Sova, S. Gobec, A. Prezelj, and U. Urleb. 2009. Novel Inhibitors of Beta-Ketoacyl-ACP Reductase From Escherichia Coli. *Chem.Biol.Interact.* 178, no. 1-3: 310-316.

Krizaj, D., S. J. DeMarco, J. Johnson, E. E. Strehler, and D. R. Copenhagen. 2002. Cell-Specific Expression of Plasma Membrane Calcium ATPase Isoforms in Retinal Neurons. *J.Comp Neurol.* 451, no. 1: 1-21.

Krstic, D., M. Colovic, N. Bosnjakovic-Pavlovic, A. Spasojevic-De Bire, and V. Vasic. 2009. Influence of Decavanadate on Rat Synaptic Plasma Membrane ATPases Activity. *Gen.Physiol Biophys.* 28, no. 3: 302-308.

Kuhn, A., D. R. Goldstein, A. Hodges, A. D. Strand, T. Sengstag, C. Kooperberg, K. Becanovic, M. A. Pouladi, K. Sathasivam, J. H. Cha, A. J. Hannan, M. R. Hayden, B. R. Leavitt, S. B. Dunnett, R. J. Ferrante, R. Albin, P. Shelbourne, M. Delorenzi, S. J. Augood, R. L. Faull, J. M. Olson, G. P. Bates, L. Jones, and R. Luthi-Carter. 2007. Mutant Huntingtin's Effects on Striatal Gene Expression in Mice Recapitulate Changes Observed in Human Huntington's Disease Brain and Do Not Differ With Mutant Huntingtin Length or Wild-Type Huntingtin Dosage. *Hum.Mol.Genet.* 16, no. 15: 1845-1861.

Kuo, T. H., K. K. Wang, L. Carlock, C. Diglio, and W. Tsang. 1991. Phorbol Ester Induces Both Gene Expression and Phosphorylation of the Plasma Membrane Ca<sup>2+</sup> Pump. *J.Biol.Chem.* 266, no. 4: 2520-2525.

Kurnellas, M. P., H. Li, M. R. Jain, S. N. Giraud, A. B. Nicot, A. Ratnayake, R. F. Heary, and S. Elkabes. 2010. Reduced Expression of Plasma Membrane Calcium ATPase 2 and Collapsin Response Mediator Protein 1 Promotes Death of Spinal Cord Neurons. *Cell Death Differ.* 17, no. 9: 1501-1510.

Kwan, C. Y., L. Belbeck, and E. E. Daniel. 1979. Abnormal Biochemistry of Vascular Smooth Muscle Plasma Membrane As an Important Factor in the Initiation and Maintenance of Hypertension in Rats. *Blood Vessels* 16, no. 5: 259-268.

Lacinova, L. 2005. Voltage-Dependent Calcium Channels. *Gen.Physiol Biophys.* 24 Suppl 1: 1-78.

Lamont, C. and W. G. Wier. 2002. Evoked and Spontaneous Purinergic Junctional Ca<sup>2+</sup> Transients (JCaTs) in Rat Small Arteries. *Circ.Res.* 91, no. 6: 454-456.

Lee, C. H., D. Poburko, K. H. Kuo, C. Seow, and C. van Breemen. 2002. Relationship Between the Sarcoplasmic Reticulum and the Plasma Membrane. *Novartis.Found.Symp.* 246: 26-41.

Lee, W. J., S. J. Roberts-Thomson, N. A. Holman, F. J. May, G. M. Lehrbach, and G. R. Monteith. 2002. Expression of Plasma Membrane Calcium Pump Isoform MRNAs in Breast Cancer Cell Lines. *Cell Signal* 14, no. 12: 1015-1022.

Lee, W. J., S. J. Roberts-Thomson, and G. R. Monteith. 2005. Plasma Membrane Calcium-ATPase 2 and 4 in Human Breast Cancer Cell Lines. *Biochem.Biophys.Res.Commun.* 337, no. 3: 779-783.

Lehotsky, J., P. Kaplan, R. Murin, and L. Raeymaekers. 2002. The Role of Plasma Membrane Ca<sup>2+</sup> Pumps (PMCA) in Pathologies of Mammalian Cells. *Front Biosci.* 7: d53-d84.

Lerman, A., B. S. Edwards, J. W. Hallett, D. M. Heublein, S. M. Sandberg, and J. C. Burnett, Jr. 1991. Circulating and Tissue Endothelin Immunoreactivity in Advanced Atherosclerosis. *N.Engl.J.Med.* 325, no. 14: 997-1001.

Liu, B. F., X. Xu, R. Fridman, S. Muallem, and T. H. Kuo. 1996. Consequences of Functional Expression of the Plasma Membrane Ca<sup>2+</sup> Pump Isoform 1a. *J.Biol.Chem.* 271, no. 10: 5536-5544.

Liu, L., Y. Ishida, G. Okunade, G. J. Pyne-Geithman, G. E. Shull, and R. J. Paul. 2007. Distinct Roles of PMCA Isoforms in Ca<sup>2+</sup> Homeostasis of Bladder Smooth Muscle: Evidence From PMCA Gene-Ablated Mice. *Am.J.Physiol Cell Physiol* 292, no. 1: C423-C431.

Luzzago, A., F. Felici, A. Tramontano, A. Pessi, and R. Cortese. 1993. Mimicking of Discontinuous Epitopes by Phage-Displayed Peptides, I. Epitope Mapping of Human H Ferritin Using a Phage Library of Constrained Peptides. *Gene* 128, no. 1: 51-57.

Mahoney, M. G., L. L. Slakey, P. K. Hepler, and D. J. Gross. 1993. Independent Modes of Propagation of Calcium Waves in Smooth Muscle Cells. *J.Cell Sci.* 104 ( Pt 4): 1101-1107.

Makani, S. and M. Chesler. 2010. Rapid Rise of Extracellular PH Evoked by Neural Activity Is Generated by the Plasma Membrane Calcium ATPase. *J.Neurophysiol.* 103, no. 2: 667-676.

Marian, M. J., H. Li, D. Borchman, and C. A. Paterson. 2005. Plasma Membrane Ca<sup>2+</sup>-ATPase Expression in the Human Lens. *Exp.Eye Res.* 81, no. 1: 57-64.

Marian, M. J., P. Mukhopadhyay, D. Borchman, and C. A. Paterson. 2008. Plasma Membrane Ca-ATPase Isoform Expression in Human Cataractous Lenses Compared to Age-Matched Clear Lenses. *Ophthalmic Res.* 40, no. 2: 86-93.

Marian, M. J., P. Mukhopadhyay, D. Borchman, D. Tang, and C. A. Paterson. 2008. The Effect of Hydrogen Peroxide on Sarco/Endoplasmic and Plasma Membrane Calcium ATPase Gene Expression in Cultured Human Lens Epithelial Cells. *Open.Ophthalmol.J.* 2: 123-129.

Martin, R., N. C. Harvey, S. R. Crozier, J. R. Poole, M. K. Javaid, E. M. Dennison, H. M. Inskip, M. Hanson, K. M. Godfrey, C. Cooper, and R. Lewis. 2007. Placental Calcium Transporter (PMCA3) Gene Expression Predicts Intrauterine Bone Mineral Accrual. *Bone* 40, no. 5: 1203-1208.

McCarron, J. G., S. Chalmers, K. N. Bradley, D. MacMillan, and T. C. Muir. 2006. Ca<sup>2+</sup> Microdomains in Smooth Muscle. *Cell Calcium* 40, no. 5-6: 461-493.

McConnell, S. J., A. J. Uveges, D. M. Fowlkes, and D. G. Spinella. 1996. Construction and Screening of M13 Phage Libraries Displaying Long Random Peptides. *Mol.Divers.* 1, no. 3: 165-176.

McLafferty, M. A., R. B. Kent, R. C. Ladner, and W. Markland. 1993. M13 Bacteriophage Displaying Disulfide-Constrained Microproteins. *Gene* 128, no. 1: 29-36.

Meldolesi, J. and T. Pozzan. 1998. The Endoplasmic Reticulum Ca<sup>2+</sup> Store: a View From the Lumen. *Trends Biochem.Sci.* 23, no. 1: 10-14.

Miller, D. J. and A. O'Dowd. 2000. Vascular Smooth Muscle Actions of Carnosine As Its Zinc Complex Are Mediated by Histamine H(1) and H(2) Receptors. *Biochemistry (Mosc.)* 65, no. 7: 798-806.

Missiaen, L., F. Wuytack, L. Raeymaekers, H. De Smedt, G. Droogmans, I. Declerck, and R. Casteels. 1991. Ca<sup>2+</sup> Extrusion Across Plasma Membrane and Ca<sup>2+</sup> Uptake by Intracellular Stores. *Pharmacol.Ther.* 50, no. 2: 191-232.

Missiaen, L., W. Robberecht, Bosch L. van den, G. Callewaert, J. B. Parys, F. Wuytack, L. Raeymaekers, B. Nilius, J. Eggermont, and H. De Smedt. 2000. Abnormal Intracellular Ca(2+)Homeostasis and Disease. *Cell Calcium* 28, no. 1: 1-21.

Mohamed, T. M., D. Oceandy, S. Prehar, N. Alatwi, Z. Hegab, F. M. Baudoin, A. Pickard, A. O. Zaki, R. Nadif, E. J. Cartwright, and L. Neyses. 2009. Specific Role of Neuronal Nitric-Oxide Synthase When Tethered to the Plasma Membrane Calcium Pump in Regulating the Beta-Adrenergic Signal in the Myocardium. *J.Biol.Chem.* 284, no. 18: 12091-12098.

Molek, P., B. Strukelj, and T. Bratkovic. 2011. Peptide Phage Display As a Tool for Drug Discovery: Targeting Membrane Receptors. *Molecules* 16, no. 1: 857-887.

Moller, J. V., B. Juul, and M. le Maire. 1996. Structural Organization, Ion Transport, and Energy Transduction of P-Type ATPases. *Biochim.Biophys.Acta* 1286, no. 1: 1-51.

Moncada, S. and E. A. Higgs. 2006. Nitric Oxide and the Vascular Endothelium. *Handb.Exp.Pharmacol.*, no. 176 Pt 1: 213-254.

Monteith, G. R. and B. D. Roufogalis. 1995. The Plasma Membrane Calcium Pump--a Physiological Perspective on Its Regulation. *Cell Calcium* 18, no. 6: 459-470.

Monteith, G. R., D. McAndrew, H. M. Faddy, and S. J. Roberts-Thomson. 2007. Calcium and Cancer: Targeting Ca<sup>2+</sup> Transport. *Nat.Rev.Cancer* 7, no. 7: 519-530.

Navedo, M. F., G. C. Amberg, R. E. Westenbroek, M. J. Sinnegger-Brauns, W. A. Catterall, J. Striessnig, and L. F. Santana. 2007. Ca(v)1.3 Channels Produce Persistent Calcium Sparklets, but Ca(v)1.2 Channels Are Responsible for Sparklets in Mouse Arterial Smooth Muscle. *Am.J.Physiol Heart Circ.Physiol* 293, no. 3: H1359-H1370.

Nicot, A., M. Kurnellas, and S. Elkabes. 2005. Temporal Pattern of Plasma Membrane Calcium ATPase 2 Expression in the Spinal Cord Correlates With the Course of Clinical Symptoms in Two Rodent Models of Autoimmune Encephalomyelitis. *Eur.J.Neurosci.* 21, no. 10: 2660-2670.

Niggli, V., E. S. Adunyah, and E. Carafoli. 1981. Acidic Phospholipids, Unsaturated Fatty Acids, and Limited Proteolysis Mimic the Effect of Calmodulin on the Purified Erythrocyte  $\text{Ca}^{2+}$  - ATPase. *J.Biol.Chem.* 256, no. 16: 8588-8592.

Niggli, V., E. S. Adunyah, J. T. Penniston, and E. Carafoli. 1981. Purified  $(\text{Ca}^{2+}$ - $\text{Mg}^{2+}$ )-ATPase of the Erythrocyte Membrane. Reconstitution and Effect of Calmodulin and Phospholipids. *J.Biol.Chem.* 256, no. 1: 395-401.

Niggli, V., M. Zurini, and E. Carafoli. 1987. Purification, Reconstitution, and Molecular Characterization of the  $\text{Ca}^{2+}$  Pump of Plasma Membranes. *Methods Enzymol.* 139: 791-808.

Oceandy, D., M. H. Buch, E. J. Cartwright, and L. Neyses. 2006. The Emergence of Plasma Membrane Calcium Pump As a Novel Therapeutic Target for Heart Disease. *Mini.Rev.Med.Chem.* 6, no. 5: 583-588.

Oceandy, D., E. J. Cartwright, M. Emerson, S. Prehar, F. M. Baudoin, M. Zi, N. Alatwi, L. Venetucci, K. Schuh, J. C. Williams, A. L. Armesilla, and L. Neyses. 2007. Neuronal Nitric Oxide Synthase Signaling in the Heart Is Regulated by the Sarcolemmal Calcium Pump 4b. *Circulation* 115, no. 4: 483-492.

Okunade, G. W., M. L. Miller, G. J. Pyne, R. L. Sutliff, K. T. O'Connor, J. C. Neumann, A. Andringa, D. A. Miller, V. Prasad, T. Doetschman, R. J. Paul, and G. E. Shull. 2004. Targeted Ablation of Plasma Membrane  $\text{Ca}^{2+}$ -ATPase (PMCA) 1 and 4 Indicates a Major Housekeeping Function for PMCA1 and a Critical Role in Hyperactivated Sperm Motility and Male Fertility for PMCA4. *J.Biol.Chem.* 279, no. 32: 33742-33750.

Osborn, K. D., A. Zaidi, A. Mandal, R. J. Urbauer, and C. K. Johnson. 2004. Single-Molecule Dynamics of the Calcium-Dependent Activation of Plasma-Membrane  $\text{Ca}^{2+}$ -ATPase by Calmodulin. *Biophys.J.* 87, no. 3: 1892-1899.

Owsianik, G., K. Talavera, T. Voets, and B. Nilius. 2006. Permeation and Selectivity of TRP Channels. *Annu.Rev.Physiol* 68: 685-717.

Pacaud, P., G. Loirand, J. L. Lavie, C. Mironneau, and J. Mironneau. 1989. Calcium-Activated Chloride Current in Rat Vascular Smooth Muscle Cells in Short-Term Primary Culture. *Pflugers Arch.* 413, no. 6: 629-636.

Pande, J., K. K. Mallhi, and A. K. Grover. 2005. A Novel Plasma Membrane  $\text{Ca}^{2+}$ -Pump Inhibitor: Caloxin 1A1. *Eur.J.Pharmacol.* 508, no. 1-3: 1-6.

Pande, J., K. K. Mallhi, and A. K. Grover. 2005. Role of Third Extracellular Domain of Plasma Membrane  $\text{Ca}^{2+}$ - $\text{Mg}^{2+}$ -ATPase Based on the Novel Inhibitor Caloxin 3A1. *Cell Calcium* 37, no. 3: 245-250.

Pande, J., K. K. Mallhi, A. Sawh, M. M. Szewczyk, F. Simpson, and A. K. Grover. 2006. Aortic Smooth Muscle and Endothelial Plasma Membrane  $\text{Ca}^{2+}$  Pump Isoforms Are Inhibited Differently by the Extracellular Inhibitor Caloxin 1b1. *Am.J.Physiol Cell Physiol* 290, no. 5: C1341-C1349.

Pande, J., M. M. Szewczyk, I. Kuszczak, S. Grover, E. Escher, and A. K. Grover. 2008. Functional Effects of Caloxin 1c2, a Novel Engineered Selective Inhibitor of Plasma Membrane  $\text{Ca}^{2+}$ -Pump Isoform 4, on Coronary Artery. *J.Cell Mol.Med.* 12, no. 3: 1049-1060.

Pande, J., M. M. Szewczyk, and A. K. Grover. 2010. Phage Display: Concept, Innovations, Applications and Future. *Biotechnol.Adv.* 28, no. 6: 849-858.

Pande, J., M. M. Szewczyk, and A. K. Grover. 2010. Phage Display: Concept, Innovations, Applications and Future. *Biotechnol.Adv.* 28, no. 6: 849-858.

Pande, J., M. M. Szewczyk, and A. K. Grover. 2011. Allosteric Inhibitors of Plasma Membrane Ca Pumps: Invention and Applications of Caloxins. *World J.Biol.Chem.* 2, no. 3: 39-47.

Paszty, K., A. R. Penheiter, A. K. Verma, R. Padanyi, A. G. Filoteo, J. T. Penniston, and A. Enyedi. 2002. Asp1080 Upstream of the Calmodulin-Binding Domain Is Critical for Autoinhibition of HPMCA4b. *J.Biol.Chem.* 277, no. 39: 36146-36151.

Paszty, K., A. K. Verma, R. Padanyi, A. G. Filoteo, J. T. Penniston, and A. Enyedi. 2002. Plasma Membrane Ca<sub>2</sub>+ATPase Isoform 4b Is Cleaved and Activated by Caspase-3 During the Early Phase of Apoptosis. *J.Biol.Chem.* 277, no. 9: 6822-6829.

Paszty, K., G. Antalfy, L. Hegedus, R. Padanyi, A. R. Penheiter, A. G. Filoteo, J. T. Penniston, and A. Enyedi. 2007. Cleavage of the Plasma Membrane Ca+ATPase During Apoptosis. *Ann.N.Y.Acad.Sci.* 1099: 440-450.

Penniston, J. T. and A. Enyedi. 1998. Modulation of the Plasma Membrane Ca<sub>2</sub>+ Pump. *J.Membr.Biol.* 165, no. 2: 101-109.

Peppiatt-Wildman, C. M., A. P. Albert, S. N. Saleh, and W. A. Large. 2007. Endothelin-1 Activates a Ca<sub>2</sub>+ -Permeable Cation Channel With TRPC3 and TRPC7 Properties in Rabbit Coronary Artery Myocytes. *J.Physiol* 580, no. Pt.3: 755-764.

Philipson, K. D., D. A. Nicoll, M. Ottolia, B. D. Quednau, H. Reuter, S. John, and Z. Qiu. 2002. The Na<sup>+</sup>/Ca<sub>2</sub><sup>+</sup> Exchange Molecule: an Overview. *Ann.N.Y.Acad.Sci.* 976: 1-10.

Pinto, Fde T. and H. P. Adamo. 2002. Deletions in the Acidic Lipid-Binding Region of the Plasma Membrane Ca<sub>2</sub>+ Pump. A Mutant With High Affinity for Ca<sub>2</sub>+ Resembling the Acidic Lipid-Activated Enzyme. *J.Biol.Chem.* 277, no. 15: 12784-12789.

Prasad, V., G. W. Okunade, M. L. Miller, and G. E. Shull. 2004. Phenotypes of SERCA and PMCA Knockout Mice. *Biochem.Biophys.Res.Comm.* 322, no. 4: 1192-1203.

Prasad, V., G. Okunade, L. Liu, R. J. Paul, and G. E. Shull. 2007. Distinct Phenotypes Among Plasma Membrane Ca<sub>2</sub>+ -ATPase Knockout Mice. *Ann.N.Y.Acad.Sci.* 1099: 276-286.

Qiu, L. Y., E. Krieger, G. Schaftenaar, H. G. Swarts, P. H. Willems, J. J. De Pont, and J. B. Koenderink. 2005. Reconstruction of the Complete Ouabain-Binding Pocket of Na,K-ATPase in Gastric H,K-ATPase by Substitution of Only Seven Amino Acids. *J.Biol.Chem.* 280, no. 37: 32349-32355.

Ray, F. R., W. Huang, M. Slater, and J. A. Barden. 2002. Purinergic Receptor Distribution in Endothelial Cells in Blood Vessels: a Basis for Selection of Coronary Artery Grafts. *Atherosclerosis* 162, no. 1: 55-61.

Razani, B., S. E. Woodman, and M. P. Lisanti. 2002. Caveolae: From Cell Biology to Animal Physiology. *Pharmacol.Rev.* 54, no. 3: 431-467.

Reddy, S., D. Benatar, and M. Gheorghiad. 1997. Update on Digoxin and Other Oral Positive Inotropic Agents for Chronic Heart Failure. *Curr.Opin.Cardiol.* 12, no. 3: 233-241.

Reinhardt, T. A., A. G. Filoteo, J. T. Penniston, and R. L. Horst. 2000. Ca<sup>2+</sup>-ATPase Protein Expression in Mammary Tissue. *Am.J.Physiol Cell Physiol* 279, no. 5: C1595-C1602.

Reinhardt, T. A., J. D. Lippolis, G. E. Shull, and R. L. Horst. 2004. Null Mutation in the Gene Encoding Plasma Membrane Ca<sup>2+</sup>-ATPase Isoform 2 Impairs Calcium Transport into Milk. *J.Biol.Chem.* 279, no. 41: 42369-42373.

Rimessi, A., L. Coletto, P. Pinton, R. Rizzuto, M. Brini, and E. Carafoli. 2005. Inhibitory Interaction of the 14-3-3(Rimessi et al. 2005) Protein With Isoform 4 of the Plasma Membrane Ca<sup>2+</sup>-ATPase Pump. *J.Biol.Chem.* 280, no. 44: 37195-37203.

Rodriguez, C., M. Slevin, R. Rodriguez-Calvo, S. Kumar, J. Krupinski, T. Tejerina, and J. Martinez-Gonzalez. 2009. Modulation of Endothelium and Endothelial Progenitor Cell Function by Low-Density Lipoproteins: Implication for Vascular Repair, Angiogenesis and Vasculogenesis. *Pathobiology* 76, no. 1: 11-22.

Saito, K., K. Uzawa, Y. Endo, Y. Kato, D. Nakashima, K. Ogawara, M. Shiba, H. Bukawa, H. Yokoe, and H. Tanzawa. 2006. Plasma Membrane Ca<sup>2+</sup> ATPase Isoform 1 Down-Regulated in Human Oral Cancer. *Oncol.Rep.* 15, no. 1: 49-55.

Salamino, F., B. Sparatore, E. Melloni, M. Michetti, P. L. Viotti, S. Pontremoli, and E. Carafoli. 1994. The Plasma Membrane Calcium Pump Is the Preferred Calpain Substrate Within the Erythrocyte. *Cell Calcium* 15, no. 1: 28-35.

Saleh, S. N., A. P. Albert, C. M. Peppiatt, and W. A. Large. 2006. Angiotensin II Activates Two Cation Conductances With Distinct TRPC1 and TRPC6 Channel Properties in Rabbit Mesenteric Artery Myocytes. *J.Physiol* 577, no. Pt 2: 479-495.

Saleh, S. N., A. P. Albert, C. M. Peppiatt-Wildman, and W. A. Large. 2008. Diverse Properties of Store-Operated TRPC Channels Activated by Protein Kinase C in Vascular Myocytes. *J.Physiol* 586, no. 10: 2463-2476.

Schnetkamp, P. P. 2004. The SLC24 Na<sup>+</sup>/Ca<sup>2+</sup>-K<sup>+</sup> Exchanger Family: Vision and Beyond. *Pflugers Arch.* 447, no. 5: 683-688.

Schuh, K., S. Uldrijan, S. Gambaryan, N. Roethlein, and L. Neyses. 2003. Interaction of the Plasma Membrane Ca<sup>2+</sup> Pump 4b/CI With the Ca<sup>2+</sup>/Calmodulin-Dependent Membrane-Associated Kinase CASK. *J.Biol.Chem.* 278, no. 11: 9778-9783.

Schuh, K., E. J. Cartwright, E. Jankevics, K. Bundschu, J. Liebermann, J. C. Williams, A. L. Armesilla, M. Emerson, D. Oceandy, K. P. Knobloch, and L. Neyses. 2004. Plasma Membrane Ca<sup>2+</sup> ATPase 4 Is Required for Sperm Motility and Male Fertility. *J.Biol.Chem.* 279, no. 27: 28220-28226.

Schultz, J. M., Y. Yang, A. J. Caride, A. G. Filoteo, A. R. Penheiter, A. Lagziel, R. J. Morell, S. A. Mohiddin, L. Fananapazir, A. C. Madeo, J. T. Penniston, and A. J. Griffith. 2005. Modification of Human Hearing Loss by Plasma-Membrane Calcium Pump PMCA2. *N.Engl.J.Med.* 352, no. 15: 1557-1564.

Schwab, B. L., D. Guerini, C. Didszun, D. Bano, E. Ferrando-May, E. Fava, J. Tam, D. Xu, S. Xanthoudakis, D. W. Nicholson, E. Carafoli, and P. Nicotera. 2002. Cleavage of Plasma Membrane Calcium Pumps by Caspases: a Link Between Apoptosis and Necrosis. *Cell Death Differ.* 9, no. 8: 818-831.

- Sepulveda, M. R., M. Berrocal-Carrillo, M. Gasset, and A. M. Mata. 2006. The Plasma Membrane Ca<sup>2+</sup>-ATPase Isoform 4 Is Localized in Lipid Rafts of Cerebellum Synaptic Plasma Membranes. *J.Biol.Chem.* 281, no. 1: 447-453.
- Shaul, P. W. and R. G. Anderson. 1998. Role of Plasmalemmal Caveolae in Signal Transduction. *Am.J.Physiol* 275, no. 5 Pt 1: L843-L851.
- Shull, G. E. 2000. Gene Knockout Studies of Ca<sup>2+</sup>-Transporting ATPases. *Eur.J.Biochem.* 267, no. 17: 5284-5290.
- Shuttleworth, T. J. 2004. Receptor-Activated Calcium Entry Channels--Who Does What, and When? *Sci.STKE.* 2004, no. 243: e40.
- Silverstein, R. S. and B. L. Tempel. 2006. Atp2b2, Encoding Plasma Membrane Ca<sup>2+</sup>-ATPase Type 2, (PMCA2) Exhibits Tissue-Specific First Exon Usage in Hair Cells, Neurons, and Mammary Glands of Mice. *Neuroscience* 141, no. 1: 245-257.
- Sima, A. V., C. S. Stancu, and M. Simionescu. 2009. Vascular Endothelium in Atherosclerosis. *Cell Tissue Res.* 335, no. 1: 191-203.
- Skou, J. C. and M. Esmann. 1981. Eosin, a Fluorescent Probe of ATP Binding to the (Na<sup>+</sup> + K<sup>+</sup>)-ATPase. *Biochim.Biophys.Acta* 647, no. 2: 232-240.
- Smith, G. P. and V. A. Petrenko. 1997. Phage Display. *Chem.Rev.* 97, no. 2: 391-410.
- Stauffer, T. P., D. Guerini, and E. Carafoli. 1995. Tissue Distribution of the Four Gene Products of the Plasma Membrane Ca<sup>2+</sup> Pump. A Study Using Specific Antibodies. *J.Biol.Chem.* 270, no. 20: 12184-12190.
- Strehler, E. E. and D. A. Zacharias. 2001. Role of Alternative Splicing in Generating Isoform Diversity Among Plasma Membrane Calcium Pumps. *Physiol Rev.* 81, no. 1: 21-50.
- Sward, K., M. Mita, D. P. Wilson, J. T. Deng, M. Susnjar, and M. P. Walsh. 2003. The Role of RhoA and Rho-Associated Kinase in Vascular Smooth Muscle Contraction. *Curr.Hypertens.Rep.* 5, no. 1: 66-72.
- Szewczyk, M. M., K. A. Davis, S. E. Samson, F. Simpson, P. K. Rangachari, and A. K. Grover. 2007. Ca<sup>2+</sup>-Pumps and Na<sup>2+</sup>-Ca<sup>2+</sup>-Exchangers in Coronary Artery Endothelium Versus Smooth Muscle. *J.Cell Mol.Med.* 11, no. 1: 129-138.
- Szewczyk, M. M., J. Pande, and A. K. Grover. 2008. Caloxins: a Novel Class of Selective Plasma Membrane Ca<sup>2+</sup> Pump Inhibitors Obtained Using Biotechnology. *Pflugers Arch.* 456, no. 2: 255-266.
- Szewczyk, M. M., J. Pande, G. Akolkar, and A. K. Grover. 2010. Caloxin 1b3: a Novel Plasma Membrane Ca(2+)-Pump Isoform 1 Selective Inhibitor That Increases Cytosolic Ca(2+) in Endothelial Cells. *Cell Calcium* 48, no. 6: 352-357.
- Takahashi, M., Y. Kondou, and C. Toyoshima. 2007. Interdomain Communication in Calcium Pump As Revealed in the Crystal Structures With Transmembrane Inhibitors. *Proc.Natl.Acad.Sci.U.S.A* 104, no. 14: 5800-5805.

Talarico, E. F., Jr., B. G. Kennedy, C. F. Marfurt, K. U. Loeffler, and N. J. Mangini. 2005. Expression and Immunolocalization of Plasma Membrane Calcium ATPase Isoforms in Human Corneal Epithelium. *Mol.Vis.* 11: 169-178.

Tempel, B. L. and D. J. Shilling. 2007. The Plasma Membrane Calcium ATPase and Disease. *Subcell.Biochem.* 45: 365-383.

Thomas, R. C. 2009. The Plasma Membrane Calcium ATPase (PMCA) of Neurones Is Electroneutral and Exchanges 2 H<sup>+</sup> for Each Ca<sup>2+</sup> or Ba<sup>2+</sup> Ion Extruded. *J.Physiol* 587, no. Pt 2: 315-327.

Thomas, R. C. 2009. The Plasma Membrane Calcium ATPase (PMCA) of Neurones Is Electroneutral and Exchanges 2 H<sup>+</sup> for Each Ca<sup>2+</sup> or Ba<sup>2+</sup> Ion Extruded. *J.Physiol* 587, no. Pt 2: 315-327.

Tiffert, T. and V. L. Lew. 2001. Kinetics of Inhibition of the Plasma Membrane Calcium Pump by Vanadate in Intact Human Red Cells. *Cell Calcium* 30, no. 5: 337-342.

Tiruppathi, C., G. U. Ahmmed, S. M. Vogel, and A. B. Malik. 2006. Ca<sup>2+</sup> Signaling, TRP Channels, and Endothelial Permeability. *Microcirculation.* 13, no. 8: 693-708.

Toustrup-Jensen, M. and B. Vilsen. 2003. Importance of Conserved Thr214 in Domain A of the Na<sup>+</sup>,K<sup>+</sup> - ATPase for Stabilization of the Phosphoryl Transition State Complex in E2P Dephosphorylation. *J.Biol.Chem.* 278, no. 13: 11402-11410.

Toyoshima, C., M. Nakasako, H. Nomura, and H. Ogawa. 2000. Crystal Structure of the Calcium Pump of Sarcoplasmic Reticulum at 2.6 Å Resolution. *Nature* 405, no. 6787: 647-655.

Toyoshima, C. and H. Nomura. 2002. Structural Changes in the Calcium Pump Accompanying the Dissociation of Calcium. *Nature* 418, no. 6898: 605-611.

Vale-Gonzalez, C., A. Alfonso, C. Sunol, M. R. Vieytes, and L. M. Botana. 2006. Role of the Plasma Membrane Calcium Adenosine Triphosphatase on Domoate-Induced Intracellular Acidification in Primary Cultures of Cerebellar Granule Cells. *J.Neurosci.Res.* 84, no. 2: 326-337.

Vale-Gonzalez, C., B. Gomez-Limia, M. R. Vieytes, and L. M. Botana. 2007. Effects of the Marine Phycotoxin Palytoxin on Neuronal PH in Primary Cultures of Cerebellar Granule Cells. *J.Neurosci.Res.* 85, no. 1: 90-98.

Van Baelen, K., L. Dode, J. Vanoevelen, G. Callewaert, H. De Smedt, L. Missiaen, J. B. Parys, L. Raeymaekers, and F. Wuytack. 2004. The Ca<sup>2+</sup>/Mn<sup>2+</sup> Pumps in the Golgi Apparatus. *Biochim.Biophys.Acta* 1742, no. 1-3: 103-112.

VanHouten, J., C. Sullivan, C. Bazinet, T. Ryoo, R. Camp, D. L. Rimm, G. Chung, and J. Wysolmerski. 2010. PMCA2 Regulates Apoptosis During Mammary Gland Involution and Predicts Outcome in Breast Cancer. *Proc.Natl.Acad.Sci.U.S.A* 107, no. 25: 11405-11410.

VanHouten, J. N. and J. J. Wysolmerski. 2007. Transcellular Calcium Transport in Mammary Epithelial Cells. *J.Mammary.Gland.Biol.Neoplasia.* 12, no. 4: 223-235.

Venema, V. J., H. Ju, R. Zou, and R. C. Venema. 1997. Interaction of Neuronal Nitric-Oxide Synthase With Caveolin-3 in Skeletal Muscle. Identification of a Novel Caveolin Scaffolding/Inhibitory Domain. *J.Biol.Chem.* 272, no. 45: 28187-28190.

Verma, A. K., A. Enyedi, A. G. Filoteo, E. E. Strehler, and J. T. Penniston. 1996. Plasma Membrane Calcium Pump Isoform 4a Has a Longer Calmodulin-Binding Domain Than 4b. *J.Biol.Chem.* 271, no. 7: 3714-3718.

Vincenzi, F. F. and H. J. Schatzmann. 1967. Some Properties of Ca-Activated ATPase in Human Red Cell Membranes. *Helv.Physiol Pharmacol.Acta* 25, no. 2: CR233-CR234.

Vinet, R. and F. F. Vargas. 1999. L- and T-Type Voltage-Gated Ca<sup>2+</sup> Currents in Adrenal Medulla Endothelial Cells. *Am.J.Physiol* 276, no. 4 Pt 2: H1313-H1322.

Wan, T. C., M. Zabe, and W. L. Dean. 2003. Plasma Membrane Ca<sup>2+</sup>-ATPase Isoform 4b Is Phosphorylated on Tyrosine 1176 in Activated Human Platelets. *Thromb.Haemost.* 89, no. 1: 122-131.

Wang, K. K., L. C. Wright, C. L. Machan, B. G. Allen, A. D. Conigrave, and B. D. Roufogalis. 1991. Protein Kinase C Phosphorylates the Carboxyl Terminus of the Plasma Membrane Ca(2+)-ATPase From Human Erythrocytes. *J.Biol.Chem.* 266, no. 14: 9078-9085.

Wang, Y., X. Deng, T. Hewavitharana, J. Soboloff, and D. L. Gill. 2008. Stim, ORAI and TRPC Channels in the Control of Calcium Entry Signals in Smooth Muscle. *Clin.Exp.Pharmacol.Physiol* 35, no. 9: 1127-1133.

Waugh, W. H. 1962. Role of Calcium in Contractile Excitation of Vascular Smooth Muscle by Epinephrine and Potassium. *Circ.Res.* 11: 927-940.

Wennmalm, A. and A. S. Petersson. 1991. Endothelium-Independent Vascular Relaxation by Histamine in the Rabbit Aorta. *Acta Physiol Scand.* 142, no. 4: 525-526.

Werth, J. L., Y. M. Usachev, and S. A. Thayer. 1996. Modulation of Calcium Efflux From Cultured Rat Dorsal Root Ganglion Neurons. *J.Neurosci.* 16, no. 3: 1008-1015.

Wieczorek, I., W. G. Haynes, D. J. Webb, C. A. Ludlam, and K. A. Fox. 1994. Raised Plasma Endothelin in Unstable Angina and Non-Q Wave Myocardial Infarction: Relation to Cardiovascular Outcome. *Br.Heart J.* 72, no. 5: 436-441.

Wilhelm, B., T. Brandenburger, H. Post, and G. Aumuller. 2008. Expression and Localization of PMCA4 in Rat Testis and Epididymis. *Histochem.Cell Biol.* 129, no. 3: 331-343.

Williams, J. C., A. L. Armesilla, T. M. Mohamed, C. L. Hagarty, F. H. McIntyre, S. Schomburg, A. O. Zaki, D. Oceandy, E. J. Cartwright, M. H. Buch, M. Emerson, and L. Neyses. 2006. The Sarcolemmal Calcium Pump, Alpha-1 Syntrophin, and Neuronal Nitric-Oxide Synthase Are Parts of a Macromolecular Protein Complex. *J.Biol.Chem.* 281, no. 33: 23341-23348.

Wilson, D. P., C. Sutherland, M. A. Borman, J. T. Deng, J. A. MacDonald, and M. P. Walsh. 2005. Integrin-Linked Kinase Is Responsible for Ca<sup>2+</sup>-Independent Myosin Diphosphorylation and Contraction of Vascular Smooth Muscle. *Biochem.J.* 392, no. Pt 3: 641-648.

Withers, S., E. J. Cartwright, and L. Neyses. 2006. Sperm Phenotype of Mice Carrying a Gene Deletion for the Plasma Membrane Calcium/Calmodulin Dependent ATPase 4. *Mol.Cell Endocrinol.* 250, no. 1-2: 93-97.

Wray, S. and T. Burdyga. 2010. Sarcoplasmic Reticulum Function in Smooth Muscle. *Physiol Rev.* 90, no. 1: 113-178.

- Wu, K. D., D. Bungard, and J. Lytton. 2001. Regulation of SERCA Ca<sup>2+</sup> Pump Expression by Cytoplasmic Ca<sup>2+</sup> in Vascular Smooth Muscle Cells. *Am.J.Physiol Cell Physiol* 280, no. 4: C843-C851.
- Wu, X., B. Chang, N. S. Blair, M. Sargent, A. J. York, J. Robbins, G. E. Shull, and J. D. Molkentin. 2009. Plasma Membrane Ca<sup>2+</sup>-ATPase Isoform 4 Antagonizes Cardiac Hypertrophy in Association With Calcineurin Inhibition in Rodents. *J.Clin.Invest* 119, no. 4: 976-985.
- Wuytack, F., L. Raeymaekers, and L. Missiaen. 2002. Molecular Physiology of the SERCA and SPCA Pumps. *Cell Calcium* 32, no. 5-6: 279-305.
- Yaar, R., L. M. Cataldo, A. Tzatsos, C. E. Francis, Z. Zhao, and K. Ravid. 2002. Regulation of the A3 Adenosine Receptor Gene in Vascular Smooth Muscle Cells: Role of a CAMP and GATA Element. *Mol.Pharmacol.* 62, no. 5: 1167-1176.
- Yakubu, M. A. and C. W. Leffler. 2002. L-Type Voltage-Dependent Ca<sup>2+</sup> Channels in Cerebral Microvascular Endothelial Cells and ET-1 Biosynthesis. *Am.J.Physiol Cell Physiol* 283, no. 6: C1687-C1695.
- Yamamoto, K., T. Sokabe, T. Matsumoto, K. Yoshimura, M. Shibata, N. Ohura, T. Fukuda, T. Sato, K. Sekine, S. Kato, M. Isshiki, T. Fujita, M. Kobayashi, K. Kawamura, H. Masuda, A. Kamiya, and J. Ando. 2006. Impaired Flow-Dependent Control of Vascular Tone and Remodeling in P2X4-Deficient Mice. *Nat.Med.* 12, no. 1: 133-137.
- Yiannikouris, F., M. Gupte, K. Putnam, and L. Cassis. 2010. Adipokines and Blood Pressure Control. *Curr.Opin.Nephrol.Hypertens.* 19, no. 2: 195-200.
- Yip, H., W. Y. Chan, P. C. Leung, H. Y. Kwan, C. Liu, Y. Huang, V. Michel, D. T. Yew, and X. Yao. 2004. Expression of TRPC Homologs in Endothelial Cells and Smooth Muscle Layers of Human Arteries. *Histochem.Cell Biol.* 122, no. 6: 553-561.
- Zacharias, D. A. and C. Kappen. 1999. Developmental Expression of the Four Plasma Membrane Calcium ATPase (Pmca) Genes in the Mouse. *Biochim.Biophys.Acta* 1428, no. 2-3: 397-405.
- Zhang, Y., S. Moreland, and R. S. Moreland. 1994. Regulation of Vascular Smooth Muscle Contraction: Myosin Light Chain Phosphorylation Dependent and Independent Pathways. *Can.J.Physiol Pharmacol.* 72, no. 11: 1386-1391.
- Zhou, C. and S. Wu. 2006. T-Type Calcium Channels in Pulmonary Vascular Endothelium. *Microcirculation* 13, no. 8: 645-656.

## 6. APPENDIX

### ***Appendix 1. To determine caloxin 1c2-binding to PMCA protein (continuation of Jyoti Pande PhD thesis)***

***Hypothesis:*** Caloxin 1c2 inhibits PMCA4 by binding to its exdom1X

***Rationale:*** Caloxin 1c2, (TAWSEVLDLLRRGGGSK) the mutant of caloxin 1b1, inhibited the  $\text{Ca}^{2+}$ - $\text{Mg}^{2+}$ -ATPase activity of PMCA in human erythrocyte ghosts with 20 x higher affinity than parent caloxin 1b1 (Pande et al. 2006) Since caloxin 1b1 was obtained for binding to PMCA4 exdom1X, it was hypothesized that the mechanism of inhibition by caloxin 1c2 involves its binding to exdom1X of PMCA4. The initial steps to test this hypothesis had already been conducted. Two derivatives of caloxin 1c2 containing biotin (at the epsilon amino group of K) and the UV cross linking group benzoyl-phenylalanine (Bpa) were synthesized. W at position 3 was substituted by Bpa in 3Bpa-1c2-biotin and S at 16 in 16Bpa-1c2-biotin. Biotin was added for the detection of the photolabel by horse radish peroxidase (HRP) conjugated streptavidin. Both probes inhibited PMCA in human erythrocyte ghosts, but as expected 3Bpa-1c2-biotin was a weaker inhibitor ( $K_i = 50 \mu\text{M}$ ), indicating that W is important for caloxin binding. Both probes UV cross-linked to a high molecular weight doublet in Western blots (approximately 240-270 kDa, detected with streptavidin-HRP) but the signal was much stronger with 3Bpa-1c2-biotin indicating again that W is crucial for caloxin 1c2 binding. Since then studies with 3Bpa-1c2-biotin were conducted. Since PMCA molecular weight is about 135 kDa and the observed doublet was twice as big it was hypothesized that the

doublet may be PMCA oligomer. The intensity of the detected high molecular weight doublet decreased only in the presence of high amounts of caloxin 1c2 or synthetic PMCA4 exdom1X peptide. The intensity of the doublet labeled with 50  $\mu\text{M}$  3Bpa-1c2-biotin decreased by 36 % and 63 % in the presence of 200  $\mu\text{M}$  and 500  $\mu\text{M}$  caloxin 1c2, respectively. The presence of 1 mM synthetic exdom1X peptide decreased the intensity of the 250-270 kDa biotinylated band by 76 %. Immunoprecipitation of the ghosts UV cross-linked with 3Bpa-1c2-biotin with an anti-PMCA antibody (5F10, Affinity Bioreagents, recognizes all PMCA) resulted in detection of the doublet of the same size (around 260 kDa) with HRP-streptavidin.

**Purification of photoadducts:** To further confirm that the high molecular weight doublet is a PMCA oligomer, the method of purification of photolabeled PMCA with streptavidin coated magnetic beads to capture biotinylated product was developed. Purification resulted in detection of a high molecular weight doublet with anti-PMCA (5F10), anti-PMCA4 (JA9) but not with anti-PMCA1 antibodies. Bands additional to the high molecular weight doublet were also detected using the 5F10 and JA9 antibodies.

**Enzymatic digestion of photoadducts:** Since the only lysine residue of caloxin 1c2 was modified, digestion of the PMCA- 3Bpa-1c2-biotin complex with the protease lys C should give a PMCA fragment with biotin still intact. Based on a protease lys C digestion pattern the expected size of the PMCA fragment including exdom1X would be 11 kDa. Toward this approach I optimized large scale UV cross-linking, protein solubilization and immunoprecipitation on streptavidin coated magnetic beads. We tried

to optimize conditions for lys C digestion, however the digested product did not give the expected 11 kDa product.

**LC MS/MS analysis:** Due to unexpected problems with enzymatic digestion, the erythrocyte ghosts UV-crosslinked to 3Bpa-1c2-biotin were solubilised, purified on streptavidin coated magnetic beads, run on a 7.5% polyacrylamide gel and the doublet was excised from the gel and sent for LC MS/MS analysis to Dr. Erol Gulcicek (W. M. Keck Facility, Yale University) for analysis. Results from LC MS/MS analysis were unexpected. The sample contained mainly alpha and beta spectrin, solute carrier family4, streptavidin, small amounts of keratin, but no PMCA4. An excess of spectrin compared to PMCA protein and its ability to interact with other proteins can possibly explain the nonspecific spectrin labeling with 3bpa1c2-biotin. The spectrin heterodimer consists of two subunits  $\alpha$  and  $\beta$  (280 and 246 kDa, respectively) and is the major protein in the erythroid membrane. Moreover it is amphiphilic and is characterized by hydrophobic stretches in its polypeptide sequence containing a large number of hydrophobic sites which can bind hydrophobic molecules (Gallagher et al. 2004). One can assume that caloxin 1c2 could be selected for binding to spectrin during affinity chromatography, however spectrin is barely solubilized with the method we use to solubilize PMCA for affinity chromatography experiments. Photolabeled ghosts (2 mg protein) are extracted twice with the buffer containing 1 % sodium deoxycholate, 0.1 % SDS and 1 % Triton X-100, while for PMCA purification 2 mg of erythrocyte ghosts protein is solubilised with 0.2 % Triton X-100. Moreover, coomassie blue stained polyacrylamide SDS gel of erythrocyte PMCA purified on calmodulin-agarose column shows only one ~140 kDa

band.

**Optimization of photolabeling of PMCA purified from erythrocyte ghosts with 3Bpa-caloxin 1c2:** To avoid spectrin contamination PMCA purified from erythrocyte ghosts were used for UV-cross-linking experiments. The UV labeling of purified PMCA with 100  $\mu\text{M}$  3Bpa-1c2-biotin for 30 min resulted in one band of expected 140 kDa size when detected with streptavidin-HRP in Western blots. Since the product was weak the conditions for detection to enhance the signal were optimized. The signal was increased when the blots were first incubated with streptavidin (0.06  $\mu\text{g/ml}$ ) and next with rabbit anti-streptavidin-HRP (1:50000). Saturation was not observed up to 400  $\mu\text{M}$  of 3Bpa-caloxin 1c2 when labelled for 30 min. Next the time course was done with 100  $\mu\text{M}$  3Bpa-caloxin 1c2.

It was hypothesized that caloxin 1c2 and caloxin 1b1 would compete with its derivative 3Bpa1c2-biotin for binding to PMCA as they were expected to bind at the same site. The photolabeling of human erythrocyte ghosts was carried out with 50  $\mu\text{M}$  3Bpa1c2-biotin with or without caloxin 1c2, caloxin 1b1 or caloxin 1b1 randomized peptide (30 and 100  $\mu\text{M}$ ). However the intensity of the labeling did not decrease in the presence of any of the peptides. This indicated that W substitution with 3Bpa, changed caloxin 1c2 selectivity for binding to its original site and that nonspecific binding occurs.

The project was discontinued. To overcome the problem of unspecific binding, caloxins with higher affinity for PMCA may be used when available.